Detection, Diversity, and Evolution of Fungal Nitric Oxide Reductases (P450nor)

A Dissertation Presented for the
Doctor of Philosophy
Degree
The University of Tennessee, Knoxville

Steven Adam Higgins
August 2017

Copyright © 2017 by Steven A. Higgins
All rights reserved.

ACKNOWLEDGEMENTS

First, I would like to say thank you to Dr. Frank E. Löffler for his continued guidance and support as a PhD mentor. I am grateful for all the obvious (and not so obvious) advice he has provided me over the past six years. Rather than force me to think inside a box, he accepted and even encouraged criticism, and fostered an environment where I could be creative, think independently, and have access to top notch research tools and collaborators. I would especially like to thank Dr. Löffler for allowing me the freedom to pursue a topic I was passionate about, even if that topic is, to paraphrase, “just some stuff that contaminated my cultures” (Frank’s reference to fungi during his PhD). Thanks again Frank.

I would also like to thank another mentor, Dr. Christopher W. Schadt, who was an excellent mentor during my one year fellowship at the Oak Ridge National Laboratory. After the fellowship ended, Dr. Schadt encouraged that I participate in regular meetings between the two of us, and although our schedules sometimes did not permit, these meetings were always productive times where I derived excellent research advice, support, and just an ear to listen when I needed it. I also would like to give a special thanks to Drs. Schadt and P. Brandon Matheny for supervising an excellent fungal ecology journal club.

Thank you to my committee, for their advice, constructive criticism, and support throughout my PhD. Your service on my committee means a great deal to me, and I hope for continued discussions, collaborations, and to keep in touch as I continue to pursue a career in academia. I would like to acknowledge Drs. Robert A. Sanford, Joanne C. Chee-Sanford, Allana Welsh, and David E. Graham for their contributions to research support and advice over the years.

Thank you to all my friends and family for your love, encouragement and guidance throughout the completion of my doctoral degree. It is a big sacrifice to allow a loved one to move away and be out of your lives, but you all have been patient, caring, and supported me all these years I have been away. I know that was not easy. Thank you. A special thanks to Dr. Ashley M. Frank for her continued love, advice, support, and hugs. You have been through the PhD machine, and have helped me complete this degree in more ways than you know. Thank you to those who may not have gotten a special mention here, but were an assuredly significant part of my life and helped me to succeed. Finally, a big thanks to my lovely hound dog, Tallulah.

ABSTRACT

Nitrous oxide (N_2O) is a gas responsible for significant ozone layer depletion and contributes to greenhouse effects in Earth's atmosphere. N_2O is primarily generated by denitrification, whereby nitrate (NO_3-) or nitrite (NO_2-) is converted to gaseous N_2O or N_2. Teragram quantities of N_2O are emitted annually from agricultural soils treated with nitrogenous fertilizers due to the activity of soil microbiota. Although bacteria and fungi harbor genes permitting denitrification, fungi lack NosZ, an enzyme responsible for reducing N_2O into inert N_2 gas. Historically, scientists have linked fungi to soil N_2O production, but uncertainty in fungal contributions remain due to the persistent use of biased, inhibitor-based methodologies used to assess fungal and bacterial contributions to soil N_2O emissions. In the following chapters, the application of PCR- and bioinformatics-based techniques to detect the nitric oxide reductase gene, *p450nor,* are presented. N_2O-producing fungi were isolated from microcosms established with two distinct agricultural soils amended with NO_3- or NO_2-. The *p450nor* PCR primers identified 49 novel *p450nor* gene amplicons from isolate and environmental DNA. Moreover, the PCR primer's utility was expanded by their incorporation into Illumina sequencing protocols, enabling analyses of 72 soil samples from two Midwest agricultural soils. Analysis of *p450nor* sequences (12,675,480 in total) revealed 69.7 and 64.6 % were classified as isolate or environmental sequences previously acquired from these soils. Analysis of fungal internal transcribed spacer (ITS2) sequences revealed 4,591 OTUs, of which 19 OTUs comprised 41.6 % of all fungal sequences. Importantly, ITS2 OTUs assigned to fungal families harboring denitrifying members suggests between 2 and 67 % of the fungal community may be denitrifiers. Finally, a phylogenomics approach was applied to explore denitrification potential across >700 fungal genomes. These analyses demonstrated a low co-occurrence of *p450nor* and other denitrification genes (*narG*, *napA*, *nirK*). Instead, 11 % of genomes were predicted to contain *p450nor* in secondary metabolism (SM) gene clusters and 35 % were localized adjacent hallmark SM genes, suggesting an undiscovered role for *p450nor* in SM. Phylogenetic analyses united *p450nor* with actinobacterial sequences involved in SM, suggesting recent horizontal gene transfer and challenging the paradigm of *p450nor*'s primary role in denitrification.

TABLE OF CONTENTS

Chapter One Introduction....1
Fungi and Nutrient Cycling....2
Fungi and the Nitrogen Cycle....4
Denitrification: loss of soil nitrogen to the atmosphere....4
Genes underlying canonical bacterial denitrification....5
Genes underlying fungal denitrification....7
Diversity of the denitrifying fungi....9
Culture-dependent methods to assess the fungal contributions to soil denitrification....10
Culture-independent methods to detect fungal denitrifiers in soil....11
Unique characteristics of anaerobic respiration in fungi....12
Uncertainty in fungal contributions to N_2O production....15
Denitrifying eukaryotes other than fungi....18
Objectives....20
Chapter Two Detection and Diversity of Fungal Nitric Oxide Reductase Genes (*p450nor*) in Agricultural Soils....21
Abstract....22
Introduction....23
Materials and Methods....25
Medium preparation....25
Fungal enrichment and isolation....25
Analytical procedures....26
Denitrification activity of fungal isolates....27
DNA extraction....27
Primer design....27
PCR conditions....28
Cloning and sequencing....30
Fungal taxonomy....30
Metagenomic analysis....30
P450nor sequence analyses....31
Nucleotide sequence accession numbers....32
Results....32
Fungal isolation....32
Fungal denitrifier morphology and taxonomy....33
p450nor and *nirK* PCR amplification....33
Soil denitrification activity....35
Metagenomic analyses....35
Discussion....35
A new means to assess fungal denitrification potential....35
Diversity of the denitrifying fungi....38
N_2O formation in soil microcosms and enrichments....39
Low sequence depth limits detection of fungal sequences in metagenomes....40

Chapter Three Dual Amplicon sequencing of fungal nitric oxide reductase (p450nor) and internal transcribed spacer (ITS2) region reveals functional, not fungal, community structure is controlled by soil edaphics 41
Abstract 42
Introduction 43
Materials and Methods 44
Soil sampling and DNA extraction 44
p450nor amplification 45
ITS2 amplification 46
p450nor and ITS2 Illumina sequencing library construction 46
p450nor and ITS2 sequence processing 47
Statistical analyses 49
Nucleotide sequence accession numbers 49
Results 50
p450nor amplicons and OTUs 50
ITS2 amplicons and OTUs 51
Overlapping taxonomy between *p450nor* and ITS2 52
Spatial and environmental controls on fungal community composition 53
Discussion 54
High-throughput sequencing enables detection of novel *p450nor* diversity 54
Contrasting spatial, pH, and moisture effects on the overall phylogenetically defined community versus functionally defined fungal communities 56
Culture-dependent approaches complement amplicon sequencing studies 56
High-throughput amplicon sequencing outcompetes shotgun metagenomics for environmental analysis of fungi 57
Chapter Four Phylogenomic Analyses Reveal Widespread Horizontal Gene Transfer of the Fungal Nitric Oxide Reductase (P450nor) and Support an Undiscovered Role for P450nor in Secondary Metabolism 59
Abstract 60
Introduction 61
Materials and Methods 64
Fungal genome acquisition 64
Comparative bionformatic analysis 64
Analysis of SM gene clusters in fungi 65
Phylogenetic analysis 66
TxtE enzyme expression, purification, and assay 69
Results 73
Fungi harbor a minimal set of evolutionarily correlated denitrification traits 73
On the origins of fungal *p450nor* 74
Evolutionary forces acting upon denitrification traits within fungi 75
Evidence for a role of *p450nor* in secondary metabolism 76
Discussion 79
Shared ancestry unites P450nor with P450s involved in SM 79
An undiscovered role for P450nor in SM? 80
The complex evolution of denitrification traits in fungi 82

Nitrate reductases in fungi were not created equal 84
Are green algae an enigmatic source of N_2O emissions? 85
Chapter Five Conclusions and Recommendations 87
List of References 93
Appendix 126
Vita 183

LIST OF TABLES

Table 2.1: NCBI identifiers and species designations for *p450nor* sequences used in PCR primer design. 128
Table 2.2: Characteristics of the *p450nor* gene-targeted primers. 131
Table 2.3: Fungal isolate N_2O production and PCR amplification characteristics. 132
Table 2.4: The SILVA 18S rRNA gene classification of 37 fungal isolates. 134
Table 2.5: *p450nor* amplicon lengths and number of introns found in amplified regions using primer set *p450nor394F*/*p450nor809R* 135
Table 3.1: Number of *p450nor* sequences generated per DNA sample and other quality control statistics per sample. 146
Table 3.2: Relative abundance of P450nor sequences aligned to reference OTUs in DNA extracted from Havana or Urbana soils. 148
Table 4.1: TxtE enzyme assay reaction components and final concentrations. 161
Table 4.2: Results from AU tests (see Materials and Methods) for the monophyly of fungal classes within *napA*, *nirK,* and *p450nor* gene trees. Where indicated, the monophyly of two lineages was also assessed. Bold font data indicate that the AU test rejected the monophyly of the taxa. Test significance was evaluated at $p \leq 0.05$. 162
Table 4.3: Results from species-tree gene-tree reconciliation using NOTUNG software for *napA*, *nirK*, and *p450nor* genes in fungi. Values are averages of solutions with standard deviations reported in parentheses. 164

LIST OF FIGURES

Figure 1.1: Comparison of fungal and bacterial denitrification pathways. The red X indicates that the *nosZ* gene is absent in Fungi. Note that Fungi only possess *nirK*, encoding the nitrite reductase, and that *Bacteria* possess alternative nitric oxide reductases, NorB and NorZ. 127
Figure 2.2: Stereoscopic images of isolate fungal groups (A) and singleton isolates (B). 139
Figure 2.3: PCR amplification of *p450nor* in fungal isolates. 140
Figure 2.4: Phylogeny of full length p450nor and *p450nor* amplicon sequences generated using PCR primers *p450nor394F/p450nor809R*. 141
Figure 2.5: N_2O production in soil microcosms amended with streptomycin and chloramphenicol to inhibit bacterial activity. 142
Figure 2.6: NO_3^- (▲), NO_2^-(■), and N_2O (○) quantities measured in Havana and Urbana soil transfer cultures. 143
Figure 2.7: Intron structure of the region amplified by primer set *p450nor394F*/*p450nor809R* in 47 *p450nor* sequences. 144
Figure 3.1: Schematic of the locations of soil sampling sites within Havana and Urbana, IL. The large brown rectangle represents the agricultural field at each site. The transect and the associated centroid sampling locations are marked by a line with arrows and circles with an X, respectively. This figure is courtesy of Drs. Allana Welsh, Joanne Chee-Sanford, and Robert Sanford. 150
Figure 3.2: Plot of amino acid conservation of translated and aligned P450nor amplicon sequences (red) compared to amino acid conservation in the reference (black). 151
Figure 3.3: Phylogenetic tree of amino acid sequence alignment of P450nor OTUs identified in DNA extracted from Havana (gold) and Urbana (purple) soils. Relative abundances of each OTU in the soil DNA are indicated by bars on the right. OTUs colored red are either P450nor soil clones from Havana and Urbana or fungal isolates previously isolated from each site. Tree scale represents amino acid substitutions per site. 152
Figure 3.4: Relative abundance of ITS2 OTUs identified in DNA extracted from soil samples collected at Havana and Urbana, IL sites. The lowest taxonomic affiliation for a given OTU is presented on the x axis and the OTU label (for reference purposes) is located above each bar. 153
Figure 3.5: ITS2 OTUs with ≥ 1 % relative abundance in (A) Urbana and (B) Havana soils. Relative abundances of OTUs between sites are displayed for comparison purposes. The OTU label is displayed above each bar as a reference and the lowest taxonomic rank assigned to an OUT is provided on the x-axis. 154
Figure 3.6: Relative abundance of fungal OTUs at the family rank within the ITS2 (above) and *p450nor* (below) amplicons. Potential for denitrification within the entire fungal community is suggested by shared taxonomic classifications between data sets. 155

Figure 3.7: Distribution of OTU relative abundances for *p450nor* (gold) and ITS2 (purple) based on family rank classifications. OTU relative abundance distributions of OTUs within Ajellomycetaceae, Nectriaceae, Aspergillaceae (top row) display little overlap, whereas OTUs within Hypocreaceae, Chaetomiaceae, and Lasiosphaeriaceae display more similar distributions. 156
Figure 3.8: Non-metric multidimensional scaling ordination of bray-curtis dissimilarity matrix of p450nor and ITS2 OUT relative abundances for Havana and Urbana soils. Stress values are reported to indicate goodness-of-fit of the ordination. Stress values ≤ 0.2 indicate suitable fit, and values ≤ 0.05 indicate a good fit (301). 157
Figure 3.9: NMDS ordination of bray-curtis pairwise distances computed for fungal ITS2 OUT relative abundances observed in Havana and Urbana soil DNA samples (top). Points within the NMDS plots are colored by centroid location within the site. Pie charts (below) detail class level taxonomic ranks of ITS2 OTUs within each centroid. Black arrows highlight specific shifts in class relative abundance between centroids that are likely driving separation between the points. Class level designation (right) for the pie charts, with black boxes highlighting classes in the pie charts that change in relative abundance between centroids. 158
Figure 3.10: Regression of NMDS ordination values (first axis) against measured pH and moisture of Havana and Urbana soil samples for the (A) ITS2 NMDS ordination and (B) p450nor NMDS ordination. 159
Figure 3.11: pH and moisture measurements by month within Havana (gold) and Urbana (purple) soil samples. 160
Figure 4.1: Schematic of the proposed TxtE nitration reaction of L-tryptophan that has been demonstrated to occur in vitro (253) (top) and the hypothesized side reaction of TxtE in N_2O formation (bottom). In some cases, presumably without the substrates for nitration (L-tryptophan, O_2) present, TxtE may react with two NO molecules to produce N_2O as demonstrated for P450nor. 166
Figure 4.2: BL21 *Escherichia coli* cell pellets following induction of cells with IPTG. Both sets of cells contain a pET28b(+) vector with or without the *txtE* gene, encoding a nitrating cytochrome P450. The darker red color of induced *E. coli* containing plasmid with the *txtE* gene suggests a large production of heme-containing protein. 167
Figure 4.3: Plot of absorbance of eluted protein fractions from metal ion affinity chromatography. An increasing absorbance at 417 nm indicates a heme-containing protein, possibly the target protein TxtE, was eluted from the column in the collected fractions. Peaks at 280 nm represent absorbance of aromatic amino acid moieties of proteins present within these fractions. ..168
Figure 4.4: SDS-PAGE gel of purified TxtE protein (20 µL) produced in IPTG-induced BL21 *Escherichia coli* cells containing the *txtE* gene in a pET28b(+) vector. Lanes contain his-tagged protein-containing fractions eluted from a nickel ion embedded affinity chromatography column. Lane labeled

"Concentrate" is the pooled fractions (13-17) after concentration using a 30 kDa cutoff MWCO filter. Outer most lanes are precision protein plus kaleidoscope protein standards. kDa, kilodalton. 169
Figure 4.5: Maximum likelihood phylogeny of the kingdom Fungi inferred from a concatenated alignment of 238 single copy marker gene amino acid sequences (see Materials and Methods). The presence/absence of key genes encoding enzymes involved in the metabolism of N-oxyanions within fungal phyla queried in the present study (A) and within individual members (B). Black squares marking branches indicate nodes with bootstrap percentages below 90%. The scale bar in (A) represents amino acid substitutions per site. The outer black bars in (B) represent the percentage (out of 1438) of conserved single copy genes in kingdom Fungi that were detected in the fungal genomes queried in the present study. Additional colored markers surrounding the tree indicate presence or absence of each gene within a fungal genome. Flavohb, flavohemiglobin genes involved in NO detoxification to NO_3^-. 169
Figure 4.6: Midpoint-rooted Bayesian phylogeny of select families of cytochrome P450 amino acid sequences from fungi, algae, and bacteria. Ancestral state reconstruction was performed using CYP55 (orange), CYP105 (green), and other CYPs (purple) to uncover the shared ancestry of algal and fungal N_2O-producing cytochrome P450s with their most recent common bacterial ancestor. The scale bar indicates substitutions per site and values above branches are posterior probabilities of the Bayesian MCMC analysis. Numbers in parentheses next to collapsed clades indicate the number of sequences in the clade. Values in pie charts are average probabilities of each character across a representative Bayesian MCMC analysis. 172
Figure 4.7: Midpoint rooted Bayesian (left) and maximum-likelihood phylogenies (right) of 301 cytochrome P450 sequences demonstrating the affiliation of P450nor with other sequences belonging to members of the bacterial phyla *Actinobacteria* and *Proteobacteria*. Black squares on branches (left tree) indicate ≥0.95 posterior probability or ≥90 % bootstrap replication (right tree). The colored legend indicates the cytochrome P450 family specified by shared amino acid identity of ≥40 % (279). 173
Figure 4.8: Bayesian tree reconstruction of actinobacterial and proteobacterial 16S rRNA gene (left) and cytochrome P450 family 105 amino acid sequences (right). Both phylogenies represent 50% majory-rule consensus trees. The tree on the left is rooted with proteobacterial sequences as outgroup to the *Actinobacteria*. The tree on the right is midpoint rooted. Nodes with posterior probabilites ≥ 0.95 are indicated by black circles on an adjacent branch. 174
Figure 4.9: Maximum-likelihood phylogenies connecting fungal species with their respective nitric oxide reductase (*p450nor*) gene sequence(s). On the left, an amino acid phylogeny of 238 concatenated single copy orthologues from fungal species in which one or more *p450nor* gene(s) were detected. The *p450nor* nucleotide phylogeny (right) demonstrates many instances of

incongruence with the fungal species phylogeny. Black dots in each phylogeny represent bootstrap percentages greater than or equal to 90%. Scale bars represent subtitutions per site. 175
Figure 4.10: Cophylogenetic plot of napA-containing fungal species (left) and the napA nucleotide tree (right). Both are ML trees where blacks docks represent bootstrap percentages ≥90 %. Scale bars indicate substitutions per site for the concatenated amino acid species phylogeny and nucleotide phylogeny, respectively. 176
Figure 4.11: Cophylogenetic plot of *nirK*-containing fungal species (left) and the *nirK* nucleotide tree (right). Both are ML trees where blacks docks represent bootstrap percentages ≥90 %. Scale bars indicate substitutions per site for the concatenated amino acid species phylogeny and nucleotide phylogeny, respectively. 177
Figure 4.12: ML phylogeny of a concatenated set of 238 amino acid sequences (A) and zoomed in view of genes surrounding *p450nor* in five of the 32 fungi (B). Black stars at the tips of the phylogeny in (A) indicate the zoomed in gene regions are depicted in (B). Fungi predicted to have p450nor contained within an SM cluster are indicated with a blue square at the end of the phylogeny. Arrows at the tips of the phylogeny represent the genomic arrangement of *p450nor* (blue asterisk) and surrounding genes. Distance between arrows are scaled representations of actual genomic distances within the genomes. Grey, light blue, and dark blue arrows represent no SM annotation, manual SM annotation, and automatic SM annotation (see Materials and Methods for details). The scale bar indicates amino acid substitutions per site and black circles indicate bootstrap percentages ≥90 %. 178
Figure 4.13: Taxonomic representation of the top 50 orthologous groups (A) and their functional annotations (B). Bars in (A) are colored by fungal class. Data points in (B) are colored according to whether they were automatically (dark blue), manually (light blue), or were not predicted (grey) to be involved in SM. 180
Figure 4.14: ML phylogenetic trees of amino acid sequences corresponding to non-ribosomal peptide synthase (A) and polyketide synthase domains (B). Domains identified in fungal genomes nearby *p450nor* are indicated by a black star. Reference domains from napdos and their corresponding chemical products are indicated by colored sections. Scale bars indicate amino acid substitutions per site. Values along branches indicate bootstrap support for the adjacent node. 181
Figure 4.15: N_2O formation at time 0 and 24 h after incubation of TxtE under anoxic conditions. 182

CHAPTER ONE
INTRODUCTION

Fungi and Nutrient Cycling

Fungi are major drivers of biotic processes in aquatic and terrestrial ecosystems (1–4). Fungi are central to the functioning of terrestrial soil habitats, where they contribute significantly to soil health and fertility, the degradation of recalcitrant carbon-rich compounds, and partitioning of soil resources to the benefit of other soil biota (e.g., nutrient transport to plants by arbuscular and ectomycorrhizal fungi) (5–7). Although fungi are touted as significant drivers of soil geochemical processes, their cryptic morphologies and low DNA content per dry weight of cell material compared to their bacterial counterparts, hamper some culture-dependent techniques to assess the ecology, function, and genetic diversity of fungi in soil. Moreover, these aforementioned factors combined with larger genome sizes also can hinder current state-of-the-art culture-independent techniques (e.g., shotgun metagenomics) from being applied to soil systems to assess fungal function and diversity (8). For these reasons, approaches aimed at combining the strengths of both culture-dependent and culture-independent techniques need to be carefully utilized for investigating the role of fungi in the soil environment (9). Despite of these limitations, our understanding of the fungal contributions to soil nutrient cycling is advancing. An excellent example of this enhanced knowledge can be found in the biomineralization of key soil metals and nutrients by fungal oxalate production. Fungi produce oxalate through enzymatic hydrolysis of oxaloacetate or glyoxylate and excrete this compound extracellularly where it can be further mineralized to CO_2 or form alter the solubility and bioavailability of potassium, phosphorous, aluminum, copper, iron, and other elements (10, 11). Under controlled laboratory conditions, this process has been shown to promote plant growth, presumably by solubilization of phosphate through ligand exchange of phosphate complexes with oxalate (12–14). Oxalate production has been observed in a variety of fungal taxa including the Ascomycota, Basidiomycota, and Zygomycota *sensu lato*, and is influenced by the carbon (C) and nitrogen (N) ratio, as well as source of C (glucose, glycerol, etc.) or N (ammonium, nitrate) (10, 11).

Many fungal species are also prodigious decomposers, and exhibit a saprotrophic lifestyle in which organic matter is mineralized to CO_2 (15). Fungal saprotrophy is of importance in woodland habitats, as fungi are predominant decomposers in the initial stages of complex organic matter (e.g., lignin, hemicellulose, pectin) breakdown in wood and leaves (15, 16). The saprotrophic fungi excrete extracellular enzymes (laccases, peroxidases) that destabilize and decompose lignin into simpler phenolic substrates, thus providing themselves access to the more readily metabolizable cellulose (17). At least for some fungal taxa, organic matter decomposition has been observed to be controlled by the observed fungal species diversity and N status of their environment (18, 19). Fungal decomposers are also biological mediators of bulk C and N movement in soils, the function of which has important implications for both the plant and microbial communities inhabiting soil (20).

Finally, fungi are well known for their ability to utilize various organic and inorganic forms of N in soil (21–23). For instance, arbuscular and ectomycorrhizal fungi are well studied for their roles in organic and inorganic N uptake and transport to associated host plants (24, 25). N is an essential nutrient for fungi as it is a requirement for generating amino acids (glutamine), cell wall precursors (N-acetylglucosamine), purines and pyrimidines in nucleosides, and a variety of additional, important N-containing biomolecules (21, 22). Hence, fungi possess several biochemical pathways to assimilate N and incorporate this element into their biomass (24, 26–34). Of these sources, ammonium and amino acids are the preferred N source, but fungi are also able to assimilate inorganic N-oxides like nitrate into ammonium via the well-studied actions of enzymes such as assimilatory nitrate and nitrite reductases, NiaD and NiiA, respectively, in *Aspergillus nidulans* and *YNR1* and *YNI1*, respectively, in yeasts (30, 31, 35). Although dissimilatory N cycling pathways occur in fungi (discussed below), assimilatory N metabolism may regulate additional N transformations depending on the N status of the cell (32). Given the diversity of life history strategies, metabolic pathways, and nutrient uptake capacity found in the kingdom Fungi, it

is no wonder that these multifarious organisms dominate soil microbial biomass in many soils (36). As a result, the nutrient cycling activity of fungi has important implications for climate change, as fungi directly and indirectly contribute to greenhouse gas (GHG) emissions and their activity may regulate microbial functional guilds that also contribute to GHG emissions (37).

Fungi and the Nitrogen Cycle

Denitrification: loss of soil nitrogen to the atmosphere

While a diversity of aerobic and anaerobic nitrogen (N) transformation pathways exist in nature (e.g., ammonium oxidation, nitrogen fixation), all are dominated by the activity of diverse microorganisms (38). Although N may also be transformed abiotically (e.g., chemodenitrification), the contributions of these reactions to the N cycle are not well understood (39, 40). More than a century of human activity related to agricultural crop production has resulted in the N cycle becoming one of Earth's most disrupted biogeochemical cycles (38). Specifically, human technology has significantly altered the N cycle, allowing for the fixation of massive quantities of nitrogen gas (N_2) via the Haber-Bosch process for use in agricultural fertilizers (41). One drastic consequence of the increasing application of agricultural fertilizers is enhanced microbial activity resulting in nitrous oxide (N_2O) production, which may account for up to one third of all soil N losses after fertilizer application (42). N_2O is a potent GHG that is 300-fold more effective at trapping infrared radiation than carbon dioxide, and additionally contributes to ozone depletion (43). Since agricultural soils are anticipated to contribute to two-thirds of all N_2O emissions by 2030, research investigating the sources (microorganisms) and mitigation strategies for gaseous N loss from these habitats is critical (44).

The process of denitrification (i.e., the formation of gaseous N products from nitrate, NO_3^-, or nitrite, NO_2^-), is implicated as a major source of increased N_2O production from soils, with pathways such as nitrification contributing to a lesser extent (38, 45). Microorganism typically perform denitrification when their

primary electron acceptor O_2 has been depleted and inorganic N-oxides are available (40). Inorganic N-oxides can serve as alternative electron acceptors under anoxic conditions, enabling the formation of an electrochemical potential energy gradient to drive ATP synthesis and promote microbial survival or growth (42). N_2O formation and release from soil via denitrification is controlled by a multitude of factors, including O_2 concentration, pH, temperature, moisture, soil type and compaction, and microbial species diversity (44, 46–48). Of these factors, O_2 concentration appears to be a key driver of not only the quantities of N_2O formed, but also on the sources of the N_2O (e.g., heterotrophic versus nitrifier denitrification) (44). Not surprisingly, transcriptional regulation of microbial genes involved in N respiration is controlled by a myriad of N- and redox-sensitive transcription factors (42).

Genes underlying canonical bacterial denitrification

Although fungi and other eukaryotes have been increasingly recognized for their potentially important role in denitrification, members of the kingdom *Bacteria* (and some Cren- and Euryarchaeota *Archaea*) have historically been the focus of intense investigation on the topic (38, 49). Bacterial denitrification is thought to be predominantly mediated by members of the diverse bacterial phylum *Proteobacteria*. However, additional members of the bacterial phyla *Firmicutes*, *Bacteroides*, *Verrucomicrobia*, *Spirochaetes*, and *Actinobacteria* have been demonstrated to perform denitrification or possess the genetic components (*nar*/*nap*, *nir*, *nor*, and *nos* gene operons) required for some or all reductions within the pathway (40, 50–55) .

The first step of canonical denitrification is the reduction of nitrate (NO_3^-) to nitrite (NO_2^-), through the activity of the Nar/Nap enzymes. The catalytic enzyme of the *nar* operon is encoded by *narG*, and is a 126 kDa (average mass) soluble protein containing a *bis*-molybdopterin guanine dinucleotide cofactor that accepts electrons from the quinol pool to reduce NO_3^- to NO_2^- (56). Accessory subunits encoded by the *narH* and *narI* loci are the β and γ subunits involved in electron

transfer and anchor the Nar protein to the cytoplasmic membrane or perform quinol oxidation, respectively (56). The periplasmic nitrate reductase, NapA, is a variably sized enzyme (70 – 105 kDa) that also utilizes a molybdopterin cofactor, but contains an additional iron sulfur cluster for accepting electrons involved in nitrate reduction (57, 58). Additional loci in the *nap* operon encode redox related proteins (NapBCGH) or encode proteins with functions related to protein maturation (NapDFL) (57). Of the redox proteins encoded in the *nap* operon, NapB has been extensively studied and provides electrons to NapA via the quinol pool (57).

The reduction of NO_2^- to nitric oxide (NO) is carried out by enzymes encoded by two evolutionarily distinct *nir* genes known as *nirS* and *nirK* in members of *Bacteria* (and to some extent the *Archaea*). No organism has been shown to possess both genes simultaneously (59, 60). The *nirS* gene encodes a dimeric, ~60 kDa soluble enzyme containing heme c and d_1 chromophore cofactors required for electron transfer and nitrite binding and reduction (59, 61). Other genes present in some, but not all *nirS*-containing microbes, are the genes *nirTBMCFDLGHJEN* which encode electron transfer, cofactor and protein maturation enzymes (59). In contrast to *nirS*, *nirK* does not appear to have additional genes encoded in an operon and is found in a greater diversity of microorganisms (54, 59, 60, 62). The *nirK* gene encodes a soluble, ~108 kDa trimeric multi-copper oxidase that catalyzes nitrite reduction to nitric oxide (59). NirK receives electrons from either a 14 kDa type 1 copper-containing (pseudo)azurin or cytochrome c_{551}; these enzymes in turn receive their electrons from membrane-bound respiratory complexes oxidizing the quinol pool (51, 59, 63, 64).

Nitric oxide is subsequently reduced to N_2O, and this is carried out by two evolutionarily related, but distinct nitric oxide reductases, NorB and NorZ (51, 59, 65). The major distinction between the two enzymes is that the 53 kDa membrane-bound NorB receives electrons from cytochrome c directly, whereas the 84.5 kDa, membrane-bound NorZ contains an additional N-terminal quinol

oxidase to generate electrons for nitric oxide reduction. This difference has resulted in the incorrect usage of the terms c*norB* and q*norB* to distinguish these genes in the literature (62, 65, 66). Additionally, the *norB* operon also contains the genes *norEFCQD* whereas *norZ* is not contained in an operon (65).

The final step in canonical denitrification is the reduction of the greenhouse has N_2O to the inert and ubiquitous N_2 gas. This step is carried out by the multicopper enzyme NosZ, a ~132 kDa soluble dimer containing two electron donating Cu_A and catalytic Cu_Z centers, each ensconced in one of either a cupredoxin or seven-bladed beta propeller protein fold (45, 67). The canonical *nos* operon is composed of *nosXRDFYL*, that encode transcription factors (NosR), copper center maturation enzymes (NosDFYL), and electron transfer reactions (NosX) (45). Recently, microorganisms not typically identified as denitrifiers (e.g., members of the *Bacteroides* and *Epsilonproteobacteria*) were observed to possess an atypical *nosZ* gene sequence, which differs from the canonical NosZ in that most contain a Sec protein secretion signal, rather than the twin arginine translocation, or TAT, motif (68, 69). Understanding the function, ecology, and diversity of bacteria containing atypical *nosZ* gene sequences is an area of ongoing research.

Genes underlying fungal denitrification

The genes underlying the fungal denitrification pathway largely overlap with their denitrifying prokaryotic counterparts, but some striking differences are also apparent (Figure 1.1, all tables and figures are located in the Appendix) (70, 71). For example, some members of the kingdom *Fungi* have been demonstrated to possess genes encoding the nitrate-reducing molybdoenzymes, NarG and NapA, and the copper-containing multicopper oxidase NirK (71, 72). Of these enzymes, NarG and NirK are reported to bear striking biochemical similarities to the prokaryotic varieties of each enzyme (73–75). As discussed above, the bacterial Nar protein complex contains β and γ subunits encoded by *narH* and *narI*, however there are no reports of these genes in fungi. In parallel with bacterial

systems, a heme-containing c-type cytochrome and azurin protein, both affiliated with electron transfer to NirK, have been identified in *Fusarium oxysporum* (73, 74). The NarG in *Fusarum oxysporum* strain MT811 has been suggested to be more similar to the Nar system of the non-denitrifying *Escherichia coli*, in which mitochondrial formate dehydrogenase activity is coupled to quinol oxidation and electron transfer to Nar (73). In contrast, fungal *nirK* is suggested to have arisen from maintenance of the *nirK* gene in the alphaproteobacterial ancestor that was endocytosed early on in eukaryotic evolution (76, 77). Both NarG and NirK are reported to be targeted to the mitochondria in fungi. This may allow NarG to generate a proton motive force and produce ATP, and NirK to act as an electron sink (73–75, 78). Although *nar* and *nir* have been extensively studied in fungi, little or no characterization of the periplasmic nitrate reductase protein, NapA, exists for fungi, in spite of reports of its higher gene prevalence in fungal genomes than *narG* (79). This observation is significant and should be investigated further since most fungal isolates examined cannot utilize nitrate to produce N_2O (70, 71, 80).

Overall, fungi appear to possess components of the early enzymatic steps of denitrification, but they lack homologs of the prokaryotic *nor* and *nos* genes that are involved in the latter steps of denitrification in bacteria. Instead, fungi have acquired a unique gene, *p450nor*, encoding a soluble, ~45 kDa heme-containing cytochrome P450 to reduce NO to N_2O (79). The *p450nor* gene has been hypothesized to have been horizontally transferred from a diverse group of actinobacterial CYP105 family cytochrome P450 sequences (79), but no critical evaluation of this hypothesis has been investigated (see chapter four for details of this analysis). Fungal P450nor is a member of the CYP55 family of cytochrome P450s and is unique among all cytochrome P450s because it has been shown to stoichiometrically convert NO to N_2O and directly bind reduced pyridine nucleotides (NADH and NADPH) (79, 81–84). These findings were noteworthy, particularly since other P450s and cytochrome c oxidase are inhibited in the presence of nitric oxide, and require additional flavoproteins and

ferredoxins to bind reduced pyridine nucleotides and donate electrons for their activity (85–88). Cytochrome c oxidase has been reported to reduce NO to N_2O, but additional reports refuted these claims, suggesting P450nor's NO reductase activity may be truly unique (89, 90).

Another unique feature regarding the genetic landscape of fungal denitrification is the absence of the N_2O reductase gene, *nosZ*, responsible for reducing N_2O to N_2 (70). Despite this absence, the complete reduction to N_2 can be accomplished through codenitrification, a process in which N from nitrite or nitric oxide is coupled with another N source (e.g., sodium azide, amines) in a nitrosation reaction to produce N_2 gas (91–93). Although codenitrification has been reported in a variety of terrestrial and aquatic habitats, there is some disagreement as to the environmental relevance of this process for fungi (91, 94). Regardless, N_2O produced by fungal P450nor potentially represents a significant source of N_2O in soils since fungi predominantly produce N_2O as the final step in denitrification (93) (see section on *Uncertainty in fungal contributions to N_2O production* for counter arguments)**.**

Diversity of the denitrifying fungi

Five decades ago, Bollag and Tung measured N_2O produced by *Fusarium oxysporum* and *F. solani* in liquid medium, and paved the way for future investigations underlying the mechanism of N_2O production in fungi (95). It was not until a decade later that Bleakley and Tiedje further confirmed a diverse assemblage of organisms, including yeasts and filamentous fungi, that could produce N_2O from N oxides (96). Nevertheless, a mechanistic explanation for fungal N_2O formation evaded researchers for almost 20 years until Hirofumi Shoun and colleagues identified additional members of the kingdom Fungi (Phylum Ascomycota) as denitrifiers and characterized the fungal enzyme P450nor as the sole N_2O-producing agent in fungi (79, 84). Since this finding, hundreds of fungal isolates by a multitude of research groups have been evaluated for their ability to form N_2O (72, 93, 97–100). Briefly, members of the

fungal phyla Ascomycota, Basidiomycota, and the recently revised Mucoromycota, have all been demonstrated to produce variable quantities of N_2O when grown in liquid medium (99). Members of a variety of fungal genera display modest rates of N_2O formation (>50 nmol $N_2O \cdot mL\ media^{-1} \cdot day^{-1}$) including *Fusarium*, *Haematonectria*, *Chaetomium*, *Coniochaeta*,Cylindrocarpon, *Albonectria*, *Trichoderma*, *Aspergillus*, *Neonectria*, *Pichia*, *Saccharomycopsis*, *Trichosporon*, *Trichosporiella*, *Trigonopsis*, *Yarrowia*, *Paecilomyces*, *Apiospora*, *Acremonium*, *Fusicolla*, *Monographella*, and *Pseudallescheria* (99, 101). Of note, only members of the genera *Fusarium*, *Gibberella*, *Haemonectria*, *Neocomospora*, *Trichoderma*, and *Trichosporon* were observed to produce N_2O at rates >1000 nmol $N_2O \cdot mL\ media^{-1} \cdot day^{-1}$, whereas most other fungi display rates that are at least an order of magnitude below this value (99). Many of these fungal genera have also been observed to produce N_2O in sterilized soil, further implicating this diverse group in soil N_2O formation (97). Given that the high N_2O producers were members of the phyla Ascomycota (class Sordariomycetes) and Basidiomycota (class Tremellomycetes), these types of fungi may be most relevant for studies regarding climate change since they potentially represent a source of N_2O emissions in soils. These fungi also possess saprotrophic and pathogenic life history strategies, and represent a dual threat to both the agriculture and horticulture industries since these enterprises utilize large quantities of N-based fertilizer and a variety of plant monocultures upon which these fungi thrive (99).

Culture-dependent methods to assess the fungal contributions to soil denitrification

The two principle methods used to assess the role of fungi in soil N_2O formation have historically relied on either directly cultivating fungal denitrifiers from soil and/or applying the substrate induced respiration inhibition (SI) technique to soil samples (72, 102–106). A variety of methods are available to cultivate fungi from soils, but liquid dilution of soil and/or spread plating are the preferred methods

(107). The choice of medium to cultivate fungi with specific activities is also a key consideration, and for denitrifying fungi the most widely employed has been a modified Czapek-Dox liquid or agar medium (99, 108). Briefly, the modified medium (preferred due to precipitation of magnesium phosphate (109)) contains glucose or sucrose as the main carbon source, and nitrate or nitrite as the sole N source. Additional modifications containing organic or ammonium-N sources have been used, depending on the purpose of the experiment (99, 110).

Although cultivation of fungal denitrifiers from a soil sample is suggestive of their presence or activity in the soil, additional methods, like SI, have been developed to directly observe *in situ* contributions of fungi to soil N_2O formation. The SI technique utilizes inhibitors of bacterial (e.g., streptomycin, chloramphenicol) and fungal (e.g., cycloheximide) activity to partition the contributions of each microbial group to a specific respiratory process (111). Since its inception by Anderson and Domsch in the early 1970s, the SI technique has been applied to assess the contribution of bacteria and fungi to carbon mineralization in a variety of soil habitats (112–116). Hence, it was not long before this technique was adopted to investigate the fungal contribution to N_2O formation in agricultural (72, 117, 118), prairie/grassland (119, 120), peatland (121), wetland sediments (122, 123), forest (124, 125), uranium and nitrate contaminated groundwater (101), and arid soils (126). The range of fungal contributions to N_2O emissions using the SI method has been estimated to be substantial, and reports range from 40 to 89 % of the total N_2O emitted from soil systems examined (99). The section *Uncertainty in fungal contributions to N_2O production* of this document reveals the inherent biases of this technique and provides commentary suggesting that bacterial contributions to N_2O production are in fact much higher than that of fungi.

Culture-independent methods to detect fungal denitrifiers in soil

With the advent of several large scale fungal genome sequencing projects, such as assembling the fungal tree of life and 1000 fungal genomes, an increasing

number of completed and partial fungal genomes containing denitrification genes are available for comparison (127, 128). Although high throughput amplicon sequencing and shotgun metagenomics are available to query the genetic potential of microbial communities, polymerase chain reaction (PCR) methods continue to be the gold standard for environmental fungal research. Hence, PCR-based methodologies have recently been developed to target a diversity of fungal denitrifiers without having to cultivate them from soils (97, 103, 129–131). Of the four genes related to denitrification in fungi, PCR primers targeting the *nirK* gene have been the preferred methodology (97, 130–132), presumably because development of degenerate primers targeting a diversity of *p450nor* genes was not feasible (refer to chapter two for additional details)(103). Moreover, the gene encoding the membrane-bound nitrate reductase, NarG, is not prevalent in available fungal genomes (refer to chapter four and reference (79) for additional details). Similarly, the *napA* gene encoding the periplasmic nitrate reductase is prevalent in fungi (79), but no evidence of a role for NapA in fungal denitrification is available and limits the utility of this marker for assaying the potential contribution of fungi to denitrification. Although widely used in fungal research, PCR-based approaches have substantial limitations (133); for example, multiple primer sets may be required to target a diversity of taxa to make them applicable to different environments, and primer bias during amplification or formation of chimeric PCR amplicons poses a challenge for downstream data analysis (134). However, fungal sequences represented only a small fraction of shotgun metagenomes (except for some simple communities with high fungal biomass (135)) and PCR methodologies still represent reliable, cost-effective tools for assessing fungal presence/absence, diversity, relative abundance, and function in soils.

Unique characteristics of anaerobic respiration in fungi

The genetic system fungi employ to respire N-oxides is unique, and multiple observations have been reported that separate anoxic N respiration in fungi from

their prokaryotic counterparts (79). For example, fungi appear to have acquired distinct genes and biochemical pathways to grow and oxidize reduced pyridine nucleotides under anoxic conditions coupled to N-oxide reduction (136). Under strictly anoxic conditions in the presence of nitrate and ethanol as the sole C source, *Fusarium oxysporum* and *Aspergillus nidulans* have been observed to perform a version of nitrate reduction to ammonium termed ammonia fermentation (137–139). However, ammonium formation from nitrate was also observed in *Aspergillus terreus* strain An4, and is thought to be an analog of the bacterial dissimilatory nitrate reduction to ammonium (DNRA) since fermentation of organic matter was not involved (140). Members of the *Bacteria* perform the nitrite reduction step of DNRA using a pentahaem cytochrome c_{552} encoded by the *nrfA* gene and, to date, no homolog has been identified in fungi (140, 141). In *A. nidulans*, ammonia fermentation is carried out by the assimilatory nitrate and nitrite reductases, NiaD and NiiA, respectively, with energy generation promoted by substrate level phosphorylation via acetate kinase (137). For *A. terreus* strain An4, DNRA was not connected to the fermentation of organic substrates, but further evidence is required to demonstrate whether the dissimilatory or assimilatory nitrate and nitrite reductases are operating in this organism (140).

Another difference between fungal and bacterial N-oxide respiration is the coupling of nitrate reduction to formate oxidation using formate dehydrogenase (73, 142). This pathway of nitrate reduction in fungi deviates from bacterial denitrifiers in that the coupling of formate oxidation to nitrate reduction is similar to anaerobic metabolism in non-denitrifying *Escherichia coli* (143). In Enterobacteria, this process requires the action of pyruvate formate lyase to produce formate and acetyl coenzyme A (acetyl-CoA), the former of which is oxidized via formate dehydrogenase to provide NADH for nitrate reduction and the latter is required to produce ATP and acetate from the activity of phosphotransacetylase and acetate kinase (137, 143). In one report of ammonia fermentation in *Fusarium oxysporum* strain MT811, pyruvate formate lyase is suggested to be operating (142), yet an analysis of >100 fungal genomes

identified genes encoding pyruvate formate lyase only in the fungal phylum Neocallimastigomycota, a group of obligately anaerobic chytrids (144). Hence, the relevance of pyruvate formate lyase in fungal ammonia fermentation seems limited, especially since an alternative pathway using, alcohol dehydrogenase, CoA-acylating aldehyde dehydrogenase, and acetyl-CoA synthetase have been suggested to be operating in both *F. oxysporum* strain MT811 and *A. nidulans* (137–139). Further exploration of the environmental relevance of the varying types of fungal nitrate respiration are required, especially given that this process has been largely observed in fungi under a limited set of conditions (in the presence of nitrate and ethanol) (138). A recent study by Ma et al. suggested that formate regulates the production of N_2O by fungi present in cultivated and uncultivated wetlands, presumably by stimulating nitrate reduction to nitrite with the addition of formate (123). Overall, fungal nitrate reduction may be relevant in anoxic systems, such as wetlands and deep sea sediments, where fungi are prevalent but their contributions to N cycling has not been firmly established (123, 140).

Much like denitrifying members of the *Bacteria*, oxygen concentration appears to be a regulatory signal for denitrification to occur in fungi (145, 146). However, in members of the *Bacteria*, N_2O is produced under anoxic conditions, whereas fungal N_2O formation is inhibited by anoxia and requires low (µmole) quantities of oxygen (95, 96, 145). Proposed explanations for the observed oxygen requirement are the need for oxygen to biosynthesize fatty acids and ergosterol, perform oxygenase reactions, and utilization of a dual aerobic/anaerobic respiration in the mitochondria (145). The fungal oxygen requirement for N_2O production is only reported for pure culture studies using fungal isolates. Enzyme assays using purified P450nor are performed under strictly anoxic conditions and N_2O production by this enzyme has been reported to be inhibited by oxygen (81, 147–152). Hence, the effect of O_2 on fungal denitrification is complex, and requires additional investigations to explain

discrepancies between biochemical and pure culture-based physiological studies,

Another interesting feature of fungal denitrification is the finding that denitrification genes are encoded within nuclear, not mitochondrial, chromosome(s) (79). Thus, fungal denitrification genes are transcribed in the nucleus, their mRNA presumably transported to the endoplasmic reticulum or mitochondria, and subsequently translated by ribosomes in either the endoplasmic reticulum or mitochondria. NarG, NirK, and P450nor activity have been detected in mitochondrial fractions of fungal lysates, and, at least for some P450nor, mitochondrial targeting signals have been detected at the carboxy terminus of the amino acid sequence (74, 75, 82, 152). Of note, the *p450nor* gene has been demonstrated to encode two isozymes of P450nor in *Fusarium oxysporum*, *Cylindrocarpon tonkiense*, and *Trichosporon cutaneum*; one isozyme being targeted to the mitochondria whereas the other is cytoplasmic and is suggested to be involved in NO detoxification (147, 153, 154). No evidence of *narG*, *napA*, or *nirK* encoding multiple isozymes have been reported, and the finding that P450nor isozymes are present in multiple species of fungi suggests it may be an important feature of P450nor function and evolution in fungi.

Uncertainty in fungal contributions to N_2O production

Increasing evidence indicates that fungi are chief contributors to denitrification in arable, grassland, and arid soils (102, 120, 155), but their contributions to N-cycling may be more widespread than is currently known. In support of these observations, several studies have reported that members of the *Fungi* are potentially significant contributors to N_2O emissions from soils, especially in agroecosystems where N input is high (38, 102, 120, 121, 123, 156). However, these observations contradict findings that the rates of N_2O production by denitrifying fungal isolates in pure culture studies are three to six orders of magnitude lower than rates of bacterial N_2O formation (99, 157), and that a majority of fungal isolates tested for denitrification often convert less than 20% of

the supplied N to N_2O in laboratory incubations (millimolar inputs produce nano- or micromolar outputs) (70, 72, 80, 99, 145).

Little or no evidence exists demonstrating fungal growth using N-oxides as terminal electron acceptors in the absence of oxygen or fermentable substrates (104, 140, 145, 157, 158), suggesting these conditions might not support fungal denitrification activity. In fact, closely related fungi examined from N_2O-forming genera do not demonstrate growth under anoxic conditions in the presence of glucose (159). Investigations of fungal genomes, a sample of which included members of denitrifying fungi, failed to identify genes encoding pyruvate:ferredoxin oxidoreductase, pyruvate:NADP+ oxidoreductase, or pyruvate formate lyase (except in *Rhizopus* and obligate anaerobic chytrids), key enzymes involved in downstream ATP synthesis and anaplerosis under anoxic conditions (144, 159). Furthermore, Herold and colleagues did not observe a significant relationship between a fungal fatty acid biomarker, linoleic acid, and potential fungal denitrification rates from soils (118). This observation is significant, given the discrepancy in contributions of fungi to N_2O formation between pure culture studies and soil incubations and the suggestion that fungal denitrification may be a detoxification mechanism (152, 157). One possible explanation for these conflicting observations is that fungi may differ in their nutritional requirements to support denitrification, and current cultivation conditions may require optimization (99). Given that denitrifying members of the *Bacteria* also face this same limitation, yet do not suffer such great disparity in rates of N_2O production, suggests additional explanations may be more plausible. For example, recent evidence supports the hypothesis that biases of the SI technique are a major cause for the observed disparity in fungal N_2O production between pure culture and soil incubations (115, 160). Specifically, the recent study by Ladan and Jacinthe demonstrates that streptomycin and cycloheximide are poor inhibitors of bacterial and fungal respiration, and that recently developed inhibitors (e.g., bronopol, 2-bromo-2-nitro-1,3-propanediol) may be more effective (160). Moreover, bacteria contributed 85 ± 7 % to N_2O

emissions across the different agricultural soils investigated, and strongly suggests that fungi are only a minor contributor to N_2O formation in these soils (160). These results contrast with a majority of previously published studies, in which fungi have been observed to contribute up to 89 % of soil N_2O emissions (99). Of note, Ladan and Jacinthe observed a significant decrease in N_2O emissions from a soil undergoing no till management for 50 years when fungicide was applied, and the authors hypothesize that fungal biomass, and therefore fungal denitrifiers, may be greater under no till managed soils (160). Although this observation is promising, no measurements of fungal or bacterial biomass or their proxies (e.g., phospholipid fatty acid analysis, quantitative PCR) were performed on any soils examined.

Indeed, only two studies have evaluated proxies of fungal or bacterial biomass in relation to fungal N_2O emissions (117, 118). Herold et al. utilized ester-linked fatty acids to quantitate and monitor fungal and bacterial biomass, whereas Chen et al. monitored the copy numbers of the internal transcribed spacer one regions and 16S ribosomal RNA genes of fungi and bacteria, respectively (117, 118). Although Chen et al. did not perform qPCR analysis on antibiotic-treated enrichments, nor did they measure fungal denitrification gene copy number, they did observe quantities of bacterial *nirK* and *norB* gene copy numbers in no antibiotic soil amendments at approximately $\geq 2 \times 10^8$ gene copies $\cdot g^{-1}$ soil, suggesting a large bacterial denitrifier response to C and N additions in the examined soils (117). Nevertheless, fungal biomass is comparable to or greater than that of their bacterial counterparts in soils (155, 161–163), and the inhibitor-based studies strongly suggest that fungi are important contributors to this process *in situ*. Overall, there does not appear to be a single explanation for the discrepancy in N_2O formation observed between fungal pure culture studies and those employing soil incubation experiments. However, soil type, age, degree of management, and microbial community composition may play a role (160), and further experiments and observations are necessary to tease apart variations due to variability among experimental designs (i.e., differences in pH,

moisture contents, C sources, soils used) among studies (99). Yet, it is difficult to conceive how such long lag times and low rates of N_2O formation displayed by denitrifying fungi, recorded in a multitude of pure culture investigations with unlimited resources, could equate to the large contributions attributed to fungi in soil N_2O emissions *in situ* (95, 101, 157).

Denitrifying eukaryotes other than fungi

Although evidence implicates fungi in N_2O formation, additional eukaryotic lineages (phyla Chlorophyta, Retaria and Cercozoa) of fresh water-inhabiting green algae and the marine benthic Protists known as foraminifers, have also been actively investigated for their capacity to perform denitrification (164–167). A recent investigation of *Chlorella vulgaris* demonstrated this algal species could produce between 4 and 23 nmol $N_2O \cdot mL\ media^{-1} \cdot day^{-1}$, depending on the size of the initial cell inoculum (165). Hence, rates of N_2O production by green algae are on par with rates of N_2O formation measured for fungal isolates (99). Furthermore, both fungi and green algae mostly fail to form N_2O when grown in the presence of nitrate and may require low oxygen tensions for N_2O formation to begin (164, 165). The exact molecular mechanisms behind green algal N_2O formation have not been determined, but recent phylogenetic analysis identified a homolog of *p450nor* in two green algal genera *Chlorella* and *Chlamydomonas* (and see chapter four for additional results and discussions) (103, 165). Moreover, Guieysse and coworkers did not detect a canonical *norB* by PCR in DNA extracted from N_2O-producing *C. vulgaris* cultures supplied with antibiotics, supporting the hypothesis of a conserved system of N_2O production by P450nor between fungi and green algae (165).

In contrast to green algae, N_2O formation by foraminifers may be the result of a gammaproteobacterial endosymbiont (168). Partial *nirK* and *nirS* gene sequences most closely related to gamma- and betaproteobacteria, respectively, were amplified from DNA extracted from allogromiid foraminifer cells collected from Santa Barbara Basin sediments off the coast of southern California (168,

169). These findings were further confirmed with fluorescence *in situ* hybridization of 16S rRNA genes suggesting active populations of *Proteobacteria* are harbored by some foraminifers and that these endobionts and foraminifers may contribute significantly to marine sediment N cycling (169–171). In spite of these results, some foraminifera cells did not possess endobionts and still performed denitrification (169); therefore, future genomic investigations of foraminifers may assist in elucidating the genetic mechanisms underlying denitrification in this diverse group of protists. Some recent evidence also points to a role for endobionts in fungal functions related to pathogenicity (e.g., rhizoxin toxin production in the genus *Rhizopus*) (172, 173), but no role for an endobiont in fungal denitrification has been established. Of note, a member of *Fusarium* has been reported to contain an endobiont involved in this species ability to oxidize elemental sulfur, and raises the possibility that other fungal endobionts may be involved in additional elemental cycling pathways in fungi (174). The fact that some fungi (e.g., ectomycorrhizal fungus *Paxillus involutus*) have been observed to produce N_2O, yet no genes related to denitrification are harbored within its genome (refer to chapter four for details) suggests the hypothesis that fungi harbor denitrifying endobionts is plausible (100).

Another interesting feature of Eukaryotes related to N cycling is their ability to store milimolar concentrations of nitrate in intracellular vacuoles (167). For instance, fungi are on the low end of nitrate storage spectrum with an intracellular nitrate concentration of 0.4 mM, whereas foraminifera and gromiids store in excess of 450 mM nitrate; nitrate storage capacity in green algae, dinoflagellates and diatoms falls somewhere within this range on the nitrate storage spectrum (167). Therefore, eukaryotic lineages are not only capable of a vast array of N transformations, but they may also directly control N availability in the environment, acting as N cycle power brokers, directly affecting N acquisition and usage by other microbial community members.

Objectives

The first objective of this dissertation included the development and application of degenerate PCR primers to target *p450nor* genes in genomic DNA from both fungal isolates and the environment. The second objective was the modification of these primers to an Illumina sequencing methodology for examining *p450nor* biogeography in a greater number of soil samples and perform analyses thereof. The final objective was to perform comparative genomics and evolutionary analyses of the *p450nor* gene and other fungal denitrification traits in hundreds of fungal genomes and provide a benchmark for future phylogenomic studies of fungal denitrification.

CHAPTER TWO

DETECTION AND DIVERSITY OF FUNGAL NITRIC OXIDE REDUCTASE GENES (*P450NOR*) IN AGRICULTURAL SOILS

The following chapter is modified from a manuscript published in 2016 in the journal *Applied and Environmental Microbiology*, volume 82, issue 10, pages 2919-2928.

Abstract

Members of the Fungi convert nitrate (NO_3^-) and nitrite (NO_2^-) to gaseous nitrous oxide (N_2O) (denitrification), but the fungal contributions to N-loss from soil remain uncertain. Cultivation-based methodologies that include antibiotics to selectively assess fungal activities have limitations and complementary molecular approaches to assign denitrification potential to fungi are desirable. Microcosms established with soils from two representative U.S. Midwest agricultural regions produced N_2O from added NO_3^- or NO_2^- in the presence of antibiotics to inhibit bacteria. Cultivation efforts yielded 214 fungal isolates belonging to at least 15 distinct morphological groups, of which 151 produced N_2O from NO_2^-. Novel PCR primers targeting the *p450nor* gene that encodes the nitric oxide (NO) reductase responsible for N_2O production in fungi yielded 26 novel *p450nor* amplicons from DNA of 37 isolates and 23 amplicons from environmental DNA obtained from two agricultural soils. The sequences shared 54-98% amino acid identity to reference P450nor sequences within the phylum *Ascomycota*, and expand the known fungal P450nor sequence diversity. *p450nor* was detected in all fungal isolates that produced N_2O from NO_2^-, whereas *nirK* (encoding the NO-forming NO_2^- reductase) was amplified in only 13-74% of the N_2O-forming isolates using two separate *nirK* primer sets. Collectively, our findings demonstrate the value of *p450nor*-targeted PCR to complement existing approaches to assess the fungal contributions to denitrification and N_2O formation.

Introduction

Denitrification is a key process responsible for loss of fixed nitrogen (N) in soils and sediments and is mediated by both abiotic and microbial processes (38, 40). Of the microorganisms involved in denitrification, members of the *Bacteria* are well-studied and considered key contributors; however, some saprotrophic fungi also conserve energy from the reduction of nitrate (NO_3^-) or nitrite (NO_2^-) to nitrous oxide (N_2O), the main end product of fungal denitrification (79, 93, 147). Fungi have been implicated in N-turnover for over 30 years (40, 79, 83), but the ecological importance of fungal contributions to denitrification remain uncertain. Potential roles of fungi in soil N-loss and greenhouse gas (i.e., N_2O) emission are underexplored and monitoring tools (e.g., quantitative or end-point PCR) to specifically address the presence and abundance of denitrifying fungi are largely lacking. To date, the majority of the known denitrifying fungal isolates reside in the phylum Ascomycota (70, 72, 156). Although some reports suggest basidiomycete and zygomycete fungi (72, 98, 156) are denitrifiers, only a few isolates are available, and it remains to be confirmed if members of other phyla harbor *nar*, *nap*, *nir,* and *nor* gene clusters implicated in steps of the denitrification pathway. Previous investigations of fungal denitrification have relied on laboratory cultivation and substrate-induced respiration inhibition (SIRIN) tests (70, 79, 98). The SIRIN technique applies NO_3^- or NO_2^- in concert with broad-spectrum antibiotics (e.g., streptomycin) or fungicides (e.g., cycloheximide) to partition the bacterial and fungal contributions to N_2O or dinitrogen (N_2) formation. These efforts suggested that fungi play a large but unrecognized role in N-turnover and N_2O flux (120, 123, 156, 175). Although the SIRIN methodology has provided valuable insight into the fungal contribution to denitrification, the application of SIRIN to soils can be problematic as incomplete inhibition can bias the observations (114, 121, 176). Hence, alternative approaches (e.g., PCR) that selectively target fungal genes involved in denitrification are desirable to advance understanding of the fungal diversity

contributing to N-cycling in environments such as soils, aquifers, and deep ocean sediments where denitrifying fungi have been cultivated (70, 101, 104, 120).

Denitrifying fungi possess a unique protein of the CYP55 family of P450 cytochromes, the cytochrome P450 nitric oxide reductase (P450nor). P450nor lacks mono-oxygenase activity and a conserved N-terminal membrane anchor domain found in other eukaryotic P450 cytochromes (66). It directly binds the electron donor NAD(P)H, but otherwise is structurally conserved and shares similarity to other cytochrome P450 proteins (66). P450nor is responsible for the reduction of nitric oxide to N_2O, the dominant end product, although N_2 formation has been observed (70, 82, 93). Denitrifying bacteria and archaea are also capable of reducing nitric oxide to N_2O, but possess a distinct gene locus (*norB*) that encodes two isozymes, cNor or qNor, each relying on a distinct electron donor (c-type cytochrome or ubiquinol pool, respectively) (59, 62). Furthermore, only bacterial and archaeal denitrifiers possess the *nosZ* gene that encodes the enzyme responsible for reduction of the greenhouse gas N_2O to inert N_2. Thus, the *p450nor* gene could serve as a diagnostic marker for fungal denitrification potential, but the lack of molecular tools targeting *p450nor* currently limits efforts to assess the contribution of fungi to N-cycling. In the present study, a translated alignment of available *p450nor* sequences identified key conserved amino acid residues within P450nor and enabled the design of *p450nor*-specific degenerate primers. We demonstrated the broad utility of these new primers by performing PCR amplification of *p450nor* genes from fungal isolates and environmental DNA obtained from two agricultural soils with distinct physicochemical properties. Metagenomic datasets derived from the same agricultural soils did not reveal the presence of fungal denitrification genes within either soil, emphasizing the value of cultivation-based efforts and the *p450nor*-targeted PCR assays for assessments of fungal contributions to denitrification in complex environmental systems such as soils.

Materials and Methods

Medium preparation

A modified Czapek liquid medium containing nitrate (2 mM) or nitrite (1 mM) (108) was utilized for fungal isolation and cultivation unless noted otherwise. Briefly, ultrapure water (≥18.0 MΩ·cm) (Milli-Q system, Millipore, Billerica, MA) was combined with (in g liter^{-1}) KCl (0.5), K_2SO_4 (0.35), magnesium glycerophosphate (0.5), and $FeCl_2$ (0.01) and the pH was adjusted to 6.8 by adding sodium hydroxide (0.5 M) before the medium was autoclaved.

Fungal enrichment and isolation

Triplicate soil cores were collected in November 2012 from agricultural sites in Havana, IL (latitude 40.296, longitude -89.994) and Urbana, IL (latitude 40.075, longitude -88.242) using a soil corer with a 30 cm depth range. Soil cores were placed in coolers and transported to the University of Illinois, Urbana-Champaign for processing. Soil aliquots (5-10 grams) from the 0-5, 5-20, and 20-30 cm depth ranges were shipped overnight on ice to the University of Tennessee. Soil samples were pooled and homogenized using aseptic technique, and 5 g of soil was added to 30 mL of oxic Czapek medium (pH 6.8) in 60-mL glass serum bottles fitted with black butyl rubber stoppers and incubated at room temperature. Microcosms (n=1 per treatment) were amended with either 2 mM sodium nitrate (NO_3^-) or 1 mM sodium nitrite (NO_2^-) as electron acceptors and either sodium acetate, sodium formate, sodium pyruvate (3 mM each), or an autoclaved, 1.5 % (w/v) milled corn and soybean plant suspension as exogenous substrates. All serum bottles were amended with 30 µg mL^{-1} of chloramphenicol (Fisher Scientific, USA) and 100 µg mL^{-1} streptomycin sulfate (Fisher Scientific, USA) from ethanolic or aqueous stocks, respectively, to inhibit bacterial growth. After 1 month of monitoring N_2O production, soil microcosms were shaken vigorously by hand, and 0.5 mL of homogenized suspension was transferred using a sterile 1-mL plastic syringe fitted with a 19 gauge needle (Becton Dickinson, Franklin Lakes, NJ) to fresh, anoxic medium containing the same carbon and nitrogen

sources as the parent microcosms. Transfer cultures (n = 2 per treatment) received 50 µg mL^{-1} each of kanamycin sulfate (Fisher Scientific, USA) and ampicillin sodium salt (Fisher Scientific, USA) from sterile aqueous stocks to inhibit bacteria that may have possessed natural resistance to the antibiotics added to the initial enrichments. Cultures were then amended with 0.6 ml filter-sterilized air (2% [v/v] headspace volume), and NO_3^-, NO_2^-, and N_2O concentrations were monitored. Following a 2-week incubation period, 2 mL of culture samples were transferred to 25 mL liquid (45°C) agar medium containing the same substrates as the parent cultures. Each tube was gently mixed and its contents poured into individual sterile plastic plates. The plates were incubated in the dark at room temperature and visually inspected each day for fungal growth. After filamentous colonies were observed, approximately 1 cm^2 agar sections containing fungal mycelia were transferred to fresh agar plates. Subsequent transfers (at least three) used 1 cm^2 agar sections of the fungal colony margins to quarter-strength R2A agar (Fisher Scientific, USA) plates containing 100 µg mL^{-1} streptomycin sulfate. Contamination was monitored by microscopic observation and avoided by routine transfer of agar sections containing hyphae of consistent appearance to fresh R2A agar plates containing streptomycin or ampicillin and kanamycin. *Aspergillus terreus* strain NRRL 255 and *Aspergillus flavus* strain NRRL 3357 were obtained from the USDA Agricultural Research Service culture collection (NRRL Collection). Both fungi were grown on quarter-strength R2A agar (Becton Dickinson, Franklin Lakes, NJ) plates amended with 50 µg mL^{-1} streptomycin for tissue collection and DNA extraction (see below).

Analytical procedures

NO_3^- and NO_2^- were measured by ion chromatography with a Dionex 3000 instrument (Dionex, Sunnyvale, CA) as described (177, 178). N_2O was monitored via 1 mL headspace injections into a MicroGC 3000A (Agilent Technologies, Palo Alto, CA) equipped with a polystyrene-divinylbenzene PlotQ column and a thermal conductivity detector. All nitrogen species were quantified using a dilution

series of standards prepared in medium. The instrument limits of detection for NO_2^-, NO_3^- and N_2O were 7, 4, and 3 µmoles, as determined by preparing replicate standards (n = 20) and following established procedures (179).

Denitrification activity of fungal isolates

Fungal isolates were tested for denitrifying potential by transferring individual 1 cm^2 agar sections to 1.5 mL plastic microcentrifuge tubes containing 1 mL of sterile water, followed by brief manual homogenization with sterile steel forceps. Then, 250 µL of the water-agar-mycelium mixture was inoculated into 26-mL Balch tubes containing 15 mL of oxic Czapek medium amended with 5 mM sodium acetate, 2 mM NO_2^-, and 100 µg mL^{-1} streptomycin. The headspace of each Balch tube was monitored over a 12 day period for N_2O production.

DNA extraction

Fungal biomass (~0.3 g wet weight) was placed in a 2-mL screw cap plastic tube containing approximately 200 mg of 0.5 mm silica and zirconium beads (Fisher Scientific, USA) and DNA was extracted following an established procedure (180) (see SM for details). Soil DNA extraction from soil samples (0.5 g of homogenized soil from 0-30 cm depth from Havana and Urbana and a separate 0-5 cm depth Havana sample) was performed using the FastDNA spin kit for soil (MP Biomedicals, Santa Ana, CA) following the manufacturer's protocol. Soil DNA concentration and purity were analyzed with a NanoDrop 2000 spectrophotometer (Thermo Scientific) and a Qubit 2.0 fluorometer (Life Technologies, Carlsbad, CA) using the dsDNA BR Assay Kit following the manufacturer's recommendations (Life Technologies).

Primer design

To design primers targeting *p450nor* gene sequences, primary literature resources and the National Center for Biotechnology Information (NCBI)

database were queried to identify available *p450nor* gene and protein sequences (181). Multiple sequence alignment was used to identify conserved residues, followed by selection of additional sequences by querying public sequence databases (GenBank, UniProt) using BLAST (182). Overall, 38 *p450nor* reference sequences were obtained and aligned using the program T-Coffee (183) followed by manual inspection. PAL2NAL (184) was used to generate a codon-aware nucleotide alignment and conserved sites were selected for forward and reverse primer binding (Table 2.1, Figure 2.1). The *p450nor* sequences of *Aspergillus terreus* strain NIH2624 and *Aspergillus flavus* strain NRRL 3357 were among the 38 sequences used for primer design (Table 2.1), and *p450nor* sequences derived from *Aspergillus terreus* strain NRRL 255 and *Aspergillus flavus* strain NRRL 3357 served as positive controls in all *p450nor*-targeted PCR assays (99, 140). Genomic DNA from the bacterium *D. lykanthroporepellens* strain BLDC-9 (ATCC BAA-1523) was used as a negative control in PCR assays.

PCR conditions

PCR assays using the primer pair *p450nor*394F and *p450nor*809R (Table 2) consisted of 9.125 µL DNase-free water (Life Technologies, Carlsbad, CA), 2.5 µL of 10 mM magnesium chloride solution (Applied Biosystems, CA, USA), 2.5 µL of *Ex Taq* 10X Buffer (Mg^{2+} free) (Clontech Laboratories, Inc., Mountain View, CA), 2.5 µL of 2.5 mM of each dNTP (Clontech), 0.5 µL each of 100 µM primers, 6.25 µL of 200 ng/µL bovine serum albumin (BSA) solution (Fisher Scientific, USA), and 0.125 µL of 5 U/µL TaKaRa *Ex Taq* DNA Polymerase (Clontech), and 1 µL DNA template (approximately 10 to 100 ng/µL) in a total reaction volume of 25 µL.

PCR conditions for *p450nor* amplification from soil DNA samples required a semi-nested approach for consistent results, with initial PCR using primers *p450nor*394F and *p450nor*1008R, followed by a second round of PCR using primers *p450nor*394F and *p450nor*809R. The initial PCR reaction contained the same ingredients as described above, except that 0.8 µL each of 25 µM primers

*p450nor*394F and *p450nor*1008R were utilized in the initial amplification reaction. Then, 1 µL of the amplicon solution was used as template DNA in a second round of PCR with primers *p450nor*394F and *p450nor*809R employing identical PCR reaction conditions as for fungal genomic DNA amplification.

Amplification of fungal *nirK* genes from isolate DNA were performed as previously described using primers nirKfF/nirKfR and fnirK2F/fnirK1R (130, 131) with the following modifications. The duration of the annealing and elongation steps were increased by 15 sec (Wei et al.) or decreased by 15 sec (Long et al.), respectively, to allow simultaneous amplification of similar sized amplicons (~450-500 bp). A total of 35 amplification cycles were performed for both the nirKfF/nirKfR and the fnirK2F/fnirK1R primer sets.

Amplification of the fungal internal transcribed spacer (ITS) was performed using primers ITS4 (185) and EF3RCNL (186). Amplification and sequencing of the nuclear small subunit ribosomal (18S rRNA) gene from fungal isolates utilized 0.5 µL each of 10 µM primers PNS1, NS1, NS3, NS4, NS7, NS8, SR6, NS19b (185, 187, 188) and the PCR conditions described for the *p450nor*394F *and p450nor*1008R primers.

All DNA amplifications were carried out on a Veriti thermal cycler (Life Technologies, Carlsbad, CA) at 95 °C for two minutes and 10 seconds, followed by 35 cycles each of 95 °C for 30 seconds, 47 °C for 45 seconds, and 72 °C for one minute (1.5 minutes for 18S rRNA genes), with a final extension step at 72 °C for seven minutes. For amplification of *p450nor* from soil DNA templates, as well as amplification of isolate ITS regions or isolate 18S rRNA genes, the annealing temperature was increased to 50, 53, or 55 °C, respectively. Annealing temperatures for amplifications with *nirK*-targeted primer pairs nirKfF/nirKfR and fnirK2F/fnirK1R were 54 and 50 °C, respectively (130, 131). For visualization of amplicons, 5 µL of the PCR assay mixture was combined with 1 µL of a loading dye solution (25 mg bromophenol blue and xylene cyanol each, and 4 g sucrose dissolved in 10 mL of ultrapure water) and loaded onto a 1 % ([w/v]) agarose gel,

and electrophoresis was conducted at 90 volts for 1 hour at an initial amperage of 200 mAmps.

Cloning and sequencing

Cloning of the ITS region and *p450nor* amplicons from DNA obtained from isolates and agricultural soil was performed using the TOPO TA cloning kit (Life Technologies, Carlsbad, CA) following manufacturer protocols. Of the 60 amplicons generated from soil DNA, 23 were selected for sequencing based on restriction digest analysis (*HaeIII* digest using NEBuffer 4 solution, New England Biolabs, Ipswitch, MA). Briefly, PCR amplicons (5 µL) were incubated at 37 °C for 12 hours in a 12 µL reaction volume (5.3 µL PCR-grade water, 1.2 µL 10X NEBuffer 4 solution, 0.5 µL *HaeIII*) and fragment patterns analyzed via gel electrophoresis. Cloned amplicons were Sanger sequenced using an ABI Big-Dye v3.1 cycle sequencing mix on an ABI 3130 analyzer (Applied Biosystems) at the University of Tennessee Molecular Biology Resource Facility. Electropherograms of sequenced amplicons were manually inspected using Geneious software (Biomatters Ltd., Auckland, New Zealand) following automatic trimming with a 0.03 error probability limit, and overlapping regions assembled *de novo* after vector sequence removal using the UniVec database within Geneious.

Fungal taxonomy

The script FungalITSPipeline.pl (189) was used to extract ITS1 and ITS2 regions from the cloned ITS sequences of the fungal isolates, and to determine taxonomic affiliations within the International Nucleotide Sequence Database Collaboration (INSDC) (190). The 18S rRNA gene sequences were annotated using the SILVA database and the SINA alignment tool (191, 192).

Metagenomic analysis

Metagenomic reads previously generated from Havana (SRR1152189) and Urbana (SRR1153387) soils (193) were retrieved from NCBI's Sequence Read

Archive and unpacked with the SRA Toolkit (194). SolexaQA++ (195) was used to trim reads with a 0.01 error probability limit (Phred score of 20) followed by discarding reads shorter than 50 nucleotides in length. This procedure resulted in a total of (including paired and single reads) 236,437,515 and 291,298,696 high quality sequences from Havana and Urbana soils, respectively. Fungal presence in the metagenomes was established by nucleotide alignment (BLASTn) against a custom ITS database provided by the FHiTINGS ITS analysis software, followed by analysis of the results with the same software (196). BLASTn alignment of the metagenomic reads against the cloned ITS sequences from the enriched fungal isolates was performed to uncover the presence/absence and relative abundance of isolated fungi within the metagenomes. A similar analysis was performed with cloned *p450nor* sequences, except a translated nucleotide alignment (BLASTx) was used.

P450nor sequence analyses

The 38 reference P450nor sequences were combined with newly obtained *p450nor* sequences from isolates and soil DNA. Following the removal of identical sequences, all sequences were aligned to the UniRef90 database with BLASTp (182, 197). Significant alignments (≥ 70% alignment length and ≥ 30% sequence identity) to eukaryotic sequences were retained for each query sequence, and hits with ≥ 90% identity to P450nor query sequences or uncertain NCBI taxonomy were removed. MAFFT *v7.130b* (198) was used with default parameters to initially align all sequences, followed by manual editing with Jalview and SEA VIEW to retain the region amplified by the primer set *p450nor*394F and *p450nor*809R (199–201). The resulting alignment consisted of 108 taxa with an average length of 153 amino acids (Min: 128, Max: 158). The alignment was analyzed with ProtTest v3.4 (202) to select an optimized evolutionary model for the aligned sequences prior to tree building. Phylogenetic reconstruction was performed using the FastTree 2 *v2.1.7 SSE3* software package (203). Approximate maximum-likelihood tree reconstruction with

FastTree 2 was performed using the Whelan and Goldman (204) amino acid substitution model with gamma distributed rate heterogeneity (discrete distribution with 4 rate categories) and the subtree-pruning-regrafting algorithm. Support for internal nodes was assessed using 5000 replications of the Shimodaira-Hasegawa test performed within FastTree 2. An additional alignment was generated using MAFFT that contained full-length sequences from a subset (n=16) of all the sequences used in phylogenetic reconstruction. This alignment was submitted to the ESPript 3.0 web server (http://espript.ibcp.fr) (205) to visualize key, conserved residues in a diversity of P450nor sequences.

Nucleotide sequence accession numbers

p450nor, ITS, and 18S rRNA gene sequences are available under GenBank accession numbers KM889490-KM889526 and KT714145-KT714154, KM889527-KM889556, and KT714155-KT714191, respectively.

Results

Fungal isolation

Fungal cultivation techniques applied to Havana and Urbana soil-derived transfer cultures produced 214 fungal isolates. Growth experiments in medium containing NO_2^- demonstrated that about two thirds of the isolates (151 out of 214) produced N_2O within a 12-day incubation period (data not shown). Based on gross morphology of mature fungal colonies, the 214 isolates from both the Havana and Urbana soils were divided into 15 groups. Then, thirty distinct isolates (including at least one representative isolate of each morphological group) were selected for further analysis (Figure 2.2). Since each morphological grouping may not align with an underlying isolate genotype, ITS region analysis was performed, which revealed 10 phylogenetically distinct groups, four of which were composed of singleton ITS sequences (Table 2.3). Five additional isolates were later selected for *p450nor* analysis based on consistent morphology with

N_2O-producing isolates in previously assigned groupings, but only 18S rRNA gene identification was performed on these isolates (Table 2.3).

Fungal denitrifier morphology and taxonomy

The majority of the representative fungal isolates were assigned to the genera *Fusarium* (teleomorph *Giberella*, 19 total) and *Trichoderma* (five total) based on ITS and 18S rRNA gene sequence analysis. Microscopic observations of mature fungal colonies corroborated these results and revealed characteristic features of both the *Fusarium* (e.g., banana-shaped, septate ascospores) and *Trichoderma* isolates (e.g., presence of green conidia aggregated into fascicles) (Figure 2.2) (206). Taxonomic prediction based on 18S rRNA gene sequence classification was successful for all but two fungal isolates. ITS sequence analysis identified these two isolates as putative *Trichoderma* sp. and *Fusarium* sp. Morphotyping (e.g., appearance of aerial hyphae with a white, feathery appearance on agar plates) and 18S rRNA gene sequence analysis assigned two additional isolates to the order Mortierellales. Other fungi isolated in this study included members of the genera *Verticillium* (1 isolate), *Humicola* (2), *Chaetomium* (3), *Podospora* (1), *Lecythophora* (1), and *Guehomyces* (1) (Table 2.3), which all belong to fungal lineages known to harbor denitrifying representatives (99).

***p450nor* and *nirK* PCR amplification**

Application of primers *p450nor*394F and *p450nor*809R consistently resulted in a DNA band between 650 and 850 bp in size. Sequencing confirmed the amplification of *p450nor* gene fragments in 23 out of 23 (100%) N_2O-producing fungal isolates (Figure 2.3; Table 2.3). Several non-specific amplicons were consistently observed 100-200 bp below the predicted *p450nor* amplicon size of 536-890 bp (Table 2.5), requiring gel extraction and cloning of the amplicons prior to sequencing. Sequence similarity among non-target amplicons indicated that they originated from a putative ATPase gene and a non-coding genomic region. Nine isolates displayed a *p450nor* amplicon but N_2O was not detected in

liquid culture under the conditions tested (Table 2.3). *nirK* amplification was detected in 17 out of 23 (74%) N_2O-producing fungal isolates using primer set nirKfF/nirKfR. Amplification of both a *p450nor* and *nirK* gene was observed in 20 out of 37 (54%) isolates. There were two instances in which *nirK* was amplified but *p450nor* could not be detected (isolate ID 50 and 141), and in 12 cases *p450nor* was amplified but *nirK* was not detected (Table 2.3). Using primer set fnirK2F/fnirK1R, *nirK* was only detected in three out of 23 (13%) N_2O-producing fungal isolates (Table 2.3).

The nested PCR amplification of soil DNA resulted in the recovery of a total of 23 environmental *p450nor* clone sequences. Pairwise nucleotide and amino acid identities of the 23 environmental *p450nor* sequences ranged from 65.8 to 100% and 63.8 to 100%, respectively. Phylogenetic analysis of the environmental *p450nor* sequences revealed the presence of five distinct soil clades (e.g., Urbana clone groups I, II and Havana clone groups I, II, III; Figure 2.4). The clone groups from both soils were affiliated with sequences of representative Sordariomyetes denitrifiers (e.g., *Fusarium* and *Trichoderma*) and *p450nor* sequences derived from N_2O-producing fungal isolates recovered from these soils (isolate ID 213 and 179; Figure 2.4). Overall, the environmental clone sequences displayed 59-100% amino acid identity with P450nor sequences from fungal isolates derived from the same agricultural soils. The alignment of the amplified region of the *p450nor* genes (approximately 160 amino acids) and P450nor tree reconstruction supported the monophyly of the cloned *p450nor* sequences with previously reported *p450nor* sequences from confirmed fungal denitrifiers (Figure 2.4). The *p450nor* sequences recovered from isolate DNA and soil DNA clustered with *p450nor* sequences from members of the Leotiomycetes (one sequence), Eurotiomycetes (one sequence), and Sordariomycetes (47 sequences), three diverse fungal lineages within the phylum Ascomycota that are known to harbor denitrifying representatives (99).

Soil denitrification activity

Previous investigations have demonstrated that most denitrifying fungal isolates lack the capacity to reduce NO_3^-. Therefore, replicate microcosms received NO_3^- or NO_2^- to assess denitrification activity. N_2O production and visible fungal biomass (i.e., hyphae) were observed in all microcosms (16 total) that received antibiotics to inhibit bacterial growth (Figure 2.5); however, N_2O formation in Havana soil microcosms amended with NO_3^- was low (Figure 2.5, top left). Havana transfer cultures amended with NO_2^- mirrored patterns observed in the NO_2^--amended soil microcosms, but N_2O formation was variable in the transfer cultures that received NO_3^- (Figure 2.6). N_2O concentrations declined in Urbana microcosms after 2 weeks of incubation, whereas N_2O production continued in Havana microcosms (Figure 2.5). A decline in NO_3^- concentration in Urbana transfer cultures was observed, but concomitant formation of N_2O did not occur (Figure 2.6).

Metagenomic analyses

BLAST analysis of the Havana and Urbana metagenomic sequences identified 5,213 and 3,373 unique reads out of 236 and 291 million reads, respectively, that were alignable to fungal ITS database sequences. Fewer than 200 reads from each metagenome aligned to ITS sequences amplified from the representative fungal isolates obtained from the same soil samples. No metagenomic reads aligned to amplified and sequenced *p450nor* (this study) or previously reported *p450nor* sequences.

Discussion

A new means to assess fungal denitrification potential

The *p450nor* sequences identified in this study formed a monophyletic group with reference *p450nor* sequences, and demonstrated the specificity of the degenerate primers for *p450nor* genes in isolate and soil DNA (Figure 2.4). New sequences sharing 54 to 98% amino acid identity to reference *p450nor*

sequences were recovered suggesting the primers allow the recovery of novel sequence diversity within the predicted 536-890 bp sequence region spanned by the conserved primer binding sites (Table 2.5). Phylogenetic analysis of the *p450nor* environmental clones permitted the identification of distinct groups (Havana clone groups I, II, III and Urbana clone group I; Figure 2.4). These data suggest that geochemical differences between Havana and Urbana soils could be driving fungal denitrifier diversity, but additional efforts are needed to conclusively demonstrate to what extent geochemical conditions determine fungal *p450nor* diversity.

Recent investigations into fungal denitrification have relied on PCR primers targeting the fungal *nirK* gene to demonstrate the NO_2^--reducing potential of the fungal community (97, 130). Although a significant advance in our ability to target fungal denitrifiers, *nirK* primer sets targeting the NO_2^--to-NO step do not directly reveal the N_2O-producing potential of the fungal community. The application of the fungal *nirK* gene-targeted primer set fnirK2F/fnirK1R (131) yielded only five positive results whereas primer set nirKfF/nirKfR (130) revealed that many (17 out of 23) of the N_2O-producing fungal isolates possessed *nirK*. Apparently, the latter primer set targets a greater diversity of fungal *nirK*, but still failed to amplify *nirK* genes from 26% of the nitrite-reducing and N_2O-producing fungal isolates. Interestingly, fungal *nirK* amplification was observed in two non-denitrifying isolates (no N_2O production observed), in which *p450nor* was not detected, and *p450nor* amplification occurred in 12 isolates but *nirK* was not detected (Table 2.3). Of these 12 organisms, five were shown to reduce NO_2^- to N_2O. These observations suggest that the characterization of fungal *nirK* sequence space is incomplete, and additional sequence information from denitrifying fungal isolates is desirable. To date, *p450nor* is the sole gene known to encode the N_2O-producing phenotype in fungi (79) and thus represents an ideal target for assessing N_2O formation potential. Due to substantial heterogeneity in available *p450nor* sequences, primer design is challenging (99), and the design of PCR primers that amplify all *p450nor* sequences, while

excluding all other sequences of the p450 gene family, will probably not be possible. Still, the new *p450nor* primers presented here represent a major advance for assessing fungal N_2O production potential.

The variable presence/absence of introns within *p450nor* genes can lead to amplicon size variations and create additional difficulties in identifying *p450nor* amplicons. To assist in identifying a range of expected amplicon sizes, we analyzed the intron structure in *p450nor* sequences from 47 *p450nor*-containing fungal genomes (Figure 2.7; Table 2.5). Overall, predicted *p450nor* amplicons contained between one and four introns and varied in size from 536 to 890 bp. Although introns or other genetic variations may prevent *p450nor* amplification, their presence within a primer binding region was observed in only a single case (*Glarea lozoyensis* strain ATCC 20868, Figure 2.7). The observed intron is more likely due to low transcript coverage observed at the *p450nor* locus in *G. lozoyensis*, since the forward primer site (present in exons of all other fungi examined) was detected within the predicted gene sequence. Primer sequence degeneracy contributes to non-specific amplification, and thus cloning and sequencing was required to confirm *p450nor* amplification. A general limitation of degenerate PCR primers is a diminished binding efficiency leading to uneven amplification of target sequences (Table 2.2). Despite these obstacles, all sequenced amplicons fell in the expected 536-890 bp size range and were identified as *p450nor*. Importantly, primers *p450nor*394F/*p450nor*809R amplified *p450nor* from all N_2O-producing isolates indicating the utility of this approach to target a broad diversity of fungal denitrifiers. In nine instances, *p450nor* was detected but N_2O was not produced by fungal isolates in liquid culture. Amplicon sequencing ruled out false positives, suggesting that the chosen cultivation conditions were not conducive for N_2O production in these isolates.

The semi-nested PCR methodology provides additional confidence to assay for the presence/absence of *p450nor* in soils where fungi may not be abundant at the time of sampling or fungal DNA is underrepresented in soil DNA extracts. Application of the semi-nested PCR approach on a dilution series of

genomic DNA extracted from *A. terreus* strain NRRL 255, *A. flavus* strain NRRL 3357, and *Fusarium graminearum* indicated a 10 to 100-fold increase in sensitivity over the direct (i.e., non-nested) approach. Experiments with dilutions of genomic DNA suggested that the semi-nested PCR approach yielded positive results when at least 3,000 to 24,000 *p450nor* gene copies were present per assay (data not shown). Thus, the non-nested PCR approach may yield false negative results (inability to detect *p450nor* when present), and failure to detect *p450nor* amplicons in isolate or environmental DNA samples should be interpreted accordingly.

Diversity of the denitrifying fungi

It is widely accepted that the majority of soil bacteria cannot be cultivated with conventional methods (207). Although this issue may not be as extensive for fungi, only 2 – 7 % of the estimated 1.5-5.1 million fungal species have been cultivated (208, 209). Furthermore, only a few hundred of the 100,000 documented fungal species have been tested for their ability to produce N_2O from N-oxyanions. Our knowledge of fungi capable of denitrification is constantly expanding, and fungal representatives spanning eight orders and three phyla have now been documented to produce N_2O (97, 99) including a diversity of organisms examined here. Therefore, it is very likely that a far greater diversity of fungi contributing to this process exists in nature than is currently acknowledged.

The enrichment and isolation techniques utilized in the present study resulted in the cultivation of fungal taxa largely representative of currently classified fungal denitrifiers. For example, several members of the genera *Fusarium* and *Trichoderma*, both known to harbor species capable of N_2O production, were cultured (72, 101, 104). Also identified were two *Mortierella* isolates (Mortierellomycotina – formally Zygomycota*)*, a genus which includes members known to produce N_2O (97, 99). Only one of the two *Mortierella* isolates produced N_2O in liquid culture after 12 days of incubation, indicating not all members of the genus may share this phenotype. Several other fungal isolates

possessed highly similar ITS regions (>99% similarity) to known denitrifiers, but not all produced N_2O under the cultivation conditions tested (Table 2.3). Similarly, a recent study demonstrated that only 50 of 113 species in the order *Hypocreales*, many belonging to the same genus (i.e., *Fusarium*), tested positive for N_2O production, suggesting the denitrifying phenotype varies even among closely related fungi (97).

N_2O formation in soil microcosms and enrichments

The Havana and Urbana site microcosms amended with NO_2^- consistently produced N_2O, but N_2O formation from NO_3^- was limited to Urbana soil microcosms. Possible explanations for this observation include a lack of fungal denitrifiers possessing nitrate reductase (*nar*/*nap*) genes, inhibition of fungal nitrate reductase activity by antibiotics intended to inhibit bacterial denitrifiers (210), or the rapid reduction of NO_3^- to ammonium in Havana soils (137). Of note, the N_2O concentration either declined or N_2O was never detected in Urbana microcosms amended with NO_3^- or NO_2^- (Figure 2.5, 2.6), likely because bacterial denitrifiers were not completely inhibited by the addition of antibiotics and consumed available N_2O. In support of this explanation, inoculation of solid medium with suspensions from Urbana soil microcosms resulted in the formation of colonies of presumably antibiotic resistant bacteria. Microscopic observations corroborated bacterial growth on antibiotic-treated solid medium. Incomplete inhibition of all or specific microbial processes is a known weakness of SIRIN analyses and may explain the observed variation in N_2O production between sites (102, 104, 120, 211). The observed variability in NO_3^- reduction is consistent with other studies describing a diversity of fungi that are incapable of reducing NO_3^- to N_2O (70, 98). Interestingly, most sequenced genomes of fungal denitrifiers possess a putative *napA* gene encoding periplasmic nitrate reductase (79), but a detailed understanding of the variation in fungal NO_3^- reduction capacity has yet to be obtained. Overall, the observed production of N_2O in microcosms established with Havana and Urbana soils is in line with the

magnitude and variability observed in other studies, in which antibiotics were employed to probe the fungal contribution to N_2O production (72, 101, 120).

Low sequence depth limits detection of fungal sequences in metagenomes

p450nor was not detected in Havana and Urbana metagenomes, but fungal presence was established by the presence of fungal ITS sequences (~ 5,200 and 3,400 reads, respectively) and alignment of >200 million metagenomic reads to the fungal isolate ITS regions (~200 reads in both metagenomes). The newly designed primer sets amplified *p450nor* genes using soil DNA extracted from the same soil samples used for metagenomics analysis, emphasizing their utility to screen for fungal denitrification potential. In most documented cases, a single *p450nor* gene copy is found per fungal genome, although exceptions have been noted (e.g., three *p450nor* gene copies were detected in *Nectria haematococca*) (Figure 2.4). Not surprisingly, the detection of single copy, protein-encoding genes in metagenomics datasets is more challenging than detecting high copy number ribosomal operons (which includes the fungal ITS region) (212). Hence, current metagenomics approaches may not be optimal for sequence detection from organisms that contribute low DNA amounts (e.g., fungi) or are present in low abundance, and increased sequencing depth of environmental DNA samples is needed to uncover the functional potential of fungi in soils (21, 22, 213).

CHAPTER THREE

DUAL AMPLICON SEQUENCING OF FUNGAL NITRIC OXIDE REDUCTASE (P450NOR) AND INTERNAL TRANSCRIBED SPACER (ITS2) REGION REVEALS FUNCTIONAL, NOT FUNGAL, COMMUNITY STRUCTURE IS CONTROLLED BY SOIL EDAPHICS

Abstract

Gene-targeted, high-throughput amplicon sequencing approaches are gaining traction as tools to investigate microbial functional diversity in a variety of environments. Fungi are increasingly recognized for their contributions to soil N_2O emissions, but culture-dependent techniques are the norm. Although available culture-independent techniques (e.g., PCR) are high-throughput, downstream cloning and sequencing of amplicons are not. Therefore, PCR primers targeting the fungal nitric oxide reductase (*p450nor*) gene were adapted to high-throughput sequencing with the Illumina MiSeq platform on 72 soil samples from two Midwest agricultural soils. Sequencing and analysis of the fungal internal transcribed spacer (ITS2) region was also performed on the same soil samples to monitor diversity patterns in the overall fungal community. Of the 79 closed-reference p450nor OTUs, 69.7 and 64.6 % of all *p450nor* sequences (12,675,480 in total) were classified as fungal isolate or environmental *p450nor* sequences affiliated with these soils. Analysis of fungal ITS2 sequences revealed 4,591 OTUs from both soils, of which 19 OTUs comprised 41.6 % of all fungal ITS2 sequences. ITS2 OTUs classified as members of fungal families known to harbor denitrifying representatives indicates that 2 to 67 % of the fungal community in each sample may be denitrifiers. Site was a significant predictor of fungal *p450nor* and ITS2 community composition, but only location within a transect predicted community composition only for fungal ITS2 sequences. The environmental variables pH and moisture were significant predictors of community composition using *p450nor*, but not ITS2, sequences, which suggest these factors may be related to fungal N_2O emissions *in situ*. Application of *p450nor* PCR primers to a high-throughput Illumina sequencing methodology revealed a wealth of novel fungal sequence diversity and highlighted the importance of several edaphic factors that may affect fungal N_2O emissions in soils. Overall, given the limited representation of fungi in shotgun metagenomic data sets, amplicon sequencing will continue to be the tool of choice to perform large-scale ecological studies exploring fungal diversity and function.

Introduction

Fungi are potentially significant contributors to N_2O production in soils, but current methods to assess the contribution of fungi to N_2O emissions predominantly rely on culture-dependent techniques (i.e., cultivation) to understand fungal denitrifier diversity and function (99). Since fungi possess a variety of diagnostic genes linked to the denitrification process, culture-independent techniques (e.g., polymerase chain reaction combined with high throughout sequencing) should be feasible, but are not routinely employed to investigate fungal denitrification. The current state of culture-independent techniques to investigate fungal denitrification mainly relies on PCR primers targeting the fungal copper-containing nitrite reductase gene (*nirK*, also found in many denitrifying bacteria) (97, 130–132). Recent PCR methodologies have been developed that also target the fungal *p450nor* gene, encoding the sole nitric oxide reductase in fungi linked to N_2O production (103, 129). Several studies exploring the functional diversity of fungal *nirK* in soils have been reported (97, 130–132), but investigation of *p450nor* may be preferable as *nirK* PCR primers may co-amplify bacterial *nirK* (132), and the direct link between P450nor activity and N_2O formation by fungi (81, 214). Although fungi are reported to be significant contributors to N_2O emissions in soil, especially in agricultural soils, data regarding *p450nor*'s presence/absence, relative abundance, and functional diversity in soils are lacking (71, 99, 102). Therefore, previously published *p450nor* PCR primers targeting the broadest diversity of *p450nor* sequences were adapted to a high throughput amplicon sequencing methodology using the Illumina MiSeq (103). Single-end Illumina sequencing of an ~400-900 bp region of the *p450nor* gene and paired-end Illumina sequencing of the fungal internal transcribed spacer (ITS2) region of the nuclear ribosomal RNA operon were performed to compare/contrast fungal functional and overall community composition. Given the previously reported prevalence and potential importance of fungi to N_2O emissions in agricultural soils, *p450nor* and ITS2 amplicon sequencing was performed on DNA extracted from 70 and 72 soil samples,

respectively, across a linear transect from two distinct agricultural soils in the Midwest Cornbelt (Illinois). The overarching hypothesis was that fungal *p450nor* and ITS2 gene diversity would differ within sites (position within a transect), between the two sites, and that community composition would differ among time points. Furthermore, these differences would be relatable to soil physical parameters including moisture and pH.

Materials and Methods

Soil sampling and DNA extraction

Soils were collected in April, June, September and November of 2013 from Havana, IL (latitude 40.296, longitude -89.994) and Urbana, IL (latitude 40.075, longitude -88.242) agricultural field sites and processed as previously described (103). Briefly, three 30 cm depth soil cores were extracted from three centroids along a transect at each site and promptly processed nearby at the University of Illinois at Urbana-Champaign (Figure 3.1). From each soil core, the top 0-5 cm depth layer was homogenized and a 0.5 g aliquot was placed into a sterile, 1.5 mL microcentrifuge tube and stored at -80 °C until further use (n = 72). Corn and soybean were planted at both Havana and Urbana sites on a yearly rotation (i.e., corn in one year and soybean in the next or vice versa). In 2013, the Havana soil was planted with soybean whereas the Urbana site contained corn crops. DNA extraction from soil samples was performed using the FAST Spin DNA kit for soil (MP Biomedicals, LLC, Santa Ana, CA, USA) following the manufacturer guidelines. Following DNA extraction, contaminating soil substances (e.g., humic acids) were removed using the OneStep PCR Inhibitor Removal kit (Zymo Research Corp., Irvine, CA, USA) and DNA quantity determined using the Qubit double stranded DNA broad range assay kit (Thermo Fisher Scientific, Inc., Waltham, MA, USA) following manufacturer's recommendations. Soil moisture was measured gravimetrically and pH using a standard pH probe calibrated to standards of known pH. Air temperature was recorded at each sampling event using an alcohol thermometer.

***p450nor* amplification**

A variable-sized fragment of the *p450nor* gene was amplified as previously described, using the semi-nested approach required to detect this sequence across a range of environmental DNA samples (103). Briefly, the initial PCR amplification required primers *p450nor*394F and *p450nor*1008R, followed by a second round of PCR cycles using primers *p450nor*394F and *p450nor*809R. The initial PCR reaction contained the same ingredients as described (103), except that all DNA samples were diluted to 10 ng/µL and PCR reactions were performed in triplicate 25 µL reaction volumes for the first round of PCR, and triplicate 50 µL reaction volumes for the second PCR amplification. In the first phase of *p450nor* amplification, each reaction contained 8.525 µL DNase-free water (Life Technologies, Carlsbad, CA), 2.5 µL of 10 mM magnesium chloride solution (Applied Biosystems, CA, USA), 2.5 µL of *Ex Taq* 10X Buffer (Mg^{2+} free) (Clontech Laboratories, Inc., Mountain View, CA), 2.5 µL of 2.5 mM of each dNTP (Clontech), 0.8 µL each of 25 µM primers *p450nor*394F and *p450nor*1008R, 6.25 µL of 200 ng/µL bovine serum albumin (BSA) solution (Fisher Scientific, USA), and 0.125 µL of 5 U/µL high fidelity TaKaRa *Ex Taq* DNA Polymerase (Clontech), and 1 µL DNA template (0.4 ng/µL final concentration) in a total reaction volume of 25 µL. In the second amplification reaction, 1 µL of the amplicon solution was used as template DNA in a second round of triplicate, 50 µL PCR reactions with the same composition as above, except ingredient volumes were doubled, and 19.25 µL DNase-free water and 1 µL each of 100 µM primers *p450nor*394F and *p450nor*809R were used in the reactions. DNA amplifications of *p450nor* gene fragments from soil were carried out on a Veriti thermal cycler (Life Technologies, Carlsbad, CA) at 95 °C for two min and 10 s, followed by 35 cycles each of 95 °C for 30 s, 50 °C for 45 s, and 72 °C for one min, with a final extension step at 72 °C for seven min. Thermocycler conditions for the second *p450nor* amplification phase were identical, except that an annealing temperature was lowered to 47 °C. In all, *p450nor* genes were

successfully amplified from 68 (94 %) soil samples, but downstream analysis was only performed on 62 samples at this time.

ITS2 amplification

A modified, two-step PCR approach to barcode tag templates with frameshifting nucleotide primers outlined in Lundberg et al. were employed for amplification of fungal ITS2 rRNA regions (215). Forward and reverse primers (0.5 µM each) were combined in the initial PCR step to maximize phylogenetic coverage of fungi, and included primers ITS3NGS1 (F1-F6), ITS3NGS2-F1, ITS4NGS3-F2, ITS4NGS4-F3, ITS4NGS5-F4, ITS4NGS10-F5, ITS4NGSR(F1-F6), and ARCH-ITS4-F1 (185, 216, Cregger et al., unpublished). Following the initial amplification, PCR products were cleaned with 17 µL of Agencourt AMPure XP beads (Beckman Coulter Inc., Pasadena, CA, USA) and eluted in 21 µL of nuclease-free water. Secondary PCR amplifications contained AMPure cleaned DNA tagged with barcoded reverse primers and forward primers listed above included in a 50 µL reaction using 20 µL of purified DNA from the initial PCR amplification step. Thermal cycler conditions consisted of denaturation at 95 ºC for 45 s followed by 32 cycles of 95 °C for 15 s, annealing at 60 °C for 30 s, and extension at 72 °C for 30 s.

***p450nor* and ITS2 Illumina sequencing library construction**

P450nor PCR reactions were analyzed by agarose gel electrophoresis and positive DNA bands were excised from the gel using a sterile razorblade and purified using the QIAquick gel extraction kit (Qiagen, Venlo, Netherlands) following manufacturer's guidelines. For library construction, P450nor PCR amplicons were ligated to Illumina MiSeq sequencing adapters using the Bioo Scientific NEXTflex Rapid DNA sequencing kit and 96 Nextflex DNA barcodes (Bioo Scientific Corp., Austin, TX, USA) following manufacturer's guidelines. All libraries were individually quantified using the Kapa Sybr Fast qPCR kit (Kapa

Biosystems, Inc., Wilmington, MA, USA) on a ViiA 7 Real-Time PCR system (Thermo Fisher Scientific, Waltham, MA, USA) after ligation, whereas libraries were qualitatively assessed both before and after ligation using an Agilent 2100 Bioanalyzer instrument and Agilent 1000 DNA kit and reagents (Agilent Technologies, Inc., Santa Clara, CA, USA). Illumina MiSeq sequencing was performed using a 17 pM library concentration with 5 % PhiX viral genomic DNA addition recommended by the v3 Illumina MiSeq kit (Illumina, Inc., San Diego, CA, USA). The MiSeq sequencer was run in single read mode for a full 600 cycles (1x600 bp), since most *p450nor* amplicons are too large to assemble with 2X300 bp sequences.

For the ITS2 rRNA region, PCR amplification was followed by pooling replicate DNA amplicons that were then purified with Agencourt AMPure XP beads (beads to DNA, 0.7 to 1 ratio). After purification, each library was analyzed for quality and PCR amplicon size on an Agilent 2100 Bioanalyzer instrument using the Agilent 7500 DNA kit and reagents. Each library was purified and analyzed on the Bioanalyzer 2-3X prior to sequencing (Illumina, San Diego, CA, USA) to only include high quality amplicons. The ITS2 Illumina DNA library (9 pM) included a 15% PhiX addition and was sequenced for 500 (2x250) cycles on the Illumina MiSeq sequencing platform.

p450nor **and ITS2 sequence processing**

p450nor amplicons were processed using Qiime v1.9.1 and FrameBot (217, 218). Briefly, the split_libraries_fastq.py script in Qiime was operated with a minimum phred score cutoff of 20, a 50 % fractional read length value for retaining a read with consecutive high quality bases, and three consecutive low quality bases required prior to trimming a read. FrameBot translates protein coding nucleotide sequences against a reference protein database considering sequencing errors that may cause a frameshift. This feature is ideal for analysis of *p450nor* amplicons, as the region spanned by *p450nor* primers used in the

present study contain intronic regions intervening the exonic regions, which may or may not occur in the same frame. Hence, FrameBot reliably identifies exons in the correct frame in *p450nor* amplicons by performing translated alignments against reference protein sequences. In addition, the 79 P450nor sequences in the reference amino acid database reflect predominant intron-exon structure of high quality *p450nor* genes. FrameBot was operated with a 40 % amino acid identity cutoff, gap opening penalty of -7, and could keep alignments of only the top protein subject in the reference database for each read. In this manner, FrameBot performs a closed-reference operational taxonomic unit (OTU) picking procedure. The generated *p450nor* OTU table was rarified to the smallest sample size of 110,440 sequences. Although closed-reference OTU-picking is sufficient for many applications, additional OTU-picking methods, such as de novo and open-reference, are recommended due to biases in use of a reference OTU library for OTU picking present in a closed-reference OTU methodology (219). Hence, additional preliminary analysis of de novo and open-reference Qiime OTU-picking methodologies was performed using *p450nor* nucleotide sequences, excluding introns, that aligned to a single region of the reference *p450nor* dataset. In this manner, a nucleotide version of closed-reference, open-reference, and de novo OTU-picking was performed using 50, 250 nt length OTUs as references clustered at 95 % identity. Reference OTUs were identified by comparison of within and among group pairwise nucleotide sequence identity of *p450nor* sequences from different genera (*Fusarium*, *Aspergillus*, *Ajellomyces*, etc.), and suggested 95 % nucleotide identity was a reliable cutoff for differentiating *p450nor* sequences at the genus level. Next, an open-reference OTU picking methodology using the 50 OTUs, followed by de novo clustering of the remaining sequences at 95 % nucleotide identity was performed. The final Qiime OTU picking strategy performed was de novo clustering at 95 % nucleotide sequence identity. Due to concern regarding inflated OTUs predicted using de novo clustering with Qiime, de novo clustering (95 % nucleotide identity cutoff) was also performed using the UPARSE pipeline (220).

ITS2 sequences were preprocessed using the PIPITS pipeline for fungal ITS data and subsequent analyses performed in Qiime and the phyloseq package in R (217, 221, 222). Briefly, paired-end reads were joined using PEAR (223), quality filtered using the FASTX toolkit using a phred score cutoff of ≥ 20, ≥ 70 % of read containing a phred score ≥ 20, and reads containing ambiguous base calls discarded (224). Following dereplication (removal of non-unique sequences), PIPITS extracts the ITS2 region using ITSx (225). Prior to de novo OTU picking using a 97 % identity cutoff, the variable length ITS2 sequences were padded with N characters to prevent spurious OTU calling by VSEARCH (a problem previously reported with UPARSE with the USEARCH algorithm for fungal ITS2 data). After OTUs were identified and N characters removed, chimeric OTUs were identified and removed and total reads were mapped to each OTU using VSEARCH, followed by taxonomic assignment using the RDP classifier against the UNITE database version 7.0 (226–228). Prior to diversity analyses, the ITS2 OTU table was rarified to 7,000 sequences per sample.

Statistical analyses

All statistical analyses were conducted in R using phyloseq and components of the VEGAN package therein (222, 229, 230). The non-parametric analysis of similarity (ANOSIM) test was performed in R with 10,000 permutations using the Bray-Curtis distance metric.

Nucleotide sequence accession numbers

All sequences were submitted to the Sequence Read Archive (https://www.ncbi.nlm.nih.gov/sra/) under SRA accessions SRR5435236 - SRR5435242 and BioProject ID PRJNA382352. Data will be released 01-16-2018 or upon publication, whichever occurs first.

Results

p450nor amplicons and OTUs

Illumina sequencing of *p450nor* amplicons from 62 soil samples resulted in the generation of a total of 19,444,409 total reads (601 nt median length), of which 12,675,480 (65.2 %) passed QC with a median length of 374 nt (Table 3.1). Hence, 38.8 % of *p450nor* read lengths were below acceptable quality limits when operating the Illumina MiSeq instrument in single read mode using the v3 MiSeq sequencing kit. A large increase in sequence diversity was observed in the translated region amplified by primers *p450nor394F*/*p450nor809R* (Figure 3.2). In many cases, the new *p450nor* sequences displayed a > 60 % drop in sequence conservation compared to the same amino acid character in the reference sequences. The drop in amino acid conservation is particularly relevant for regions reference positions 15 – 30, 79 – 105, 127 – 132, and 170 – 196 (Figure 3.2). The first region corresponds to a protein-coding region only found in two out of five *Metarhizium p450nor* sequences and is encoded by the amino acid characters RQVTRPVHRFHCLTSPY. All other P450nor sequences have a gap in the amino acid alignment in this region. Nevertheless, *Metarhizium* sequences comprise 1.4 % relative abundance of all environmental *p450nor* sequences, and their alignment contributes to the observed drop in sequence conservation in this region. The regions 79 -105 and 170 - 196 encode ALPIPSH-IIYDILGIPIEDFEYLSGC and PGHIEKLDVVQIAFLLLVAGNATVVSM, respectively, in the reference P450nor sequence of *Aspergillus flavus* strain NRRL 3357 and correspond to two alpha helical regions within the P450nor protein structure.

Using the 79 closed reference OTUs identified in Havana and Urbana soils, 69.7 and 64.6 %, respectively, of all sequences mapped to OTUs belonging to cloned environmental or isolate *p450nor* sequences generated in an earlier sampling of these soils by Higgins et al. (103) (Figure 3.3). For example, the reference *p450nor* OTUs of fungal isolates 67 and 74, both of which are affiliated

with the genus *Fusarium* and were previously isolated from Urbana and Havana soils, were observed to have a combined relative abundance of 34.9 and 26.4 % in DNA extracted from Urbana and Havana soils, respectively (Figure 3.3). *p450nor* OTUs from fungal species not derived from previous cultivation efforts in Havana or Urbana soils possessing a relative abundance of ≥ 2 % were members of the genera *Colletotrichum*, *Fusarium*, *Ajellomyces*, *Trichoderma*, *Paracoccidioides*, *Pseudogymnoascus*, and *Aspergillus* (Table 3.2). A large disparity in relative abundances for some reference OTUs was observed between soils (Figure 3.3, Table 3.2). For example, some OTUs were predominantly detected in Havana soils (clones HC C1 and A7, isolate 213, and *Metarhizium anisopliae*) whereas others dominated in DNA extracted from Urbana soils (clone UC F2, isolates 185 and 112). Overall, most *p450nor* sequences identified from both soils were affiliated with OTUs belonging to fungal class Sordariomycetes.

Preliminary OTU clustering of *p450nor* nucleotide sequences (250 nt length) using Qiime closed-reference, open-reference, and de novo OTU picking strategies resulted in the identification of 18, 16,056, and 98,528 OTUs, respectively. De novo clustering with the UPARSE pipeline resulted in 22,180 OTUs after chimera removal. Additional analyses with nucleotide sequence-based OTUs were not performed due to the requirement of further analysis and retesting to confirm their validity.

ITS2 amplicons and OTUs

Of the 13,262,960 paired-end ITS2 reads generated, 11,659,328 (87.9 %) were joined and of those joined reads only 12,938 (0.1 %) were discarded. Of the 11,646,390 sequences input to ITSx ITS region extractor, 10,827,594 (92.9 %) contained a fungal ITS2 region. Analysis of the ITS2 regions amplified from Havana and Urbana soil DNA with the PIPITS pipeline resulted in the identification of 4,848 OTUs, of which 4,591 (94.6 %) were classified within the kingdom Fungi. Of these fungal ITS2 OTUs, 19 were observed to have a relative

abundance ≥ 1 % and contributed to 41.6 % of all the fungal sequences (Figure 3.4). The two most abundant OTUs (OTU8 and OTU5) were 4.7 and 4.1 % of all ITS2 sequences and belonged to unidentified members of the family Nectriaceae and order Pleosporales (Figure 3.4). When inspecting relative abundance of OTUs within each site individually, some important similarities, as well as differences, became immediately apparent. For instance, the two most abundant OTUs within each site are classified as an unidentified member of the family Nectriaceae (OTU8) and *Talaromyces* sp. NRRL 62997 (OTU3) and are observed to have a relative abundance of 8.2 and 8.6 % within the Urbana and Havana soil DNA, respectively (Figure 3.5). Of note, OTU8 is also the most abundant OTU observed across both soils, and appears to exist predominantly in Urbana soils (0.1 % relative abundance in Havana). The *Talaromyces* OTU3 also exhibited a site specific preference, and was absent (0.001 %) in Havana soil DNA (Figure 3.5). The Havana and Urbana soils shared 8 out of a total of 43 (18.6 %) OTUs with ≥ 1 % relative abundance between both sites. Six of these OTUs could not be classified below the rank of order, the remaining two OTUs were classified to the genera *Fusarium* (OTU13) and *Alternaria* (OTU9). These shared OTUs comprised 20.7 % of the OTU relative abundance observed within the data set.

Overlapping taxonomy between *p450nor* and ITS2

Although one-to-one direct comparison between the OTUs in the two data sets is not possible, the shared taxonomic ranks observed between the *p450nor* and ITS2 community may be indicative of the overall fungal community's capacity for N_2O production. For example, between 2 and 67% of the fungal community in all samples examined may be capable of denitrification based on shared taxonomic affiliation at the rank of family (Figure 3.6). Although the relative abundance of *p450nor* and ITS2 markers overlapped considerably for some families, this was not true for all families (top row, Figure 3.7). For example, the relative abundance of *p450nor* OTUs classified as members of the Nectriaceae within each sample

ranged between 34.1 to 88.5 % (median = 57.7 %), whereas relative abundances of ITS2 OTUs classified as members of the Nectriaceae were between 0.45 and 65.5 % (median = 5.85 %). In contrast, *p450nor* and ITS2 OTUs classified as members of the family Chaetomiaceae had median relative abundances of 0.87 and 0.98 % and ranged from 0.05 – 16.6 % and 0.09 – 18.1 %, respectively (bottom row, Figure 3.7).

Spatial and environmental controls on fungal community composition

Non metric multidimensional scaling (NMDS) ordination performed on *p450nor* and ITS2 OTU tables resulted in two punctate distributions that appeared to align well with soil of origin (Figure 3.8). Indeed, site was a significant predictor of fungal *p450nor* (ANOSIM R = 0.62, p = 0.001) and ITS2 (ANOSIM R = 0.82, p = 0.001) community composition (Figure 3.8). However, location along a transect within each field site was not a significant predictor for the *p450nor* community ($p > 0.05$, data not shown). In contrast, location within a site was a significant predictor of the overall fungal community in Havana (ANOSIM R = 0.07, p = 0.001) and Urbana (ANOSIM R = 0.26, p = 0.001), but the trend was more apparent at centroids within the Urbana soil (Figure 3.9). Analysis of diversity among seasons within a site revealed no significant relationships among these two variables for both *p450nor* and ITS2 data ($p > 0.05$, data not shown). Furthermore, there was no significant relationship between soil pH and moisture on the overall fungal community NMDS ordination values (ITS2) (Figure 3.10A). However, a significant negative (Adjusted R^2 = 0.63, p = 6.1 E-15, slope = -0.17) and positive relationship (Adjusted R^2 = 0.36, p = 1.8 E-7, slope = 0.02) of soil pH and moisture, respectively, on values from the first axis of the NMDS ordination from the *p450nor* community NMDS ordination was observed (Figure 3.10B).

Discussion

High-throughput sequencing enables detection of novel *p450nor* diversity

Adapting the degenerate *p450nor* primers *p450nor394F* and *p450nor809R* to a high-throughput sequencing methodology on the Illumina MiSeq platform is a significant advancement for investigations of the fungal contributions to N_2O emissions. For example, the high-throughput Illumina sequencing developed here resulted in the generation of >12 million *p450nor* sequences, whereas initial efforts with sequencing and cloning and months of effort reported in Chapter Two resulted in only 49 sequences (103). Given the recent identification of a large diversity of fungi capable of denitrification and their demonstrated contributions to N_2O emissions in soil, fast and reliable, culture-independent methodologies will enable new insights into the fungal contribution to denitrification (97, 99).

Although millions of sequences were generated using the Illumina MiSeq platform, the closed-reference OTU picking methodology used in the present study is limiting because OTUs are defined *a priori* and may not be representative of environmental sequence diversity (218). However, closed-reference OTU picking is useful for removing co-amplified, non-target sequences present in the data set and can represent a first-pass analysis to determine a baseline of diversity of sequences present in a sample or samples. Although only 79 P450nor amino acid sequences were used for close-reference OTU picking with FrameBot, these OTUs are representative of the dominant N_2O-producing fungal genera currently known (99). Nevertheless, sequence databases and culture collections will likely never represent the actual diversity present in the environment. Therefore, attempts at additional OTU-calling using *p450nor* nucleotide sequences was performed, and resulted in a much larger than anticipated number of OTUs. For example, the de novo OTU picking in Qiime resulted in ~100,000 OTUs, a much larger number than the 79 OTUs used for closed-reference OTU picking with FrameBot. Qiime's clustering methodology has been suggested to over inflate the number of OTUs (220), and the ~16,000

and ~22,000 OTUs predicted by open-reference and de novo OTU picking in Qiime and UPARSE, respectively, are much more similar to one another. Hence, there appears to be a large discrepancy in the number of OTUs determined using different methodologies. Another factor potentially contributing to the large number of *p450nor* OTUs predicted with Qiime and UPARSE are biases propagated during amplification. More than one round of PCR amplification is required to generate sufficient quantities of *p450nor* amplicon for Illumina sequencing library preparation. This is due to presence of inhibitors, high degeneracy of the *p450nor* primers *p450nor394F*/*p450nor809R*, and the low number of *p450nor* copies present compared to the overall soil metagenome content. Due to the large number of amplification cycles (70 in this two round procedure), DNA polymerase-induced mutations and template-switching both bias the result and lead to an inflated number of OTUs when examining P450nor diversity (231–234). Additionally, the 95 % nucleotide identity used may be inappropriate for identifying species-level OTUs for functional genes broadly across the tree and additional representatives and phylogenetic methods should be explored (e.g., aligning reads to a well curated phylogeny) (235).

Overall, we observed a strong overlap in taxonomic assignments of OTUs between *p450nor* and ITS2 (Figure 3.7), suggesting that both methods are complementary. However, caution in interpreting these comparisons is required since both methods use different primers and target different gene regions. The sum of the median relative abundances of OTUs belonging to fungal lineages known to contain fungal denitirifers is 10.02 %, suggesting denitrifying fungi may be a significant fraction of the overall fungal community. Although not every member of a taxonomic group will share the same function, the presence of specific taxa can be indicative of functional potential and has led to the development of key tools to predict function from presence/absence in the overall community (Langille et al. 2013, PICRUSt tool). Overlap in taxonomic assignments of *p450nor* and ITS2 OTUs in the same samples is further support that these methodologies, though not directly comparable, may be able to inform

one another. Future studies addressing the application of multiple primer sets in concert to amplify DNA from communities of known composition may help identify strengths and limitations of the current approach.

Contrasting spatial, pH, and moisture effects on the overall phylogenetically defined community versus functionally defined fungal communities

Previous investigations of soil fungal communities have observed a weak or absent effect of soil pH on fungal diversity, and may be related to the ability of fungi to remain active under a wide range of pH conditions (6, 236). Hence, a lack of an observed relationship between the NMDS ordination (representing the fungal community) and pH was not surprising. Annual precipitation has been demonstrated to have an effect on fungal diversity and GHG emissions, and more diverse fungal communities are present under low precipitation conditions (237). Although moisture and pH vary among sites and within months at a site (Figure 3.11), no significant relationship between the NMDS ordination and these variables was observed. In contrast, both pH and moisture were observed to be significant predictors of *p450nor* community structure, and suggests that these soil properties may regulate the relative abundance of fungal community members containing *p450nor*. Additional research should be conducted to explore the expressed fungal rRNA and p450nor mRNA in soil, as significant differences in relative abundance of active community members have been observed (e.g., high relative DNA abundance ≠ high rRNA or mRNA abundance), and future efforts should compare both molecules for at least a few samples when drawing conclusions about the effects of independent variables on community composition.

Culture-dependent approaches complement amplicon sequencing studies

Based on a best hit, reference-based OTU-calling strategy, the most abundant OTUs were those previously amplified directly from Havana or Urbana soil or

from isolates enriched at these sites (Figure 3.3). Although other members of the reference data set not affiliated with Havana or Urbana clones or isolate *p450nor* sequences were detected, two-thirds of the sequences mapped to reference sequences originally isolated from these soils. This observation highlights the power of using both culture-dependent and –independent approaches to studying function within a community. Without reference sequences derived from the soils under investigation, it is possible that much fewer sequences would have aligned to the reference OTUs or that community composition of *p450nor* could become compromised. Furthermore, the identification of abundant reference OTUs belonging to fungal isolates indicate that these isolates may be representative of the overall site soil environments. These isolates may therefore prove to be invaluable for testing hypotheses regarding factors affecting N_2O emissions by P450nor in a laboratory setting and extrapolating results to the field.

High-throughput amplicon sequencing outcompetes shotgun metagenomics for environmental analysis of fungi

High-throughput sequencing studies using shotgun metagenomics has become a routine method for analysis of the microbial community in a variety of environments (193, 213, 238, 239). However, recent gene-targeted sequencing approaches have been increasing in favor, largely due to a lack of signal from specific functional genes of interest in shotgun metagenomic studies (232, 240, 241). This is particularly relevant for fungi, as they often constitute a low proportion of shotgun metagenome sequence reads, and are largely absent from shotgun metagenomes generated from DNA extracted from Havana and Urbana soils (103). Indeed, one report of fungi dominating a shotgun metagenome generated using environmental DNA is from a low species diversity acid mine drainage (135), and is not representative of most environments. We are unable to detect the *p450nor* gene in shotgun metagenomes generated from these soils, but amplification using *p450nor*-targeted PCR primers allows their identification and analysis. Therefore amplification-based methodologies utilizing high-

throughput technologies will continue to be advantageous for investigations of fungal communities and functions over large spatial scales.

CHAPTER FOUR

PHYLOGENOMIC ANALYSES REVEAL WIDESPREAD HORIZONTAL GENE TRANSFER OF THE FUNGAL NITRIC OXIDE REDUCTASE (P450NOR) AND SUPPORT AN UNDISCOVERED ROLE FOR P450NOR IN SECONDARY METABOLISM

Abstract

An expanding body of scientific literature recognizes fungi as significant contributors to soil nitrous oxide (N_2O) emissions by way of a unique fungal nitric oxide reductase (P450nor); however, uncertainty in fungal contributions to soil N_2O emissions remain due to continued use of biased bacterial inhibitor assays, and observations of both low rates and high variability in N_2O formation by fungal isolates grown on inorganic N sources. To reconcile these rather conflicting observations and provide a benchmark phylogenomic analysis of fungal denitrifiers, we sought to survey the genes underlying fungal denitrification in >700 fungal genomes. Of 167 *p450nor*–containing fungal genomes identified, 0, 18, and 29 % also harbored *narG*, *napA* or *nirK*, respectively, additional diagnostic markers of denitrification potential. The low co-occurrence observed between these traits demonstrates a strong disconnect between *p450nor* presence/absence and additional markers required for true denitrification. Ancestral state reconstruction supported the monophyly of *p450nor* and actinobacterial P450s involved in secondary metabolism (SM), but studies investigating additional roles for fungal *p450nor* are lacking. SM cluster analysis of genomic regions containing *p450nor* with antiSMASH predicted 19 (11%) regions to be putative SM clusters. Moreover, 59 (35%) genomes harbor hallmark SM genes adjacent to *p450nor*, and provides additional contextual evidence linking *p450nor* to SM. These diverse, *p450nor*-containing gene clusters are widespread among the Ascomycota and challenges the existing paradigm of *p450nor's* primary function in nitric oxide reduction and fungi's reported importance in soil N_2O emissions.

Introduction

Increased human reliance on fixed nitrogen (N) fertilizers derived from the Haber-Bosch process to meet the agricultural demands of an expanding global population has greatly contributed to a 20 % rise in the atmospheric quantity of the potent greenhouse gas, nitrous oxide (N_2O), over the last half-century (38, 242). N_2O is primarily formed in soil by denitrifying members of the *Bacteria* and *Archaea* (40), a prevailing view that has been recently challenged by experiments reporting abundant, soil-inhabiting fungi may contribute from 40 to 95% of total soil N_2O emissions (99). Notably, fungi are touted as significant sources of N_2O emissions from agroecosystems (72, 102), which are landscapes expected to contribute up to two-thirds of the total N_2O emissions by 2030 (44). N_2O formation in fungi is catalyzed by P450nor, a heme-containing cytochrome P450 (hereafter P450), that catalyzes the two electron reduction of nitric oxide (NO) to N_2O (81, 149, 243). The *p450nor* gene is found exclusively in fungi and green algae, and has been exploited as a distinctive biomarker in molecular assays to identify and quantify fungal denitrifiers in soil (103, 129, 244).

Despite these observations, fungal contributions to N_2O emissions remain uncertain. For example, investigations using pure cultures of fungal denitrifiers have demonstrated a poor mass balance between inorganic N inputs and the quantities of N_2O formed, and display roughly three to six orders of magnitude lower N_2O production rates compared to denitrifying bacterial isolates (70, 96, 98, 99). Furthermore, no direct evidence links N respiration in fungal isolates to increases in fungal biomass under strictly anoxic conditions (140, 145). Likewise, no significant relationship between fungal biomass and potential denitrification rates were observed in soil incubations under anoxic conditions (118). Above all, the biases associated with soil respiration inhibition studies have not been appropriately corrected or accounted for in investigations of fungal denitrification, and may substantially inflate contributions of fungi to soil N_2O emissions (115, 160). Therefore, these observations led us to question whether there might exist

some alternative explanation for the presence and function of denitrifying traits in fungi.

Biochemical and cultivation-based studies have provided a framework for ongoing investigations of the microbial contributions to N_2O formation in the environment, but significant cost reductions and innovations in sequencing technologies have enabled the generation of (meta)genomic data sets that provide unique opportunities to study the diversity, evolution, and function of genes encoding key N cycling processes (62, 193, 245, 246). The scientific community has benefitted greatly from such studies, but to our knowledge no extensive bioinformatic analyses have been undertaken to explore the genetic determinants of fungal N_2O production. Due in large part to the efforts of the 1,000 Fungal Genomes and Assembling the Fungal Tree of Life (AFTOL) projects, there has been a steady rise in genomic sequence data for members of the fungal kingdom (128, 247). Hence, large scale phylogenomic analyses have the potential to uncover the genomic and evolutionary context of genetic components of fungal N cycling that can ultimately inform the scientific community and assist in directing research efforts. Here we present a survey of key denitrification components present in hundreds of fungal genomes and critically explore the evolutionary origins of P450nor, the only known P450 directly involved in N_2O formation.

Fungi containing *p450nor* may also harbor other genes involved in denitrification, including the copper containing nitrite reductase gene (*nirK*), which is reported to possess an alphaproteobacterial origin in fungi consistent with endosymbiotic theory (77, 79). Furthermore, genes encoding membrane bound or periplasmic nitrate reductases (*narG*, *napA*) have been observed in Fungi (79), but their evolutionary origins and distribution within the Kingdom Fungi have not been examined. Although *p450nor* is touted as belonging solely to eukaryotic microorganisms, previous investigations have hypothesized an actinobacterial origin for *p450nor* (79, 248–250). Of note, *Actinobacteria* are not widely recognized as canonical denitrifying bacteria and few studies of their

denitrification capacity exist (55, 92, 251). Most members of the *Actinobacteria* possess a truncated denitrification pathway or lack a canonical nitric oxide reductase gene (*nor*) (except members of *Corynebacterium* and *Propionibacterium*) (92, 252). Hence, both members of the Fungi and *Actinobacteria* share a reduced or incomplete denitrification pathway with a potentially limited capacity to perform denitrification. Consistent with the horizontal gene transfer (HGT) hypothesis of *p450nor* is the observation of shared amino acid similarity between fungal P450nor and actinobacterial P450s of the CYP105 family, many of which are actively investigated for their contributions to secondary metabolism (SM) (79, 253). For example, *Streptomyces turgidiscabies* strain Car8 harbors a *txtE* gene encoding a novel member of the CYP107 family (closely related to the CYP105 family) (254). Binding of NO and O_2 by TxtE results in nitration of L-tryptophan, which is subsequently converted to the potent plant cellulose synthase inhibitor, thaxtomin A. TxtE is also the only other P450 observed to directly utilize NO as a substrate (254, 255). Furthermore, P450nor and TxtE are evolutionarily distinct from bacterial *nor* and the possibility of P450nor possessing a role in nitration reactions in fungal SM has not been explored. Horizontal gene transfer (HGT) between Fungi and *Actinobacteria* has been reported for other SM traits, such as the type I polyketide synthase genes (256), and begs the question: if *p450nor* was acquired by HGT from *Actinobacteria*, is it now involved in SM or denitrification? The present hypothesis suggests that *p450nor* was acquired from *Actinobacteria* and evolved to fill a novel role in denitrification (79, 249). A more parsimonious explanation is that *p450nor* retained its ancestral function in SM (nitration reactions), and is now a widely conserved trait being selected for in fungi. However, critical experimental and phylogenomic analyses of the evolutionary origins of *p450nor* and its functions are lacking to support this hypothesis.

In the present study, a evidence supporting a role for *p450nor* in secondary metabolism is presented suggesting that N_2O formation in fungi and

Actinobacteria lacking the canonical bacterial *nor* may be incidental. Of note, widespread HGT of *p450nor* was observed between and within fungal phyla that emphasizes a greater mobility of this trait compared to other denitrification genes in fungi. Ancestral state reconstruction analysis definitively supported the affiliation of P450nor with a diverse clade of P450s involved in SM. Genomic surveys of regions immediately surrounding *p450nor* revealed many diagnostic SM genes encoding functions such as polyketide synthases, non-ribosomal peptide synthases, and terpene cyclases; many of which were also corroborated by biosynthetic gene cluster prediction tools. Taken together, these results support the more parsimonious hypothesis of a biological role for P450nor in SM rather than N_2O production. Such findings could have significant implications for both applied and environmental microbiology, since the prediction of novel fungal SM clusters could directly benefit pharmaceutical and agricultural industries and our understanding of fungal ecology as a whole.

Materials and Methods

Fungal genome acquisition

Available draft and complete fungal genomes from the National Center for Biotechnology Information and the Joint Genome Institute (JGI) were accessed on March 16th, 2016 and downloaded from the respective database utilities. In all, 712 fungal genomes were queried, and only 45 fungal genomes (identified to contain *p450nor*) from JGI were used to circumvent disclosure issues.

Comparative bionformatic analysis

The database of 1438 amino acid sequences of fungal single copy orthologs from the BUSCO tool v1.1b (257) were provided as queries to the tool genblastG search tool v1.0.138 (258) to search for and identify homologous gene models of these single copy orthologs in the genomes under investigation. The genblastG tool performs amino acid alignment of a protein query against a six frame

translated nucleotide subject sequence (genome) to find optimal alignment. Once found, genblastg performs heuristic analysis to piece the appropriate gene model back together from high-scoring segment pairs identified using blast alignment. Of these gene models identified, 238 were used for phylogenetic tree reconstruction (see below) and were annotated using the PfamScan (259, 260) against the Pfam A database (261) and blastp (182) against the uniprot database (262) with default settings. The genblastG tool was also used to perform amino acid alignment of protein sequences involved in denitrification or NO detoxification (NapA, NarG, NirK/NirS, NorB, P450nor, NosZ, and flavohemoglobins (263)). Fungal denitrification proteins used in downstream phylogenetic analysis genomes were manually curated against full length fungal reference sequences to ensure that an accurate gene model was predicted for each organism in which the gene was detected. After identification of these genes in fungal genomes, queries of the fungal NapA, NirK, NarG, and P450nor amino acid sequences, were performed against the plant, archaea, bacteria, protozoa, and fungi RefSeq protein databases (264) to identify similar sequences in each taxonomic group. Significant alignments (≥ 60 % query coverage and ≥ 35 % amino acid identity) were combined with the fungal sequences and saved for further phylogenetic analysis.

Analysis of SM gene clusters in fungi

Fungal gene clusters were identified with the antiSMASH tool (265) with default settings. Additional genes +/- 20 genes up and downstream of p450nor were evaluated using PfamScan (259) searches with default settings against the SM profile Hidden Markov Models of antiSMASH. Protein sequences matching antiSMASH HMM models were given an “automatic” SM function status and were colored blue. Additional function annotation was performed by hmmscan searches with HMMER3 against the eggNOG (266) database of orthologous protein groups to derive functional annotations for these proteins. These annotations were manually identified as being putatively involved in SM if they

possessed literature entries suggesting an involvement in SM or had functions related to methyl transfer, oxidation-reduction reactions, glycosyl transferases, fungal specific transcription factors, and other protein functions that may be important for SM (265). These annotations were colored light blue. All other annotations were colored grey since there was no obvious connection to SM.

Phylogenetic analysis

Phylogenetic reconstruction of the fungal species tree was performed using concatenated amino acid sequences from 238 single copy orthologs found in ≥ 90 % of all genomes used in the analysis. The genomes of *Melampsora pinitorqua* strain Mpini7, *Puccinia arachidis*, and *Microbotryum_lychnidis-dioicae* strain p1A1 Lamole were excluded from analysis due to an insufficient number of informative sites and inconsistent placement within the fungal tree. Alignment of amino acid sequences was performed individually on all 238 individual BUSCO gene models present within each organism was performed using MAFFT v7.130b (198) with linsi alignment tuning parameters within the software (--maxiterate 1000 and –localpair settings used). Individual alignments were subsequently concatenated using in-house python scripts, resulting in a 65,897 column alignment which was subjected to phylogenetic analyses with FastTree2 (203) using refined tree reconstruction settings for slower, more exhaustive search of the tree space than default settings (-bionj –slow –gamma –spr 4 –lg –mlacc 2 and –slownni settings). Individual trees from each BUSCO alignment were also constructed using FastTree2, and the resultant alignments and trees subjected to coalescent tree reconstruction using ASTRAL-II software (267).

The predicted amino acid and nucleotide sequences (introns removed) of fungal *napA*, *nirK*, and *p450nor* gene models were aligned using the MAFFT settings described above. The resulting alignment was subjected to further manual refinement in JalView and SeaView software (200, 201). Maximum-likelihood (ML) and Bayesian phylogenetic inference was performed on both nucleotide and amino acid alignments using RAxML and MrBayes 3.2 (268, 269).

Selection of the optimal evolutionary model for ML tree reconstruction was performed using prottest (270) (amino acid alignment) and jmodeltest (271) (nucleotide alignment) software prior to ML tree reconstruction. Optimal evolutionary models for amino acid alignment in Bayesian analysis were estimated from the alignment using MrBayes software. Briefly, the alignment was provided to MrBayes, and the software allowed to run using a mixed amino acid model with 4 chains. The analysis was performed for 1,000,000 generations with sampling performed everything 1,000th generation and the resulting output evaluated with the sump command. For all amino acid ML analyses, either the LG (272) (NapA, p450nor) or JTT (273) models (NirK) were chosen, whereas for nucleotide sequences, the GTR (274) model with variation in rate heterogeneity among sites was chosen as the optimal evolutionary model for each gene. Amino acid models identified in MrBayes were the WAG (204) (NapA and P450nor) or the JTT model (NirK). As with ML tree reconstruction of nucleotide sequences, the GTR model with rate heterogeneity among sites was also used for Bayesian tree reconstruction. For phylogenetic analysis of fungal NapA, NirK, and P450nor with additional RefSeq protein sequences, the LG (ML) or WAG (Bayesian) were selected in the respective phylogenetic software. All amino acid tree reconstruction utilized gamma distributed rate heterogeneity among sites, and additional tree reconstruction parameters were estimated from the alignment.

Phylogenetic analysis with RAxML was performed by sampling 20 starting trees and performing 1,000 replicate bootstrap analyses. The tree with the best likelihood score was compared to the 1,000 replicates in RAxML to generate the final tree. Bayesian tree construction was performed using 3 independent runs with 6 chains for 5,000,000 generations. Output from MrBayes was evaluated with the sump and sumt commands within the software to ensure Markov Chain Monte Carlo chain mixing and convergence (potential scale reduction factor of 1.0) and standard deviation of split frequencies ~ 0.01 or lower. MrBayes output was also visualized in the program Tracer to ensure convergence was reached.

BayesTraits software was used to perform phylogenetically informed correlations between binary traits (i.e., the presence or absence of two denitrification markers) and ancestral state reconstruction (275). For trait correlations, 800 ML trees produced using FastTree2 on 800 amino acid bootstrapped alignments of the 709 fungal taxa was used as input. An additional file containing presence/absence data for each denitrification trait was also used as input. BayesTraits was first operated in ML mode (100 ML tries setting) to generate parameter estimates for dependent (trait correlation) and independent (no trait correlation) models. These parameter estimates were then input to BayesTraits, and three independent runs of the software in Bayesian mode using the dependent and independent model of trait correlation between the two traits being compared were started. The runs were performed for 1,000,000 generations with samples taken every 1,000th generation and a burn-in of 50,000 generations. A stepping stone analysis (100 stones, 10,000 samples) was performed to generate log marginal likelihood values used in for Bayes factor (BF) calculations to test which model (correlation or no correlation) fits the data best. BFs are comparable to a likelihood ratio test for model selection, and the larger the Bayes Factor the more certainty there is in the more complex, dependent model (indicating trait correlation) fitting the data. Hence, a BF of 1 is weak or no favor of trait correlation, but a BF of 10 indicates strong selection of the dependent model and trait correlation. A similar analysis is performed for ancestral state reconstruction, except that 1,875 p450nor trees from a Bayesian analysis was used as input to the MultiState method of the software. MultiState analyses were run for 5,500,000 generations with sampling every 2,000th generation and a burn-in of 500,000 generations. The probability of a given character state at a node within the tree was averaged over all generations after the burn-in period and used to determine support for the state of a tree node.

Approximately unbiased (AU) tests were performed in the program CONSEL (276) using default settings to test the hypothesis of monophyly of specific clades within the phylogeny. The negative log likelihood values from of

the observed nucleotide gene phylogenies input into CONSEL were -140,261, -37,782, -111,531 for *napA*, *nirK* and *p450nor*, respectively. The observed negative log likelihood scores for amino acid phylogenies of NapA, NirK, and P450nor were -65,158, -14,197, and -44,171, respectively. Species-tree gene-tree reconciliation with NOTUNG (277, 278) was performed with a duplication cost of 2, loss cost of 1, and a variable transfer cost from 3 to 15. All other settings were default. NOTUNG ignores incomplete lineage sorting as an evolutionary mechanism when both a rooted species and gene tree are used as input, and hence only provides estimations of gene duplication, loss, and transfer events.

TxtE enzyme expression, purification, and assay

To test for N_2O production by a P450 related to *p450nor* but known to have a primary role in SM, a pET28b(+) plasmid containing a kanamycin resistance marker and the *txtE* gene from *Streptomyces scabies* strain 87-22 was obtained. The *txtE* gene, encoding a CYP105 family nitrating P450 monoxygenase, previously codon optimized for expression in *Escherichia coli* was graciously provided by Dr. Frances H. Arnold and was subsequently transformed into BL21 *E. coli* cells (255). Expression of *txtE* was performed as previously described (255). Briefly, BL21 *E. coli* transformed with pET28b(+) containing *txtE* or pET28b(+) without *txtE* (hereafter *txtE*+ and *txtE*-) were grown in a 37 °C incubator overnight in 100 mL terrific broth (Merck Millipore, Billerica, MA, USA) containing 50 µg/mL kanamycin sulfate (Sigma-Aldrich, St. Louis, MO, USA) with shaking at 225 rpm. Cells of *txtE*+ and *txtE*- (5 % inoculum) were then added to Hyper broth (AthenaES, Baltimore, MD, USA) containing 50 µg/mL kanamycin sulfate and 5 % (v/v) of glucose nutrient mix (AthenaES) and were placed into a 37 °C incubator with shaking at 225 rpm for four h. The *txtE*+ and *txtE*- cultures were then removed from the incubator and allowed to rest at room temperature for 1 h with shaking at 225 rpm. Each culture was then chemically induced with 0.5 mM isopropyl β-D-1-thiogalactopyranoside (IPTG, Sigma-Aldrich) and 0.25

mM 5-α-levulinic acid (Sigma-Aldrich) was added as a precursor for heme production, an essential cofactor in the TxtE enzyme. After induction, cultures were placed on a room temperature shaker at 220 rpm for 24 h. After this time, 50 mL *txtE*+ and *txtE*- cell aliquots were transferred into 50 mL sterile falcon tubes and centrifuged at 4,000 g and 4 °C for 10 min. Cell pellets were stored at -80 °C until further use.

Prior to cell lysis, the *txtE*+ and *txtE*- cells pellets were placed on ice to thaw, and resuspended in 5 mL of 25 mM Tris buffer, pH 8.0 by vortexing. Cell resuspensions were centrifuged at 4,000 g for 10 min at 4 °C, the supernatant removed, and an additional 5 mL of Tris buffer was used to resuspend cells a second time. The *txtE*+ and *txtE*- cell suspensions were then transferred to a sterile, 25 mL borosilicate glass tube and cells were lysed by sonication in an ice water bath using a Branson sonifier (Emerson Industrial Automation, St. Louis, MO, USA) instrument with five rounds of 30 sec sonication, and 30 sec rest on ice between sonication. During operation, the sonifier was set to a power setting of 2 and constant duty cycle for the 30 sec sonication period. Following sonication, 1.5 mL aliquots of *txtE*+ and *txtE*- cells aliquots were transferred to prechilled 1.5 mL microcentrifuge tubes and centrifuged at 20,817 g for 25 min at 4 °C to clarify the cell lysate.

The TxtE enzyme was purified at room temperature from clarified cell lysate using immobilized metal ion affinity chromatography on the AKTA Prime fast protein liquid chromatography system (GE Healthcare, Little Chalfont, UK) equipped with a 1 mL column volume HisTrap HP column cartridge (GE Healthcare). Cell lysate from *txtE*+ and *txtE*- cells was loaded into a 5 mL injection loop and injected onto the instrument at 1.0 mL/min for 6 column volumes using binding buffer A (25 mM Tris HCl, 100 mM NaCl, 30 mM imidazole). Then, a linear gradient of elution buffer B (25 mM Tris HCl, 100 mM NaCl, 300 mM imidazole) was added over 20 column volumes at 1 mL/min until 100 % concentration of buffer B was reached. After 52 minutes, 100 % buffer A was loaded for another 8 column volumes and resulted in a 60 min total run time.

Eluted buffer fractions containing protein were collected in nonsterile plastic tubes and placed on ice immediately following elution from the AKTA Prime system. Fractions were monitored by UV absorption spectrophotometry at 280 nm wavelength on PrimeView software. Fractions expected to contain eluted TxtE proteins were also monitored by absorption at 417 nm wavelength using a Beckman spectrophotometer. All fractions containing ≥20 % maximal absorbance at 417 nm were pooled (usually 8 mL total) and buffer exchanged with 25 mM Tris buffer, pH 8.0 on a 30 kDa MWCO filter (Merck Millipore) following manufacturer guidelines. Purified TxtE (100 µL aliquots) was stored at -80 °C until use. Purified TxtE was quantified using the Bradford assay (Bio-Rad Laboratories, Inc., Hercules, CA, USA) following manufacturer's protocols and measuring TxtE absorbance at 417 nm and a molar absorptivity value of 91,000 M^{-1} cm^{-1} (255, 279).

The successful purification of the TxtE protein was also confirmed by polyacrylamide gel electrophoresis using a Mini Protean 3 gel cassette assembly and voltage source and 12 % acrylamide Protean pre-cast gels (Bio-Rad Laboratories, Inc., Hercules, CA, USA). The 10 – 250 kDa Precision Protein Plus Kaleidoscope prestained protein standards (Bio-Rad) were used to evaluate purified protein mass. Briefly, the acrylamide gel was loaded into the gel cassette system and a 1 X concentration of running buffer (Tris/Glycine/SDS, Bio-Rad) was added to the cassette container. Then, 1:1 mixture of protein sample (as well as standards) to laemmli sample buffer (Bio-Rad) was combined and added into a lane of the Protean pre-cast gel. The voltage source was connected and electrophoresis carried out at 200 V for 45 min. After the run, the gel was rinsed with Milli-Q water and stained using coomassie brilliant blue G-250 solution (0.125 % coomassie G-250) in destain solution (50 % methanol, 10 % glacial acetic acid, 40 % milli-Q water) and stained for 40 min. Following staining, the gel was rinsed with Milli-Q water and destained for one h in the destain solution. Finally, the gel was removed from the destain, rinsed with Milli-Q water, and allowed to soak in Milli-Q water overnight before imaging.

TxtE enzyme assays were performed under oxic, hypoxic, and anoxic treatment conditions. In the oxic treatment, all assay reactions were prepared and monitored in an air atmosphere. Hypoxic conditions are defined as enzyme reactions that were prepared in air, but added to sealed glass vessels containing only N_2 gas. Hence, some oxygen dissolved in the liquid will be present. Anoxic conditions are defined as reactions that were prepared solely in an anoxic glove bag (N_2 and H_2 gas atmosphere) and gas measurements taken by N_2 flushed syringe needles. Reactions were prepared in 1.5 mL microcentrifuge tubes and transferred to 6 mL borosilicate glass vials sealed with a black butyl rubber stopper. All reactions were prepared in a final volume of 500 µL in 25 mM Tris buffer (pH 8.0) and contained 18 µL TxtE (1.9 µM or 0.09 mg/mL final concentration), 10 µL spinach ferredoxin (0.02 mg/mL, Sigma Aldrich), 10 µL spinach ferredoxin NADP+ reductase (0.008 U/mL, Sigma-Aldrich), 27 µL of 18.5 mM stock solution of β-nicotinamide adenine dinucleotide 2’ phosphate, reduced in 25 mM Tris buffer (pH 8) (~1 mM, Alfa Aesar, Haverhill, MA, US), 25 µL of 10 mM diethylamine NONOate diethylammonium salt (DEANO) solution in 25 mM Tris buffer (500 µM final conc., Sigma-Aldrich), and 10 µL L-tryptophan in 0.5 M NaOH (5 mM final conc., Sigma-Aldrich). The reaction was started by addition of DEANO solution. Gas measurements were taken at time zero and after 24 hours to monitor N_2O production.

N_2O was monitored by manual gas injections (100 µL) into a 7890A gas chromatograph equipped with a micro electron capture detector (Agilent Technologies, Santa Clara, CA, USA). Dilution standards of N_2O were prepared in 6 mL glass vessels capped with black butyl rubber stoppers. Limit of detection and limit of quantification were determined by repeated measurements (n = 7) of N_2O at a quantity (45 nanomoles total mass N_2O) eliciting an output response three to five times above the noise of the output when measuring a sample blank (no N_2O). The standard deviation of peak areas obtained from these seven measurements was multiplied by a value of three and ten to determine the limit of

detection (29 nanomoles) and limit of quantification (91 nanomoles) for N_2O measurements obtained during the TxtE assays, respectively (179).

The various assay components (Table 4.1), a schematic of the proposed reactions (Figure 4.1), and images of protein purification (Figure 4.2, 4.3, 4.4) can be found in the Appendix.

Results

Fungi harbor a minimal set of evolutionarily correlated denitrification traits

The two overarching aims of the present study were to enhance our understanding of the evolution and comparative genomics of denitrification traits in fungi, and to provide additional lines of evidence to assist in resolving uncertainty surrounding fungal contributions to N_2O emissions. At present, a combination of advances in sequencing technologies and collaborative fungal sequencing efforts have yielded a wealth of genomic resources ripe for bioinformatic investigations regarding fungal denitrification. Therefore, we began by performing bioinformatic surveys of 712 fungal genomes to identify homologs of canonical bacterial and fungal denitrification genes (*narG*, *napA*, *norB*, *nirK*, *nosZ, p450nor*) (Figure 4.5A). Of the complete gene set investigated, only *narG*, *napA*, *nirK*, and *p450nor* were detected in the fungal genomes analyzed (Fig. 4.5A). The gene encoding the membrane bound respiratory nitrate reductase (*narG*) was detected in only three fungal genomes (0.42 %), In contrast, the genes predicted to encode the periplasmic nitrate reductase, *napA*, and the copper containing nitrite reductase, *nirK*, were detected in 75 (10.5 %) and 82 (11.5 %) of the 712 fungal genomes analyzed, respectively (Figure 4.5B). P450nor gene sequences were observed in 167 (23 %) of the fungal genomes analyzed, and lends support to the claim that P450nor-mediated N_2O production is widespread in fungi (Figure 4.5) (97). Of note, *p450nor* homologs were also detected in three genomes of freshwater inhabiting green algae, *Chlorella variabilis*, *Chlamydomonas reinhardtii*, and *Monoraphidium neglectum*,

expanding the known distribution of *p450nor* to this enigmatic group of photosynthetic microbes.

Not only did the genomic surveys demonstrate a disparity in the abundances observed among distinct denitrification traits, but they also revealed a remarkably limited co-occurrence between *p450nor* and other denitrification traits in the fungal genomes. Since *p450nor* is the sole trait known to encode N_2O formation in fungi, the co-occurrence of these genes should be indicative of the capacity for true, or complete, dissimilatory denitrification processes by fungi and not alternative processes (e.g., N oxide detoxification). For example, no co-occurrence of the genes *narG*, *nirK*, and *p450nor* were observed, while co-occurrence of *napA*, *nirK*, and *p450nor* was observed in only 10.8 % of 167 fungal genomes possessing *p450nor*. Sets of at least two co-occurring denitrification traits *narG* and *p450nor*, *napA* and *p450nor*, and *nirK* and *p450nor* were 0, 18 and 29 % of the 167 *p450nor*-containing fungi investigated. The lack of observed co-occurrence between *narG* and *p450nor* was mirrored by Bayesian trait evolution analysis using BayesTraits software that suggests no correlation between *p450nor* and *narG* (average log Bayes Factor 0.11 ± 0.29). However, correlated evolution between *napA* and *p450nor* and *nirK* and *p450nor* were strongly supported by the observed data, with average log Bayes Factor values of 12.2 ± 0.11 and 31.3 ± 0.04, respectively.

On the origins of fungal *p450nor*

Ancestral character state reconstruction strongly supported the monophyly of *p450nor* with three orthologous sequences from members of the green algal phylum Chlorophyta and a diversity of P450 enzymes classified within the P450 family CYP105 (Figure 4.6) (280). Representative sequences of the bacterial CYP105 family of P450s include diverse actinobacterial genera such as *Streptomyces*, *Frankia*, *Nocardia*, *Saccharopolyspora*; however, a sizeable number (n = 5) of these sequences were determined to be of proteobacterial origin with sequences representing members from the genera *Paracoccus*,

Burkholderia, and *Halomonas*. Alignment of fungal P450nor amino acid sequences to the NCBI RefSeq protein database identified 230 bacterial sequences with significant alignment (≥ 65 % query coverage, ≥ 35 % amino acid identity), of which ~6 % (n = 13) were of proteobacterial origin (Figure 4.7). Gene tree-species tree comparisons of 60% identity clustered P450 amino acid sequences (n = 57) and cognate 16S rRNA genes (n = 55) supported HGT of one or more actinobacterial P450s to members of the *Alpha*-, *Beta*-, and *Gammaproteobacteria* (Figure 4.8). Furthermore, ancestral character state reconstruction overwhelmingly supported *Actinobacteria* as the root (*P* Root (*Actinobacteria*) = 0.99 ± 0.06). When forcing the root state of the P450 phylogeny to be *Proteobacteria* (simple model) and comparing to the complex model where the root is allowed to vary, the simple model with a proteobacterial root was not supported (average log Bayes Factor = 0.03 ± 0.18).

Evolutionary forces acting upon denitrification traits within fungi

Examination of a cophylogenetic plot of *p450nor* gene and species trees provided evidence for many HGT events, examples of which included support for HGT between different fungal phyla (Ascomycota and Basidiomycota) and potential transfer within and among classes of the Ascomycota (Figure 4.9). For example, the monophyly of five fungal classes (Dothideomycetes, Eurotiomycetes, Leotiomycetes, Sordariomycetes, and Tremellomycetes), represented by both amino acid and nucleotide *p450nor* phylogenies, were not supported by AU tests (Table 4.2, p ≤ 0.05), and provides additional support for widespread HGT of *p450nor* within these fungal lineages. Additional gene tree species tree reconciliation using NOTUNG software was also performed to detect and quantify duplication (GD), transfer (GT), and loss (GL) events. Of the three denitrification traits analyzed, the *p450nor* phylogenies had the greatest predicted number of GT events, ranging from 4 to 15 GT events predicted using strict GT costs (11 and 15, Table 4.3). At GT costs below 9, no temporally consistent optimal solutions were reached. Using the same stringent GT costs,

the predicted number of GT events detected for *napA* and *nirK* were much lower, and ranged from 1 to 3 and 0 to 1 GT events for each gene, respectively. The reduced number of detectable GT events for *napA* and *nirK* were also apparent from cophylogenetic plots of each gene compared to cophylogenetic plots for *p450nor* (Figure 4.10, 4.11). GD and GL appear to be significant forces shaping the evolution of *nirK* in fungi, and may explain the failure of the AU test to reject the monophyly of *nirK* lineages despite visual discord between fungal lineages within the species and gene trees (Figure 4.11, Table 4.2). Although GT events detected for *napA* were lower than *p450nor* at high GT costs, GT may still represent a significant evolutionary force contributing to the observed distribution of *napA* in extant fungal lineages. For example, at a more modest GT cost of 7, the number of *napA* GT events detected in the amino acid phylogeny substantially increased to 14, whereas no temporally consistent optimal solutions were reached for the *napA* nucleotide phylogeny. Moreover, AU tests rejected the monophyly of three Ascomycota (Dothideomycetes, Leotiomycetes, and Sordariomycetes) and one Basidiomycota (Pucciniomycetes) lineage within the *napA* phylogeny (Table 4.2, $P \leq 0.05$).

Evidence for a role of *p450nor* in secondary metabolism

To assess these genomes for evidence of a potential role for *p450nor* in SM, genes encoded within genomic regions approximately 50 kb up and downstream of *p450nor* were queried for functions related to SM (see Materials and Methods). Analysis of the genomic regions from 167 *p450nor*-containing fungal genomes using the popular biosynthetic gene cluster prediction tool antiSMASH resulted in the detection of putative biosynthetic gene clusters containing *p450nor* in 19 (11 %) of the 167 genomes analyzed. The number of open reading frames in a predicted SM cluster ranged from 34 to 97, spanning 21,086 to 55,473 nucleotides along the DNA sequence provided to antiSMASH. Of the 19 clusters, a diversity of products were predicted to be produced that included nonribosomal peptides (7), polyketides (5), terpenes (2), hybrid terpene-

polyketide-indoles (2), indole (1), and other (2) categories. Interestingly, the fact that antiSMASH was able to flag 11% of *p450nor*-containing genomic regions as putative biosynthetic gene clusters suggests these may be more closely related to well characterized clusters, and that the other 89% of *p450nor*-containing genomic regions may harbor novel, previously undiscovered gene regions potentially involved in the production of uncharacterized secondary metabolites. Further inspection of genes surrounding *p450nor* predicted to encode hallmark SM features (e.g., polyketide synthases, terpene cyclases, dimethylallyl tryptophan synthases) detectable by curated antiSMASH profile Hidden Markov Models increased this number to 59 (35 %) of the 167 genomes analyzed. The observed distribution of automatic and manually curated protein-coding genes surrounding *p450nor* in 32 additional *p450nor*-containing fungi reveals that manual annotation efforts are helpful in uniting SM clusters in diverse fungi (Figure 4.12A, 4.12B).

Ortholog clustering of 3484 protein coding genes surrounding *p450nor* resulted in the identification of 1364 orthologous groups (OGs). The 100 most abundant OGs contained an average of 11.9 ± 7.7 proteins per cluster, of which 21 OGs (343 proteins, 9.8 % of total) were predicted by antiSMASH profile Hidden Markov Models to possess significant alignment to curated proteins or domains demonstrated to be involved in SM. The other 1264 OGs contained an average of 1.5 ± 1.2 proteins per cluster, of which 60 OGs (139 proteins, 3.9 % of total) were also predicted to be involved in SM. As protein membership within an OG decreased, taxonomic diversity of the proteins within that cluster also declined (Figure 4.13 A). Of note, the OG comprised of P450nor was predicted to be involved in SM by significant alignment (average alignment bit score 124.5 ± 20.7, n=178) to the antiSMASH profile Hidden Markov Model of the CYP105 NovI, responsible for the formation of the beta-hydroxy-tyrosine intermediate of the aminocoumarin antibiotic novobiocin (data not shown). Functional annotations of proteins in the top 50 OGs were representative of hallmark SM

functions, and suggests additional fungi possess related protein functions but may not be predicted by antiSMASH to be involved in SM (Figure 4.13B).

Analysis of eight C-type condensation domains and 10 ketosythase (KS) condensation domains identified with NaPDoS (281) in non-ribosomal peptide and polyketide synthases, respectively, enabled the prediction of potential product classes that could be produced from fungal *p450nor*-containing SM clusters (Figure 4.14A, 4.14B).

p450nor duplications and gene transfer events may enhance diversity of produced SMs

Of the 178 *p450nor* sequences identified, 11 (6%) were detected as additional gene copies within the 167 *p450nor*-containing fungal genomes examined. Of these 11 sequences, one sequence each from *Pseudogymnoascus* sp. strain VKM F-4517 and *Nectria haematococca* strain mpVI 77-13-4 appear to be xenologs, or horizontally acquired, and the other eight sequences appear to be duplications occurring prior to (six) or following (three) a speciation event. One *p450nor* gene from *Pseudogymnoascus* sp. strain VKM F-4517 appears to have been laterally acquired from organisms related to *Thelebolus microsporus* strain ATCC 90970 since all *p450nor* from *Pseudogymnoascus* sp. form a monophyletic assemblage except for this sequence. An alternative, though less parsimonious, explanation would be that a duplication of *p450nor* occurred prior to the split of *Pseudogymnoascus* and *Thelebolus* (both Leotiomycetes) and subsequent gene loss in all *Pseudogymnoascus* examined except for *Pseudogymnoascus* sp. strain VKM F-4517. The *p450nor* xenolog in *Nectria haematococca* strain mpVI 77-13-4 is most closely related to five *p450nor* gene sequences of *Aspergillus* species in the fungal class Eurotiomycetes.

TxtE does not mediate NO reduction to N_2O

The enzyme assays performed with purified TxtE under anoxic conditions did not demonstrate N_2O production by this member of the CYP107 family of P450s

(Figure 4.15). No detectable quantities of N_2O were produced under oxic and hypoxic assay conditions (data not shown). Treatments without NO donor or NADPH did not produce N_2O, and suggests a reaction between NADPH and NO may occur to form N_2O under anoxic conditions (Figure 4.15). Of note, no detectable N_2O was formed in the L-4-nitrotryptophan-producing control (containing all assay components) under anoxic conditions.

Discussion

Shared ancestry unites P450nor with P450s involved in SM

Of the *p450nor* gene sequences identified, most were detected in members of the Ascomycota (n = 164) and only a few Basidiomycota (n = 3). N_2O production has also been reported for fungal isolates assigned to the recently revised phylum Mucoromycota (99, 282); hence, N_2O production may be restricted to the Dikarya, and not all Fungi as has been previously reported (97) Importantly, the *p450nor* gene was the most abundant denitrification trait detected in the sample of fungal genomes investigated, with more than two-fold higher abundance than other denitrification traits examined. Previous sequence analyses of *p450nor* have suggested a shared ancestry of *p450nor* with a large group of cytochrome P450s of the CYP105 family from the bacterial phylum *Actinobacteria* (79, 249). The main rationale for a bacterial origin of *p450nor* was the observation of a shared amino acid identity of P450nor with these bacterial proteins and initial phylogenetic comparisons of P450nor with other P450s (79, 248–250). Although these analyses invoke horizontal gene transfer as a potential mechanism explaining the observed discrepancy in *p450nor* presence in fungi, critical phylogenetic investigations were not performed, and thus little evidence was available to support a gene transfer hypothesis of *p450nor*. Ancestral state reconstruction analysis directly linked *p450nor* to the bacterial phylum *Actinobacteria*. Members of the *Proteobacteria* also possess CYP105 P450s, but additional phylogenetic analysis demonstrated that these too, likely originated

from members of the *Actinobacteria* (Figure 4.8). These results indicate that the evolutionary history of CYP105 P450s and fungal-actinobacterial interactions are complex, and may have led to the acquisition of a gene from a novel cytochrome P450 family (250, 253).

An undiscovered role for P450nor in SM?

p450nor encodes the only P450 reported to enable NO reduction to N_2O in fungi, and phylogenetic analyses reported here strongly supported the acquisition of fungal *p450nor* by horizontal transfer from one or more actinobacteral P450s in the CYP105 family. Of note, a recent investigation identified a related P450, TxtE, shown to catalyze the nitration of L-tryptophan using NO, which is subsequently modified to form the cellulose synthase inhibitor thaxtomin A (254, 255). NO has long been known to be an inhibitor of cytochrome activity in general (88), and the finding that two related enzymes with strikingly different functions related to NO was unexpected. Hence, the observation that *p450nor* likely originated from a diverse clade of actinobacterial genes encoding TxtE and other P450s involved in SM (253) led to the hypothesis that P450nor is involved in SM as well. P450nor has been previously suggested to act as an electron sink for respiratory denitrification, provide a novel mechanism for NO detoxification, and now comparative genomic and phylogenetic evidence links P450nor to a previously undiscovered role in SM (71, 79). Although a role for P450nor in NO detoxification cannot be definitively ruled out, additional mechanisms of NO detoxification are present in a majority (75 %) of *p450nor*-containing fungi, and suggests that P450nor is not required for NO detoxification to occur in these fungi. The hypothesis that P450nor may play a respiratory role as an electron sink in denitrification is also unlikely since P450s are not involved in respiratory processes (85). Furthermore, production of N_2O by P450nor in a majority of fungi does not demonstrate signs of a respiratory function (e.g., low mass balance between N species added and the N species produced). The SMs predicted to be produced by biosynthetic clusters predicted to involve P450nor are diverse

and include terpenoids, nonribosomal peptides, polyketides, and other complex metabolites (Figure 4.14). Moreover, a sizeable proportion (35 %) of gene regions surrounding *p450nor* also contained gene predicted to encode hallmarks of SM. Although automated methods for identifying SM clusters in fungi were employed, they clearly are limited since only 11 % of *p450nor*-containing genomic regions were predicted compared to those identified with expert annotation. Therefore, manual curation efforts are still required for mining valuable novel biosynthetic gene clusters in fungi.

Although purified enzymes assays with TxtE, a related P450 known to bind NO, failed to demonstrate fortuitous N_2O formation by this SM enzyme, a variety of metabolites containing nitro functional groups are being identified in fungal genera known to harbor denitrifying representatives (283). Furthermore, nitration of chemical species may represent a novel mechanism to enhance toxicity or specificity of a metabolite (284). It is suspected that P450nor may have a similar role in either nitration (NO_2 addition) or nitrosylation (NO addition) reactions with metabolites produced in SM. Therefore, the acquisition of *p450nor* and incorporation nearby additional SM features may be adaptive and have been selected for in fungal lineages where it occurred. This is supported by the widespread distribution of *p450nor* across the phylum Ascomycota, and is supported by additional reports of HGT between members of the *Actinobacteria* and Fungi in enhancing SM (285). Another unknown related to P450nor's role in SM is a putative substrate. To date, P450nor is only known to bind electron donors NADH or NADPH, and has no additional substrate other than NO. Two related P450s, TxtE and NovI, both share some similarity in substrate scope in that L-tryptophan and L-tyrosine are intermediates in the final SMs produced in their respective pathways (thaxtomin A and novobiocin production, respectively) (254, 286). Therefore, it seems plausible that P450nor may also bind or use aromatic amino acids as a substrate during SM production. Interestingly, TxtE requires an NO synthase to produce NO for use in the nitration of L-tryptophan by TxtE (254). Since *nirK* and *p450nor* are evolutionarily correlated, and few

reports exist of NO synthases in fungi, it is tempting to suggest that NirK may be an NO donor for P450nor activity in SM. Importantly, 14 genes predicted to encode nitrite reductases have been found nearby *p450nor* and supports the idea that NO donation to P450nor may be important for a potential function in SM.

The finding that TxtE did not produce N_2O was surprising given the shared function of these enzymes in NO binding (254). However, given the large amount of sequence divergence separating P450nor from its closest actinobacterial relative (Figure 4.6), it is plausible that P450nor may have acquired mutations permitting N_2O formation following its transfer from an actinobacterial donor. P450s in general exhibit a low degree of sequence similarity, but have remarkably identical structures that may confer substrate specificity (85, 287, 288). Since most CYP105 P450s examined to date all share a functional role in SM, P450nor evolving a novel function related to NO reduction is less parsimonious. Given that rates and quantities of N_2O formed by fungal isolates is low compared to denitrifying bacterial isolates, it seems likely that NO reduction might not be a primary function of P450nor, though further experimentation is required to support this claim. Enzyme assays of P450nor NO reduction have largely been performed by a single laboratory group (79, 81, 289), and further experimentation by independent laboratories is required to exclude the possibility that N_2O production by P450nor is not a secondary outcome of a primary SM role, or an artifact of *in vitro* experimental conditions.

The complex evolution of denitrification traits in fungi

Although much emphasis has been placed on understanding the biochemical basis of N_2O formation in fungi (71, 147, 289), less attention has been afforded to the evolution of *p450nor*, the sole trait postulated to be responsible for conferring N_2O production in fungi. The presence of gaps in our understanding of *p450nor* evolution represents a significant deficiency in our knowledge of fungal denitrification. For example, N_2O production from closely related fungal isolates

has been observed to be highly variable (80, 97, 103, 175), but the underlying evolutionary forces (e.g., HGT, gene gain/loss, and incomplete lineage sorting) that may account for the observed variability in fungal N_2O production had not been previously examined. Therefore, a multiple lines of evidence approach to investigate and quantify the forces shaping the evolution of denitrification traits present within fungi was undertaken. Many HGT events between distantly related fungal lineages was observed using gene tree species tree comparisons of both nucleotide and amino acid phylogenies constructed using ML and Bayesian methods. Exact numbers of HGT events may be challenging to quantify given the level of uncertainty in deeply branching nodes of the functional genes trees reported here and under sampled nature of the phylogenetic diversity of fungal genomes, but nonetheless a clear signal indicating tens of HGT events was observed using gene tree-species tree reconciliation. Gene loss and duplication events were also high (Table 4.3), and closely related fungal species display a high degree of variability in their presence/absence of denitrification traits. While a growing number of studies have implicated fungi in N_2O emissions in the soil environment, few if any studies have attempted to quantify the abundance, activity, and distribution of these gene markers across a variety of environments and none have linked them to fungal growth. Therefore, significant doubt and room for further investigations utilizing a variety of methods to correlate fungal growth with dissimilation of inorganic N-oxides would be instructive and provide additional support for or against a role for fungi in denitrification.

Although a significant disparity was observed in the co-occurrence between denitrification traits within fungal genomes, interaction among fungal species containing parts of the pathway to perform denitrification may explain these findings. For example, the genes of the denitrification pathway in *Bacteria* are known to be modular, and mutualistic interactions by microbial species harboring discrete steps in denitrification may suffice to perform this process in the environment (54, 59, 290). However, in bacterial and archaeal denitrifiers, investigators have been able to demonstrate growth linked to dissimilation of N-

oxides, which has not been conclusively demonstrated for fungi. Furthermore, a distinct correlation was detected between *p450nor* and additional denitrification traits, and although gene co-occurrence is not overwhelming within genomes, the presence of *p450nor* and additional denitrification traits within similar fungal lineages is largely correlated. However, trait correlation between *p450nor* and other denitrification traits should be interpreted with caution. Other undisclosed factors (e.g., shared ecological niche, selection pressures) related to the life history strategies of the fungi sharing these traits may explain their shared distribution equally well.

Nitrate reductases in fungi were not created equal

The low number of *narG* genes observed within fungal genomes reinforces observations of a limited capacity for dissimilatory NO_3^- reduction in fungi (70, 96, 98). Interestingly, reports of dissimilatory nitrate reduction in fungi began as early as the1960s (291, 292), yet relatively little is known about the capacity of fungi to perform nitrate reduction coupled to respiration under anoxic conditions. Most investigations demonstrate N_2O formation by fungi in the presence of NO_2^-, but much lower or no N_2O formation when grown in the presence of NO_3^-. Several investigations of select fungi containing NarG have been conducted and suggest fungi perform dissimilatory NO_3^- reduction when *narG* is present, but biochemical evidence regarding a role for NapA in fungal NO_3^- dissimilation are unavailable. The observation that *napA* is more abundant in fungal genomes compared to *narG* may suggest an overlooked yet important function for NapA in fungi. Nevertheless, the fact that a multitude of fungal genera harboring *napA* demonstrate low or no production of N_2O when grown in the presence of NO_3^- is perplexing (70). One potential explanation for the observed disparity in the abundance of different genes encoding NO_3^- and NO_2^- reducing enzymes is the modularity of genes present within the ancestral bacterial operon; genes encoding modular enzymatic processes may be acquired and maintained at a higher rate in the recipient genome than less modular, larger genes systems

(293). In some members of the *Bacteria*, NapA and NirK are thought to function in the absence of other genes of the *nap* and *nir* operon, and suggests modularity as a plausible explanation for the observed abundance of *napA* and *nirK* genes in fungi. In addition, preexisting genes encoding compatible or promiscuous protein chaperones and electron transfer proteins present in the fungal ancestor in which *nap* or *nir* genes were acquired may have led to the stabilization and selection of these key denitrification traits in fungi. Although modular genes may be acquired at higher rates than genes with complex associations, acquisition or maintenance of modular genes does not necessarily guarantee correct functioning of the encoded products.

Are green algae an enigmatic source of N_2O emissions?

A variety of green algae have been reported to produce N_2O, the production of which could, at least in part, be attributed to the presence of *p450nor* within this lineage (164, 165). A recent study by Plouviez et al. linked P450nor to N_2O production in *Chlamydomonas reinhardtii* and observed lower N_2O production from cultures subjected to RNA interference of *p450nor* transcripts (294). Although this is a novel finding, the total amounts (nanomoles) and rate of N_2O produced by green algae is on par with fungal production, and is hence three to six orders of magnitude lower than bacterial rates of N_2O production (99). Green algae also display a poor mass balance between the N added and the N formed as N_2O, and suggests that N_2O formation within *Chlamydomonas reinhardtii* is not a respiratory process (294). Furthermore, genes encoding NapA or NirK were not detected in the algal genomes; however, a 295 amino acid long NirK-like protein domain (54% identity to bacterial NirK) contained in an 1,868 amino acid length ERD4-related membrane protein (NCBI accession XP_001702327.1) is encoded by the *Chlamydomonas reinhardtii* genome (77). More recent analysis has shown that *E*arly *R*esponsive to *D*ehydration 4 proteins are upregulated in response to dehydration and other stresses and contain a DUF221 domain, which at least for *Arabidopsis thaliana*, has been demonstrated to be a calcium

permeable stress-gated cation channel and is found in a large diversity of eukaryotes, including fungi (295, 296). Hence, it is tempting to posit that nitrite-induced stress detected by the NirK domain may induce a calcium-mediated regulatory cascade in *Chlamydomonas*. Alignment of this protein to the *Chlorella* and *Monoraphidium* proteomes resulted in the identification of significant hits only to the N-terminal calcium permeable stress-gated cation channel, and no significant alignments to the C-terminal cupredoxin domains related to NirK were detected, and suggests this domain is unique to ERD4 proteins in *Chlamydomonas reinhardtii*. The presence of a NirK-like region contained within the *Chlamydomonas* ERD4 protein may indicate either an altered function for NirK, or possibly a poor gene call, and suggestions that green algae contain a *nirK* gene should be tempered until further experimentation and analysis are conducted (77). Green algae have been demonstrated to produce NO during nitrite assimilation, and suggests that P450nor may be part of an alternative mechanism for NO detoxification or possess an alternative function in green algae (297). Given the evidence linking *p450nor* to SM and the low amounts of N_2O observed to be formed by green algae suggests an alternative role for P450nor in either detoxification or SM within this lineage.

CHAPTER FIVE
CONCLUSIONS AND RECOMMENDATIONS

The two predominant groups of microorganisms implicated in N_2O emissions from soil are denitrifying members of the *Bacteria* and Fungi (40). The denitrifying activity of microorganisms is particularly robust in agroecosystems due to large inputs of reactive nitrogen into the soil (298). Agricultural soils pose a significant challenge for management decisions related to climate change due to trade-offs in crop productivity related to fertilizer addition and greenhouse gas emissions (44). Fungi have gained significant attention for their potential contributions to soil N_2O emissions mainly due to observations of their large contributions to N_2O emissions (40 – 89 %) in antibiotic treated soil incubations, and that fungi have no known ability to convert N_2O to inert N_2 (except see codenitrification) (79, 99). Despite these observations, molecular tools targeting *p450nor*, a fungal gene encoding a nitric oxide reductase, were lacking even though the development of such tools could enhance the detection of fungal denitrification potential in soils. Development of a successful degenerate *p450nor* PCR primers was made possible by previous investigations on structural studies of P450nor (288), and careful alignment and inspection of both nucleotide and amino acid sequences for suitable regions for primer design (103). The primers *p450nor394F* and *p450nor809R* enabled the detection of *p450nor* genes from a diversity of fungal isolates and environmental samples, thus streamlining the process of detecting fungal denitrification potential. Although additional PCR methodologies are available, *p450nor* PCR primers are a significant advance in the molecular biologist's toolkit since this is the sole trait posited to be directly responsible for N_2O formation in fungi.

The *p450nor* gene is twice as abundant as other denitrification markers (e.g., *nirK*) in fungal genomes based on genomic investigations, and further supports the utility of *p450nor*-targeted PCR primers for querying fungal denitrification potential. A limitation of the *p450nor* PCR primer set is that they are not applicable to quantitative PCR due to the size of the amplified region and their degeneracy. However, these limitations may be balanced by our successful recent application of these primers to gene-targeted metagenomics. The

complexity of microbial communities present in environmental samples limits the application of shotgun metagenomics for studies of functional diversity (241). Hence, gene-targeted, high-throughput amplicon sequencing is currently the most practical method to investigate the functional diversity of one or more functional genes within environmental samples (232). Application of *p450nor* PCR primers to an Illumina MiSeq sequencing methodology enabled the identification of novel sequence diversity present within two agricultural soils. Importantly, it demonstrated that fungal communities containing *p450nor* are spatially stratified over large distances (kilometers), but not so at small spatial scales (meters). Comparison of the *p450nor* community with environmental variables revealed that soil pH and moisture are related to p450nor-containing fungi community structure. Hence, these findings provide a foundation for future controlled experiments investigating how pH and moisture truly affect *p450nor* abundance, diversity, and function. Comparison of direct amplification and sequencing of *p450nor* sequences from soils also revealed that our cultivation efforts also were representative of fungal denitrifiers based on the large number of sequences aligning to previously amplified *p450nor* sequences from these isolates. These isolates will also allow additional opportunities to explore *p450nor* function and activity in a controlled setting and enabling extrapolation to the environment due to the large relative abundance these organisms possess in the soil. Although an advancement, the application of degenerate *p450nor* primers to high-throughput sequencing presents issues in interpretation of downstream analyses (e.g., OTU inflation using de novo clustering), and future investigations should explore how amplification conditions impact the results of *p450nor* amplicon sequencing.

In addition to environmental sequencing, genomic sequencing efforts aimed at fungal isolates have paved the way for investigations into comparative genomics and phylogenetic analysis of fungal denitrification traits. The exploration of *p450nor* and additional denitrification markers in fungal genomes revealed that fungal denitrification traits have a complex evolutionary history

marked by gene duplications, loss, and abundant gene transfer events between distantly related fungal lineages (e.g., between Ascomycota and Basidiomycota). Furthermore, denitrification traits were observed to be largely restricted to the phylum Ascomycota. The ancestral state reconstruction of *p450nor* supported the affiliation of *p450nor* with cytochrome P450s found in members of the Actinobacteria that are well known for their roles in secondary metabolism (SM). This observation, coupled with observations that fungal isolates demonstrate a poor capacity for N_2O formation, spurred genomic investigations of gene regions surrounding *p450nor* and the resulting identification of SM hallmarks nearby *p450nor* genes as a potential alternative functional role for these proteins. The predictive SM cluster tool antismash supported these observations, but could only predict 11 % of the 167 *p450nor*-containing gene regions to be involved in SM, while additional manual curations increased this number to 35 %. Additional support for a role for *p450nor* in SM comes from the discovery of TxtE, an additional cytochrome P450 related to P450nor that is capable of using NO as a substrate. Taken together, these findings suggest an ancestral horizontal transfer of a cytochrome P450 involved in SM from members of the *Actinobacteria* to the Fungi, which subsequently radiated, through a multitude of complex evolutionary events, into a majority of members in the largest, most diverse phylum of fungi the Ascomycota. The identification of a role for P450nor in SM is transformative because it challenges the prevailing view that P450nor is a significant contributor to denitrification, a process in which several studies have suggested is dominated by fungi in soils (99). Furthermore, a role for P450nor in SM provides a more plausible, alternative explanation to optimization of culture conditions as an explanation for observations that fungi in controlled settings convert only very small quantities of supplied nitrate or nitrite to N_2O (299). The observation that the related TxtE enzyme performs a nitration reaction using L-tryptophan as a substrate enabled the hypothesis that P450nor performs a similar nitration or NO-related reaction, and lays the groundwork for future liquid chromatography

mass spectrometry methodologies to detect such substrates in *p450nor*-containing fungi.

A growing number of observations recorded by scientists using biochemical, physiological, molecular, and environmental systems all indicate that fungi are nitrous oxide forming microorganisms (71, 79, 99). The evidence is overwhelming and few arguments can be mustered against the observation that fungi produce N_2O. That being said, there is a striking difference between observations of N_2O-forming activity of fungal isolates in the lab, and those made in soils where a portion of the fungal activity has been partitioned using bactericides (72, 99, 120). Laboratory studies using isolates would suggest that NO reduction to N_2O by fungal isolates is largely cometabolic, involved in detoxification, or perhaps in some rare instances, linked to N-oxide respiration (see *Neocomospora vasinfecta* (72)). Observations from substrate-induced respiration inhibition (SI) studies of soils would suggest that fungi are prodigious N_2O-producing microorganisms, and has received attention in the climate arena due to their inability to reduce N_2O further to inert N_2 gas. Rather than continue to identify weaknesses in both laboratory incubations and respiration inhibition studies, the adoption of low bias, alternative methodologies should be adopted to investigate the fungal contribution to N_2O emissions in soil. For example, methodologies using stable isotopes, of which several are reported for fungal denitrification (299, 300), combined with targeted omics or quantitative PCR methodologies might be one strategy to correlate biogeochemical activity with fungal relative abundance. Alternatively, a multiple lines of evidence approach could be utilized when performing SI studies that account for uncertainty in the success of inhibition by a selected antimicrobial compound. For example, fungal biomass could be monitored using fatty acid esters and ergosterol or leucine incorporation and acetate into ergosterol methodologies could be performed to investigate bacterial and fungal growth in the presence of inhibitors (115, 118). Furthermore, the relative abundance of bacterial and fungal *nirK* or *p450nor*

genes or transcripts may be investigated due to recent advances in PCR primer methodologies for targeting these sequences (103, 129, 130, 132).

LIST OF REFERENCES

1. **Wainwright M**. 1988. Metabolic diversity of fungi in relation to growth and mineral cycling in soil — a review. Trans. Br. Mycol. Soc. **90**:159–170.

2. **Wainwright M**. 1981. Mineral transformations by fungi in culture and in soils. Zeitschrift für Pflanzenernährung und Bodenkd. **144**:41–63.

3. **Wang G**, **Wang X**, **Liu X**, **Li Q**. 2012. Diversity and biogeochemical function of planktonic fungi in the ocean, p. 71–88. *In* Raghukumar, C (ed.), Biology of Marine Fungi. Springer Berlin Heidelberg, Berlin.

4. **Gadd GM**. 2007. Geomycology: biogeochemical transformations of rocks, minerals, metals and radionuclides by fungi, bioweathering and bioremediation. Mycol. Res. **111**:3–49.

5. **Xu L**, **Ravnskov S**, **Larsen J**, **Nilsson RH**, **Nicolaisen M**. 2012. Soil fungal community structure along a soil health gradient in pea fields examined using deep amplicon sequencing. Soil Biol. Biochem. **46**:26–32.

6. **Rousk J**, **Brookes PC**, **Bååth E**. 2009. Contrasting soil pH effects on fungal and bacterial growth suggest functional redundancy in carbon mineralization. Appl. Environ. Microbiol. **75**:1589–1596.

7. **Banitz T**, **Johst K**, **Wick LY**, **Schamfuß S**, **Harms H**, **Frank K**. 2012. Highways versus pipelines: contributions of two fungal transport mechanisms to efficient bioremediation. Environ. Microbiol. Rep. 211-218.

8. **Lindahl BD**, **Kuske CR**. 2014. Metagenomics for study of fungal ecology, p. 384. *In* Martin, F (ed.), The ecological genomics of fungi, 1st ed. John Wiley & Sons, Inc., Ames, IA.

9. **Singh P**, **Raghukumar C**, **Meena RM**, **Verma P**, **Shouche Y**. 2012. Fungal diversity in deep-sea sediments revealed by culture-dependent and culture-independent approaches. Fungal Ecol. **5**:543–553.

10. **Gadd GM**. 1999. Fungal production of citric and oxalic acid: Importance in metal speciation, physiology and biogeochemical processes, p. 47–92. *In* Physiology, RKPBT-A in M (ed.), . Academic Press.

11. **Dutton M V**, **Evans CS**. 1996. Oxalate production by fungi: its role in pathogenicity and ecology in the soil environment. Can. J. Microbiol. **42**:881–895.

12. **Khan MS**, **Zaidi A**, **Wani PA**. 2007. Role of phosphate-solubilizing microorganisms in sustainable agriculture — A review. Agron. Sustain. Dev. **27**:29–43.

13. **Bhatti JS**, **Comerford NB**, **Johnston CT**. 1998. Influence of oxalate and soil organic matter on sorption and desorption of phosphate onto a spodic horizon. Soil Sci. Soc. Am. J. **62**:1089–1095.

14. **Richardson AE**, **Simpson RJ**. 2011. Soil microorganisms mediating phosphorus availability update on microbial phosphorus. Plant Physiol. **156**:989–996.

15. **Ingold CT**, **Hudson HJ**. 1993. Ecology of saprotrophic fungi, p. 145–157. *In* The Biology of Fungi. Springer Netherlands.

16. **Osono T**. 2007. Ecology of ligninolytic fungi associated with leaf litter decomposition. Ecol. Res. **22**:955–974.

17. **Bugg TDH**, **Ahmad M**, **Hardiman EM**, **Rahmanpour R**. 2011. Pathways for degradation of lignin in bacteria and fungi. Nat. Prod. Rep. **28**:1883–1896.

18. **Setälä H**, **McLean MA**. 2004. Decomposition rate of organic substrates in relation to the species diversity of soil saprophytic fungi. Oecologia **139**:98–107.

19. **Koide RT**, **Malcolm GM**. 2009. N concentration controls decomposition rates of different strains of ectomycorrhizal fungi. Fungal Ecol. **2**:197–202.

20. **Frey SD**, **Six J**, **Elliott ET**. 2003. Reciprocal transfer of carbon and nitrogen by decomposer fungi at the soil–litter interface. Soil Biol. Biochem. **35**:1001–1004.

21. **Griffin DH**. 1994. Fungal physiology, 2nd ed. Wiley-Liss, Inc., New York,

New York, USA.

22. **Deacon JW**. 2005. Fungal Biology, 4th ed. Wiley-Blackwell, Hoboken, NJ.

23. **Geisseler D**, **Horwath WR**, **Joergensen RG**, **Ludwig B**. 2010. Pathways of nitrogen utilization by soil microorganisms – A review. Soil Biol. Biochem. **42**:2058–2067.

24. **Hawkins H-J**, **Johansen A**, **George E**. 2000. Uptake and transport of organic and inorganic nitrogen by arbuscular mycorrhizal fungi. Plant Soil **226**:275–285.

25. **Chalot M**, **Brun A**. 1998. Physiology of organic nitrogen acquisition by ectomycorrhizal fungi and ectomycorrhizas. FEMS Microbiol. Rev. **22**:21–44.

26. **Kusnan MB**, **Klug K**, **Fock HP**. 1989. Ammonia assimilation by *Aspergillus nidulans*: [15N] ammonia study. Microbiology **135**:729–738.

27. **Macheda ML**, **Hynes MJ**, **Davis MA**. 1999. The *Aspergillus nidulans gltA* gene encoding glutamate synthase is required for ammonium assimilation in the absence of NADP-glutamate dehydrogenase. Curr. Genet. **34**:467–471.

28. **Holmes AR**, **Collings A**, **Farnden KJF**, **Shepherd MG**. 1989. Ammonium assimilation by *Candida albicans* and other yeasts: Evidence for activity of glutamate synthase. Microbiology **135**:1423–1430.

29. **Kusnan MB**, **Berger MG**, **Fock HP**. 1987. The involvement of glutamine synthetase/glutamate synthase in ammonia assimilation by *Aspergillus nidulans*. Microbiology **133**:1235–1242.

30. **Johnstone IL**, **McCabe PC**, **Greaves P**, **Gurr SJ**, **Cole GE**, **Brow MAD**, **Unkles SE**, **Clutterbuck AJ**, **Kinghorn JR**, **Innis MA**. 1990. Isolation and characterisation of the *crnA-niiA-niaD* gene cluster for nitrate assimilation in *Aspergillus nidulans*. Gene **90**:181–192.

31. **Siverio JM**. 2002. Assimilation of nitrate by yeasts. FEMS Microbiol. Rev.

26:277–284.

32. **Marzluf GA**. 1997. Genetic regulation of nitrogen metabolism in the fungi. Microbiol. Mol. Biol. Rev. **61**:17–32.

33. **Marzluf GA**. 1993. Regulation of sulfur and nitrogen metabolism in filamentous fungi. Annu. Rev. Microbiol. **47**:31–55.

34. **Crawford NM**, **Arst, Jr. HN**. 1993. The molecular genetics of nitrate assimilation in fungi and plants. Annu. Rev. Genet. **27**:115–146.

35. **Slot JC**, **Hibbett DS**. 2007. Horizontal transfer of a nitrate assimilation gene cluster and ecological transitions in fungi: a phylogenetic study. PLoS One **2**:e1097.

36. **Joergensen RG**, **Wichern F**. 2008. Quantitative assessment of the fungal contribution to microbial tissue in soil. Soil Biol. Biochem. **40**:2977–2991.

37. **Burke DJ**, **Smemo KA**, **López-Gutiérrez JC**, **DeForest JL**. 2012. Soil fungi influence the distribution of microbial functional groups that mediate forest greenhouse gas emissions. Soil Biol. Biochem. **53**:112–119.

38. **Canfield DE**, **Glazer AN**, **Falkowski PG**. 2010. The evolution and future of Earth's nitrogen cycle. Science **330**:192–6.

39. **Hansen HCB**, **Koch CB**, **Nancke-Krogh H**, **Borggaard OK**, **Sørensen J**. 1996. Abiotic nitrate reduction to ammonium: Key role of green rust. Environ. Sci. Technol. **30**:2053–2056.

40. **Zumft WG**. 1997. Cell biology and molecular basis of denitrification. Microbiol. Mol. Biol. Rev. **61**:533–616.

41. **Schrock RR**. 2006. Reduction of dinitrogen. Proc. Natl. Acad. Sci. U. S. A. **103**:17087.

42. **Cabello P**, **Roldán MD**, **Castillo F**, **Moreno-Vivián C**. 2009. Nitrogen Cycle, p. 299–321. Third (ed.). Academic Press, Oxford

43. **Wuebbles DJ**. 2009. Nitrous oxide: no laughing matter. Science. **326**:56–57.

44. **Hu H-W**, **Chen D**, **He J-Z**. 2015. Microbial regulation of terrestrial nitrous oxide formation: understanding the biological pathways for prediction of emission rates. FEMS Microbiol. Rev. **39**:729–749.

45. **Pauleta SR**, **Dell'Acqua S**, **Moura I**. 2013. Nitrous oxide reductase. Coord. Chem. Rev. **257**:332–349.

46. **Enwall K**, **Throbäck IN**, **Stenberg M**, **Söderström M**, **Hallin S**. 2010. Soil resources influence spatial patterns of denitrifying communities at scales compatible with land management. Appl. Environ. Microbiol. **76** :2243–2250.

47. **Cavigelli M.A.**, **Robertson G.P.** 2001. Role of denitrifier diversity in rates of nitrous oxide consumption in a terrestrial ecosystem. Soil Biol. Biochem. **33**:14.

48. **Wallenstein MD**, **Myrold DD**, **Firestone M**, **Voytek M**. 2006. Environmental controls on denitrifying communities and denitrification rates: insights from molecular methods. Ecol. Appl. **16**:2143–2152.

49. **Cabello P**, **Roldán MD**, **Moreno-Vivián C**. 2004. Nitrate reduction and the nitrogen cycle in *Archaea*. Microbiology **150**:3527–46.

50. **Knowles R**. 1982. Denitrification. Microbiol. Rev. **46**:43–70.

51. **Chen J**, **Strous M**. 2013. Denitrification and aerobic respiration, hybrid electron transport chains and co-evolution. Biochim. Biophys. Acta - Bioenerg. **1827**:136–144.

52. **Verbaendert I**, **Boon N**, **Vos P**, **Heylen K**. 2011. Denitrification is a common feature among members of the genus *Bacillus*. Syst Appl Microbiol. **34**.

53. **Verbaendert I**, **De Vos P**, **Boon N**, **Heylen K**. 2011. Denitrification in gram-positive bacteria: an underexplored trait. Biochem. Soc. Trans.

39:254–258.

54. **Graf DRH**, **Jones CM**, **Hallin S**. 2014. Intergenomic comparisons highlight modularity of the denitrification pathway and underpin the importance of community structure for N_2O emissions. PLoS One **9**.

55. **Shoun H**, **Kano M**, **Baba I**, **Takaya N**, **Matsuo M**. 1998. Denitrification by actinomycetes and purification of dissimilatory nitrite reductase and azurin from *Streptomyces thioluteus*. J. Bacteriol. **180**:4413–4415.

56. **Moreno-Vivián C**, **Cabello P**, **Martínez-Luque M**, **Blasco R**, **Castillo F**. 1999. Prokaryotic nitrate reduction: molecular properties and functional distinction among bacterial nitrate reductases. J. Bacteriol. **181**:6573–6584.

57. **Sparacino-Watkins C**, **Stolz JF**, **Basu P**. 2014. Nitrate and periplasmic nitrate reductases. Chem. Soc. Rev. **43**:676–706.

58. **Gonzalez PJ**, **Rivas MG**, **Mota CS**, **Brondino CD**, **Moura I**, **Moura JJG**. 2013. Periplasmic nitrate reductases and formate dehydrogenases: Biological control of the chemical properties of Mo and W for fine tuning of reactivity, substrate specificity and metabolic role. Coord. Chem. Rev. **257**:315–331.

59. **Philippot L**. 2002. Denitrifying genes in bacterial and archaeal genomes. Biochim. Biophys. Acta - Gene Struct. Expr. **1577**:355–376.

60. **Averill BA**. 1996. Dissimilatory nitrite and nitric oxide reductases. Chem. Rev. **96**:2951–2964.

61. **Weeg-Aerssens E**, **Wu WS**, **Ye RW**, **Tiedje JM**, **Chang CK**. 1991. Purification of cytochrome cd1 nitrite reductase from *Pseudomonas stutzeri* JM300 and reconstitution with native and synthetic heme d1. J. Biol. Chem. **266**:7496–7502.

62. **Jones CM**, **Stres B**, **Rosenquist M**, **Hallin S**. 2008. Phylogenetic analysis of nitrite, nitric oxide, and nitrous oxide respiratory enzymes reveal a complex evolutionary history for denitrification. Mol. Biol. Evol. **25**:1955–66.

63. **Kukimoto M**, **Nishiyama M**, **Tanokura M**, **Adman ET**, **Horinouchi S**. 1996. Studies on protein-protein interaction between copper-containing nitrite reductase and pseudoazurin from *Alcaligenes faecalis* S-6. J. Biol. Chem. **271**:13680–13683.

64. **Ye RW**, **Fries MR**, **Bezborodnikov SG**, **Averill BA**, **Tiedje JM**. 1993. Characterization of the structural gene encoding a copper-containing nitrite reductase and homology of this gene to DNA of other denitrifiers. Appl. Environ. Microbiol. **59** :250–254.

65. **Zumft WG**. 2005. Nitric oxide reductases of prokaryotes with emphasis on the respiratory, heme–copper oxidase type. J. Inorg. Biochem. **99**:194–215.

66. **Hendriks J**, **Oubrie A**, **Castresana J**, **Urbani A**, **Gemeinhardt S**, **Saraste M**. 2000. Nitric oxide reductases in bacteria. Biochim. Biophys. Acta - Bioenerg. **1459**:266–273.

67. **Rosenzweig AC**. 2000. Nitrous oxide reductase from Cu_A to Cu_Z. Nat. Struct. Biol. **7**:169-171.

68. **Sanford RA**, **Wagner DD**, **Wu Q**, **Chee-Sanford JC**, **Thomas SH**, **Cruz-García C**, **Rodríguez G**, **Massol-Deyá A**, **Krishnani KK**, **Ritalahti KM**, **Nissen S**, **Konstantinidis KT**, **Löffler FE**. 2012. Unexpected nondenitrifier nitrous oxide reductase gene diversity and abundance in soils . Proc. Natl. Acad. Sci. **109** (48): 19709-19714.

69. **Jones CM**, **Graf DRH**, **Bru D**, **Philippot L**, **Hallin S**. 2013. The unaccounted yet abundant nitrous oxide-reducing microbial community: a potential nitrous oxide sink. Isme J. **7**: 417-426.

70. **Shoun H**. 1992. Denitrification by fungi. FEMS Microbiol. Lett. **94**:277–281.

71. **Morozkina E V.**, **Kurakov A V.** 2007. Dissimilatory nitrate reduction in fungi under conditions of hypoxia and anoxia: A review. Appl. Biochem. Microbiol. **43**:544–549.

72. **Mothapo N V**, **Chen H**, **Cubeta MA**, **Shi W**. 2013. Nitrous oxide producing activity of diverse fungi from distinct agroecosystems. Soil Biol. Biochem.

66:94–101.

73. **Uchimura H**, **Enjoji H**, **Seki T**, **Taguchi A**, **Tsakaya N**, **Shoun+ H**. 2002. Nitrate reductase-formate dehydrogenase couple involved in the fungal denitrification by *Fusarium oxysporum*. J. Biochem. **131** :579–586.

74. **Kobayashi M**, **Shoun H**. 1995. The copper-containing dissimilatory nitrite reductase involved in the denitrifying system of the fungus *Fusarium oxysporum*. J. Biol. Chem. **270**:4146–4151.

75. **Kobayashi M**, **Matsuo Y**, **Takimoto A**, **Suzuki S**, **Maruo F**, **Shoun H**. 1996. Denitrification, a novel type of respiratory metabolism in fungal mitochondrion. J. Biol. Chem. **271**:16263–16267.

76. **Gray MW**, **Burger G**, **Lang BF**. 1999. Mitochondrial evolution. Science. **283**:1476–1481.

77. **Kim S**, **Fushinobu S**, **Zhou S**, **Wakagi T**, **Shoun H**. 2009. Eukaryotic *nirK* genes encoding copper-containing nitrite reductase: originating from the protomitochondrion? Appl. Environ. Microbiol. **75**:2652–2658.

78. **Takaya N**, **Kuwazaki S**, **Adachi Y**, **Suzuki S**, **Kikuchi T**, **Nakamura H**, **Shiro Y**, **Shoun H**. 2003. Hybrid respiration in the denitrifying mitochondria of *Fusarium oxysporum*. J. Biochem. **133**:461–465.

79. **Shoun H**, **Fushinobu S**, **Jiang L**, **Kim S-W**, **Wakagi T**. 2012. Fungal denitrification and nitric oxide reductase cytochrome P450nor. Philos. Trans. R. Soc. Lond. B. Biol. Sci. **367**:1186–94.

80. **Tsuruta S**, **Takaya N**, **Zhang L**, **Shoun H**, **Kimura K**, **Hamamoto M**, **Nakase T**. 1998. Denitrification by yeasts and occurrence of cytochrome P450nor in *Trichosporon cutaneum*. FEMS Microbiol. Lett. **168**:105–110.

81. **Nakahara K**, **Tanimoto T**, **Hatano K**, **Usuda K**, **Shoun H**. 1993. Cytochrome P-450 55A1 (P-450dNIR) acts as nitric oxide reductase employing NADH as the direct electron donor. J. Biol. Chem. **268** :8350–8355.

82. **Shoun H**, **Tanimoto T**. 1991. Denitrification by the fungus *Fusarium oxysporum* and involvement of cytochrome P-450 in the respiratory nitrite

reduction. J. Biol. Chem. **266**:11078–11082.

83. **Shoun H**, **Sudo Y**, **Seto Y**, **Beppu T**. 1983. Purification and properties of a cyotchrome P-450 of a fungus, *Fusarium oxysporum*. J. Biochem. **94**:1219–1229.

84. **Shoun H**, **Suyama W**, **Yasui T**. 1989. Soluble, nitrate/nitrite-inducible cytochrome P-450 of the fungus, *Fusarium oxysporum*. FEBS Lett. **244**:11–14.

85. **Guengerich FP**, **Munro AW**. 2013. Unusual cytochrome P450 enzymes and reactions. J. Biol. Chem. **288**:17065–17073.

86. **McLean JK**, **Leys D**, **Munro WA**. 2015. Microbial Cytochromes P450, p. 261–407. *In* Ortiz de Montellano, (ed.), Cytochrome P450 Structure, Mechanism, and Biochemistry. Springer International Publishing, Cham, Switzerland.

87. **Wink DA**, **Osawa Y**, **Darbyshire JF**, **Jones CR**, **Eshenaur SC**, **Nims RW**. 1993. Inhibition of cytochromes P450 by nitric oxide and a nitric oxide-releasing agent. Arch. Biochem. Biophys. **300**:115–123.

88. **Sarti P**, **Giuffré A**, **Forte E**, **Mastronicola D**, **Barone MC**, **Brunori M**. 2000. Nitric oxide and cytochrome c oxidase: Mechanisms of inhibition and NO degradation. Biochem. Biophys. Res. Commun. **274**:183–187.

89. **Zhao XJ**, **Sampath V**, **Caughey WS**. 1995. Cytochrome c oxidase catalysis of the reduction of nitric oxide to nitrous oxide. Biochem. Biophys. Res. Commun. **212**:1054–1060.

90. **Stubauer G**, **Giuffrè A**, **Brunori M**, **Sarti P**. 1998. Cytochrome c oxidase does not catalyze the anaerobic reduction of NO. Biochem. Biophys. Res. Commun. **245**:459–465.

91. **Spott O**, **Russow R**, **Stange CF**. 2011. Formation of hybrid N_2O and hybrid N_2 due to codenitrification: First review of a barely considered process of microbially mediated N-nitrosation. Soil Biol. Biochem. **43**:1995–2011.

92. **Kumon Y**, **Sasaki Y**, **Kato I**, **Takaya N**, **Shoun H**, **Beppu T**. 2002. Codenitrification and denitrification are dual metabolic pathways through which dinitrogen evolves from nitrate in *Streptomyces antibioticus*. J. Bacteriol. **184**:2963–2968.

93. **Tanimoto T**, **Hatano K**, **Kim D**, **Uchiyama H**, **Shoun H**. 1992. Co-denitrification by the denitrifying system of the fungus *Fusarium oxysporum*. FEMS Microbiol. Lett. **93**:177–180.

94. **Phillips RL**, **Song B**, **McMillan AMS**, **Grelet G**, **Weir BS**, **Palmada T**, **Tobias C**. 2016. Chemical formation of hybrid di-nitrogen calls fungal codenitrification into question. Sci. Rep. **6**:39077.

95. **Bollag J-M**, **Tung G**. 1972. Nitrous oxide release by soil fungi. Soil Biol. Biochem. **4**:271–276.

96. **Bleakley BH**, **Tiedje JM**. 1982. Nitrous oxide production by organisms other than nitrifiers or denitrifiers. Appl. Environ. Microbiol. **44** :1342–1348.

97. **Maeda K**, **Spor A**, **Edel-Hermann V**, **Heraud C**, **Breuil M-C**, **Bizouard F**, **Toyoda S**, **Yoshida N**, **Steinberg C**, **Philippot L**. 2015. N_2O production, a widespread trait in fungi. Sci. Rep. **5**.

98. **Tsuruta S**, **Takaya N**, **Zhang L**, **Shoun H**, **Kimura K**, **Hamamoto M**, **Nakase T**. 1998. Denitrification by yeasts and occurrence of cytochrome P450nor in *Trichosporon cutaneum*. FEMS Microbiol. Lett. **168**:105–110.

99. **Mothapo N**, **Chen H**, **Cubeta MA**, **Grossman JM**, **Fuller F**, **Shi W**. 2015. Phylogenetic, taxonomic and functional diversity of fungal denitrifiers and associated N_2O production efficacy. Soil Biol. Biochem. **83**:160–175.

100. **Prendergast-Miller MT**, **Baggs EM**, **Johnson D**. 2011. Nitrous oxide production by the ectomycorrhizal fungi *Paxillus involutus* and *Tylospora fibrillosa*. FEMS Microbiol. Lett. **316**:31–35.

101. **Jasrotia P**, **Green SJ**, **Canion A**, **Overholt WA**, **Prakash O**, **Wafula D**, **Hubbard D**, **Watson DB**, **Schadt CW**, **Brooks SC**, **Kostka JE**. 2014. Watershed-scale fungal community characterization along a pH gradient in a subsurface environment cocontaminated with uranium and nitrate. Appl.

Environ. Microbiol. **80**:1810–1820.

102. **Chen H**, **Mothapo N V**, **Shi W**. 2014. The significant contribution of fungi to soil N_2O production across diverse ecosystems. Appl. Soil Ecol. **73**:70–77.

103. **Higgins SA**, **Welsh A**, **Orellana LH**, **Konstantinidis KT**, **Chee-Sanford JC**, **Sanford RA**, **Schadt CW**, **Löffler FE**. 2016. Detection and diversity of fungal nitric oxide reductase genes (*p450nor*) in agricultural soils. Appl. Environ. Microbiol. **82**:2919–2928.

104. **Cathrine SJ**, **Raghukumar C**. 2009. Anaerobic denitrification in fungi from the coastal marine sediments off Goa, India. Mycol. Res. **113**:100–109.

105. **Jirout J**. 2015. Nitrous oxide productivity of soil fungi along a gradient of cattle impact. Fungal Ecol. **17**:155–163.

106. **Lavrent'ev RB**, **Zaitsev SA**, **Sudnitsyn II**, **Kurakov A V**. 2008. Nitrous oxide production by fungi in soils under different moisture levels. Moscow Univ. Soil Sci. Bull. **63**:178–183.

107. **O'Donovan A**, **Gupta VK**, **Tuohy MG**. 2013. Fungal specimen collection and processing, p. 67–72. *In* Gupta, VK, Tuohy, MG, Ayyachamy, M, Turner, KM, O'Donovan, A (eds.), Laboratory protocols in fungal biology. Springer New York.

108. **Atlas RM**. 2004. Handbook of microbiological media, 3rd ed. CLC Press, Boca Raton.

109. 2017. Czapek dox agar (modified). Oxoid Ltd.

110. **Su F**, **Takaya N**, **Shoun H**. 2004. Nitrous oxide-forming codenitrification catalyzed by cytochrome P450nor. Biosci. Biotechnol. Biochem. **68**:473–475.

111. **Bååth E**, **Anderson T-H**. 2003. Comparison of soil fungal/bacterial ratios in a pH gradient using physiological and PLFA-based techniques. Soil Biol. Biochem. **35**:955–963.

112. **Anderson JPE**, **Domsch KH**. 1975. Measurement of bacterial and fungal contributions to respiration of selected agricultural and forest soils. Can. J. Microbiol. **21**:314–322.

113. **Anderson JPE**, **Domsch KH**. 1973. Quantification of bacterial and fungal contributions to soil respiration. Arch. Mikrobiol. **93**:113–127.

114. **Johnson CK**, **Vigil MF**, **Doxtader KG**, **Beard WE**. 1996. Measuring bacterial and fungal substrate-induced respiration in dry soils. Soil Biol. Biochem. **28**:427–432.

115. **Rousk J**, **Demoling LAA**, **Bååth E**, **Bååth E**. 2009. Contrasting short-term antibiotic effects on respiration and bacterial growth compromises the validity of the selective respiratory inhibition technique to distinguish fungi and bacteria. Microb. Ecol. **58**:75–85.

116. **Bailey VL**, **Smith JL**, **Bolton Jr. H**. 2002. Fungal-to-bacterial ratios in soils investigated for enhanced C sequestration. Soil Biol. Biochem. **34**:997–1007.

117. **Chen H**, **Mothapo N V**, **Shi W**. 2015. Fungal and bacterial N_2O production regulated by soil amendments of simple and complex substrates. Soil Biol. Biochem. **84**:116–126.

118. **Herold MB**, **Baggs EM**, **Daniell TJ**. 2012. Fungal and bacterial denitrification are differently affected by long-term pH amendment and cultivation of arable soil. Soil Biol. Biochem. **54**:25–35.

119. **Laughlin RJ**, **Rütting T**, **Müller C**, **Watson CJ**, **Stevens RJ**. 2009. Effect of acetate on soil respiration, N_2O emissions and gross N transformations related to fungi and bacteria in a grassland soil. Appl. Soil Ecol. **42**:25–30.

120. **Laughlin RJ**, **Stevens RJ**. 2002. Evidence for fungal dominance of denitrification and codenitrification in a grassland soil. Biogeochemistry **66**:1540–1548.

121. **Yanai Y**, **Toyota K**, **Morishita T**, **Takakai F**, **Hatano R**, **Limin SH**, **Darung U**, **Dohong S**. 2007. Fungal N_2O production in an arable peat soil in Central Kalimantan, Indonesia. Soil Sci. Plant Nutr. **53**:806–811.

122. **Seo DC**, **DeLaune RD**. 2010. Fungal and bacterial mediated denitrification in wetlands: influence of sediment redox condition. Water Res. **44**:2441–50.

123. **Ma WK**, **Farrell RE**, **Siciliano SD**. 2008. Soil formate regulates the fungal nitrous oxide emission pathway. Appl. Environ. Microbiol. **74**:6690–6.

124. **Spokas K**, **Wang D**, **Venterea R**, **Sadowsky M**. 2006. Mechanisms of N_2O production following chloropicrin fumigation. Appl. Soil Ecol. **31**:101–109.

125. **Castaldi S**, **Smith KA**. 1998. Effect of cycloheximide on N_2O and NO_3^- production in a forest and an agricultural soil. Biol. Fertil. Soils **27**:27–34.

126. **Marusenko Y**, **Huber DP**, **Hall SJ**. 2013. Fungi mediate nitrous oxide production but not ammonia oxidation in aridland soils of the southwestern US. Soil Biol. Biochem. **63**:24–36.

127. **Grigoriev I V**, **Nikitin R**, **Haridas S**, **Kuo A**, **Ohm R**, **Otillar R**, **Riley R**, **Salamov A**, **Zhao X**, **Korzeniewski F**, **Smirnova T**, **Nordberg H**, **Dubchak I**, **Shabalov I**. 2014. MycoCosm portal: gearing up for 1000 fungal genomes. Nucleic Acids Res. **42**:D699–D704.

128. **Martin F**, **Cullen D**, **Hibbett D**, **Pisabarro A**, **Spatafora JW**, **Baker SE**, **Grigoriev I V**. 2011. Sequencing the fungal tree of life. New Phytol. **190**:818–821.

129. **Novinscak A**, **Goyer C**, **Zebarth BJ**, **Burton DL**, **Chantigny MH**, **Filion M**. 2016. Novel *P450nor* gene detection assay used to characterize the prevalence and diversity of soil fungal denitrifiers. Appl. Environ. Microbiol. **82**:4560–4569.

130. **Wei W**, **Isobe K**, **Shiratori Y**, **Nishizawa T**, **Ohte N**, **Ise Y**, **Otsuka S**, **Senoo K**. 2015. Development of PCR primers targeting fungal *nirK* to study fungal denitrification in the environment. Soil Biol. Biochem. **81**:282–286.

131. **Long A**, **Song B**, **Fridey K**, **Silva A**. 2015. Detection and diversity of copper containing nitrite reductase genes (*nirK*) in prokaryotic and fungal

communities of agricultural soils. FEMS Microbiol. Ecol. **91**:1–9.

132. **Chen H**, **Yu F**, **Shi W**. 2016. Detection of N_2O-producing fungi in environment using nitrite reductase gene (*nirK*)-targeting primers. Fungal Biol. **120**:1479–1492.

133. **Kwok S**, **Chang SY**, **Sninsky JJ**, **Wang A**. 1994. A guide to the design and use of mismatched and degenerate primers. PCR Methods Appl. **3**:S39–47.

134. **Lindahl BD**, **Nilsson RH**, **Tedersoo L**, **Abarenkov K**, **Carlsen T**, **Kjøller R**, **Kõljalg U**, **Pennanen T**, **Rosendahl S**, **Stenlid J**, **Kauserud H**. 2013. Fungal community analysis by high-throughput sequencing of amplified markers – a user's guide. New Phytol. **199**:288–299.

135. **Mosier AC**, **Miller CS**, **Frischkorn KR**, **Ohm RA**, **Li Z**, **LaButti K**, **Lapidus A**, **Lipzen A**, **Chen C**, **Johnson J**, **Lindquist EA**, **Pan C**, **Hettich RL**, **Grigoriev I V**, **Singer SW**, **Banfield JF**. 2016. Fungi contribute critical but spatially varying roles in nitrogen and carbon cycling in acid mine drainage. Front. Microbiol. **7**:238.

136. **Müller M**, **Mentel M**, **van Hellemond JJ**, **Henze K**, **Woehle C**, **Gould SB**, **Yu R-Y**, **van der Giezen M**, **Tielens AGM**, **Martin WF**. 2012. Biochemistry and evolution of anaerobic energy metabolism in Eukaryotes. Microbiol. Mol. Biol. Rev. **76**:444–495.

137. **Takasaki K**, **Shoun H**, **Yamaguchi M**, **Takeo K**, **Nakamura A**, **Hoshino T**, **Takaya N**. 2004. Fungal ammonia fermentation, a novel metabolic mechanism that couples the dissimilatory and assimilatory pathways of both nitrate and ethanol. Role of acetyl CoA synthetase in anaerobic ATP synthesis. J. Biol. Chem. **279**:12414–20.

138. **Takaya N**. 2002. Dissimilatory nitrate reduction metabolisms and their control in fungi. J. Biosci. Bioeng. **94**:506–510.

139. **Zhou Z**, **Takaya N**, **Nakamura A**, **Yamaguchi M**, **Takeo K**, **Shoun H**. 2002. Ammonia fermentation, a novel anoxic metabolism of nitrate by fungi. J. Biol. Chem. **277**:1892–1896.

140. **Stief P**, **Fuchs-Ocklenburg S**, **Kamp A**, **Manohar C-S**, **Houbraken J**, **Boekhout T**, **de Beer D**, **Stoeck T**. 2014. Dissimilatory nitrate reduction by *Aspergillus terreus* isolated from the seasonal oxygen minimum zone in the Arabian Sea. BMC Microbiol. **14**:35.

141. **Welsh A**, **Chee-Sanford JC**, **Connor LM**, **Löffler FE**, **Sanford RA**. 2014. Refined NrfA phylogeny improves PCR-Based *nrfA* gene detection. Appl. Environ. Microbiol. **80**:2110–2119.

142. **Kuwazaki S**, **Takaya N**, **Nakamura A**, **Shoun H**. 2003. Formate-forming fungal catabolic pathway to supply electrons to nitrate respiration. Biosci. Biotechnol. Biochem. **67**:937–939.

143. **Stewart V**. 1988. Nitrate respiration in relation to facultative metabolism in enterobacteria. Microbiol. Rev. **52**:190–232.

144. **Stairs CW**, **Roger AJ**, **Hampl V**. 2011. Eukaryotic pyruvate formate lyase and its activating enzyme were acquired laterally from a firmicute. Mol. Biol. Evol. **28**:2087–2099.

145. **Zhou Z**, **Takaya N**, **Sakairi MAC**, **Shoun H**. 2001. Oxygen requirement for denitrification by the fungus *Fusarium oxysporum*. Arch. Microbiol. **175**:19–25.

146. **Tomura D**, **Obika E**, **Fukamizu K**, **Shoun I**. 1994. Nitric oxide reductase cytochrome P-450 gene, CYP 55, of the fungus *Fusarium oxysporum* containing a potential binding-site for FNR, the transcription factor involved in the regulation of anaerobic growth of *Escherichia coli*. J. Biochem. **116**:88–94.

147. **Usuda K**, **Toritsuka N**, **Matsuo Y**, **Kim DH**, **Shoun H**. 1995. Denitrification by the fungus *Cylindrocarpon tonkinense*: anaerobic cell growth and two isozyme forms of cytochrome P-450nor. Appl. Environ. Microbiol. **61**:883–889.

148. **Kaya M**, **Matsumura K**, **Higashida K**, **Hata Y**, **Kawato A**, **Abe Y**, **Akita O**, **Takaya N**, **Shoun H**. 2004. Cloning and enhanced expression of the cytochrome P450nor gene (*nicA*; CYP55A5) encoding nitric oxide reductase from *Aspergillus oryzae*. Biosci. Biotechnol. Biochem. **68**:2040–

2049.

149. **Shiro Y**, **Fujii M**, **Iizuka T**, **Adachi S**, **Tsukamoto K**, **Nakahara K**, **Shoun H**. 1995. Spectroscopic and kinetic studies on reaction of cytochrome P450nor with nitric oxide: Implication for its nitric oxide reduction mechanism. J. Biol. Chem. **270**:1617–1623.

150. **Zhang L**, **Shoun H**. 2008. Purification and functional analysis of fungal nitric oxide reductase cytochrome P450nor, p. 117–133. *In* Poole, RK (ed.), Globins and other nitric oxide-reactive proteins, Part B. Academic Press, Cambridge, MA.

151. **Daiber A**, **Nauser T**, **Takaya N**, **Kudo T**, **Weber P**, **Hultschig C**, **Shoun H**, **Ullrich V**. 2002. Isotope effects and intermediates in the reduction of NO by P450NOR. J. Inorg. Biochem. **88**:343–352.

152. **Takaya N**, **Suzuki S**, **Kuwazaki S**, **Shoun H**, **Maruo F**, **Yamaguchi M**, **Takeo K**. 1999. Cytochrome P450nor, a novel class of mitochondrial cytochrome P450 involved in nitrate respiration in the fungus *Fusarium oxysporum*. Arch. Biochem. Biophys. **372**:340–346.

153. **Nakahara K**, **Shoun H**. 1996. N-Terminal processing and amino acid sequence of two isoforms of nitric oxide reductase cytochrome P450nor from *Fusarium oxysporum*. J. Biochem. **120** :1082–1087.

154. **Zhang L**, **Takaya N**, **Kitazume T**, **Kondo T**, **Shoun H**. 2001. Purification and cDNA cloning of nitric oxide reductase cytochrome P450nor (CYP55A4) from *Trichosporon cutaneum*. Eur. J. Biochem. **268**:3198–3204.

155. **Crenshaw C**, **Lauber C**, **Sinsabaugh R**, **Stavely L**. 2008. Fungal control of nitrous oxide production in semiarid grassland. Biogeochemistry **87**:17–27.

156. **Wei W**, **Isobe K**, **Shiratori Y**, **Nishizawa T**, **Ohte N**, **Otsuka S**, **Senoo K**. 2014. N_2O emission from cropland field soil through fungal denitrification after surface applications of organic fertilizer. Soil Biol. Biochem. **69**:157–167.

157. **Kurakov A V**, **Nosikov AN**, **Skrynnikova E V**, **L'vov NP**. 2000. Nitrate reductase and nitrous oxide production by *Fusarium oxysporum* 11dn1 under aerobic and anaerobic conditions. Curr. Microbiol. **41**:114–119.

158. **Tanimoto T**, **Nakahara K**, **Shoun H**. 1992. Diauxic growth of *Fusarium oxysporum* during aerobic culture in the presence of nitrate/nitrite. Biosci. Biotechnol. Biochem. **56**:2058–2059.

159. **Wells JM**, **Uota M**. 1970. Germination and growth of five fungi in low-oxygen and high-carbon dioxide atmospheres. Phytopathology **60**:50–53.

160. **Ladan S**, **Jacinthe P-A**. 2016. Evaluation of antibacterial and antifungal compounds for selective inhibition of denitrification in soils. Environ. Sci. Process. Impacts. **18**: 1519-1529.

161. **Frostegård A**, **Bååth E**. 1996. The use of phospholipid fatty acid analysis to estimate bacterial and fungal biomass in soil. Biol. Fertil. Soils **22**:59–65.

162. **Helgason BL**, **Walley FL**, **Germida JJ**. 2009. Fungal and bacterial abundance in long-term no-till and intensive-till soils of the Northern Great Plains. Soil Sci. Soc. Amer. J. **73** (1): 120-127.

163. **Baldrian P**, **Merhautová V**, **Cajthaml T**, **Petránková M**, **Šnajdr J**. 2010. Small-scale distribution of extracellular enzymes, fungal, and bacterial biomass in *Quercus petraea* forest topsoil. Biol. Fertil. Soils **46**:717–726.

164. **Weathers PJ**. 1984. N_2O evolution by green algae. Appl. Environ. Microbiol. **48**:1251–1253.

165. **Guieysse B**, **Plouviez M**, **Coilhac M**, **Cazali L**. 2013. Nitrous oxide (N_2O) production in axenic *Chlorella vulgaris* microalgae cultures: evidence, putative pathways, and potential environmental impacts. Biogeosciences **10**:6737–6746.

166. **Risgaard-Petersen N**, **Langezaal AM**, **Ingvardsen S**, **Schmid MC**, **Jetten MSM**, **Op den Camp HJM**, **Derksen JWM**, **Pina-Ochoa E**, **Eriksson SP**, **Peter Nielsen L**, **Peter Revsbech N**, **Cedhagen T**, **van der Zwaan GJ**. 2006. Evidence for complete denitrification in a benthic foraminifer. Nature **443**:93–96.

167. **Kamp A**, **Høgslund S**, **Risgaard-Petersen N**, **Stief P**. 2015. Nitrate storage and dissimilatory nitrate reduction by eukaryotic microbes. Front. Microbiol. **6**:1492.

168. **Bernhard JM**, **Edgcomb VP**, **Casciotti KL**, **McIlvin MR**, **Beaudoin DJ**. 2012. Denitrification likely catalyzed by endobionts in an allogromiid foraminifer. ISME J **6**:951–960.

169. **Bernhard JM**, **Casciotti KL**, **McIlvin MR**, **Beaudoin DJ**, **Visscher PT**, **Edgcomb VP**. 2012. Potential importance of physiologically diverse benthic foraminifera in sedimentary nitrate storage and respiration. J. Geophys. Res. **117**:1–14.

170. **Nomaki H**, **Chikaraishi Y**, **Tsuchiya M**, **Toyofuku T**, **Ohkouchi N**, **Uematsu K**, **Tame A**, **Kitazato H**. 2014. Nitrate uptake by foraminifera and use in conjunction with endobionts under anoxic conditions. Limnol. Oceanogr. **59**:1879–1888.

171. **Piña-Ochoa E**, **Høgslund S**, **Geslin E**, **Cedhagen T**, **Revsbech NP**, **Nielsen LP**, **Schweizer M**, **Jorissen F**, **Rysgaard S**, **Risgaard-Petersen N**. 2010. Widespread occurrence of nitrate storage and denitrification among Foraminifera and Gromiida. Proc. Natl. Acad. Sci. **107** :1148–1153.

172. **Partida-Martinez LP**, **Hertweck C**. 2005. Pathogenic fungus harbours endosymbiotic bacteria for toxin production. Nature **437**:884–888.

173. **Ibrahim AS**, **Gebremariam T**, **Liu M**, **Chamilos G**, **Kontoyiannis DP**, **Mink R**, **Kwon-Chung KJ**, **Fu Y**, **Skory CD**, **Edwards John E. J**, **Spellberg B**. 2008. Bacterial endosymbiosis is widely present among Zygomycetes but does not contribute to the pathogenesis of Mucormycosis. J. Infect. Dis. **198**:1083–1090.

174. **X. S**, **T. S**, **Y. O**, **A. K**, **J. G**, **Katayama Y**. 2010. Oxidation of elemental sulfur by *Fusarium solani* strain THIF01 harboring endobacterium *Bradyrhizobium* sp. Microb. Ecol. **60**:96–104.

175. **Shoun H**. 1992. Fungal denitrification and cytochrome P-450. J. Agric. Chem. Soc. Japan **66**:154–157.
176. **Blagodatskaya E**, **Dannenmann M**, **Gasche R**, **Butterbach-Bahl K**.

2010. Microclimate and forest management alter fungal-to-bacterial ratio and N_2O-emission during rewetting in the forest floor and mineral soil of mountainous beech forests. Biogeochemistry **97**:55–70.

177. **Banihani Q**, **Sierra-Alvarez R**, **Field J**. 2009. Nitrate and nitrite inhibition of methanogenesis during denitrification in granular biofilms and digested domestic sludges. Biodegradation **20**:801–812.

178. **Yoon S**, **Sanford RA**, **Löffler FE**. 2013. *Shewanella* spp. use acetate as an electron donor for denitrification but not ferric iron or fumarate reduction. Appl. Environ. Microbiol. **79**:2818–2822.

179. **Long GL**, **Winefordner JD**. 1983. Limit of detection. A closer look at the IUPAC definition. Anal. Chem. **55**:712A–724A.

180. **Hughes KW**, **McGhee LL**, **Methven AS**, **Johnson JE**, **Petersen RH**. 1999. Patterns of geographic speciation in the genus *Flammulina* based on sequences of the ribosomal ITS1-5.8S-ITS2 area. Mycologia **91**:978–986.

181. **Geer LY**, **Marchler-Bauer A**, **Geer RC**, **Han L**, **He J**, **He S**, **Liu C**, **Shi W**, **Bryant SH**. 2009. The NCBI BioSystems database. Nucleic Acids Res. .

182. **Altschul SF**, **Gish W**, **Miller W**, **Myers EW**, **Lipman DJ**. 1990. Basic local alignment search tool. J. Mol. Biol. **215**:403–410.

183. **Notredame C**, **Higgins DG**, **Heringa J**. 2000. T-coffee: a novel method for fast and accurate multiple sequence alignment. J. Mol. Biol. **302**:205–217.

184. **Suyama M**, **Torrents D**, **Bork P**. 2006. PAL2NAL: robust conversion of protein sequence alignments into the corresponding codon alignments. Nucleic Acids Res. **34** :W609–W612.

185. **White TJ**, **Bruns T**, **Lee S**, **Taylor J**. 1990. Amplification and direct sequencing of fungal ribosomal RNA genes for phylogenetics, p. 479. *In* Innis, MA, Gelfand, DH, Sninsky, JJ, White, TJ (eds.), PCR protocols: A guide to methods and applications. Academic Press, San Diego.

186. **Lord NS**, **Kaplan CW**, **Shank P**, **Kitts CL**, **Elrod SL**. 2002. Assessment of

fungal diversity using terminal restriction fragment (TRF) pattern analysis: comparison of 18S and ITS ribosomal regions. FEMS Microbiol. Ecol. **42**:327–337.

187. **Hibbett DS**. 1996. Phylogenetic evidence for horizontal transmission of group I introns in the nuclear ribosomal DNA of mushroom-forming fungi. Mol. Biol. Evol. **13** :903–917.

188. **O'Donnell K**, **Cigelnik E**, **Benny GL**. 1998. Phylogenetic relationships among the *Harpellales* and *Kickxellales*. Mycologia **90**:624–639.

189. **Nilsson RH**, **Bok G**, **Ryberg M**, **Kristiansson E**, **Hallenberg N**. 2009. A software pipeline for processing and identification of fungal ITS sequences. Source Code Biol. Med. **4**:1.

190. **Nakamura Y**, **Cochrane G**, **Karsch-Mizrachi I**. 2013. The international nucleotide sequence database collaboration. Nucleic Acids Res. **41**:D21–D24.

191. **Pruesse E**, **Peplies J**, **Glöckner FO**. 2012. SINA: Accurate high-throughput multiple sequence alignment of ribosomal RNA genes. Bioinforma. **28** :1823–1829.

192. **Pruesse E**, **Quast C**, **Knittel K**, **Fuchs BM**, **Ludwig W**, **Peplies J**, **Glöckner FO**. 2007. SILVA: a comprehensive online resource for quality checked and aligned ribosomal RNA sequence data compatible with ARB. Nucleic Acids Res. **35** :7188–7196.

193. **Orellana LH**, **Rodriguez-R LM**, **Higgins S**, **Chee-Sanford JC**, **Sanford RA**, **Ritalahti KM**, **Löffler FE**, **Konstantinidis KT**. 2014. Detecting nitrous oxide reductase (*nosZ*) genes in soil metagenomes: method development and implications for the nitrogen cycle. MBio **5**:e01193–14.

194. **Leinonen R**, **Sugawara H**, **Shumway M**. 2010. The sequence read archive. Nucleic Acids Res. 1–3.

195. **Cox M**, **Peterson D**, **Biggs P**. 2010. SolexaQA: At-a-glance quality assessment of Illumina second-generation sequencing data. BMC Bioinformatics **11**:485.

196. **Dannemiller KC**, **Reeves D**, **Bibby K**, **Yamamoto N**, **Peccia J**. 2014. Fungal high-throughput taxonomic identification tool for use with next-generation sequencing (FHiTINGS). J. Basic Microbiol. **54**:315–321.

197. **Suzek BE**, **Huang H**, **McGarvey P**, **Mazumder R**, **Wu CH**. 2007. UniRef: comprehensive and non-redundant UniProt reference clusters. Bioinforma. **23** :1282–1288.

198. **Katoh K**, **Asimenos G**, **Toh H**. 2009. Multiple alignment of DNA sequences with MAFFT. Methods Mol. Biol. **537**:39–64.

199. **Clamp M**, **Cuff J**, **Searle SM**, **Barton GJ**. 2004. The Jalview Java alignment editor. Bioinforma. **20** :426–427.

200. **Waterhouse AM**, **Procter JB**, **Martin DMA**, **Clamp M**, **Barton GJ**. 2009. Jalview Version 2—a multiple sequence alignment editor and analysis workbench. Bioinforma. **25** :1189–1191.

201. **Galtier N**, **Gouy M**, **Gautier C**. 1996. SEAVIEW and PHYLO_WIN: two graphic tools for sequence alignment and molecular phylogeny. Comput. Appl. Biosci. **12**:543–548.

202. **Darriba D**, **Taboada GL**, **Doallo R**, **Posada D**. 2011. ProtTest 3: fast selection of best-fit models of protein evolution. Bioinforma. **27** :1164–1165.

203. **Price MN**, **Dehal PS**, **Arkin AP**. 2010. FastTree 2 – approximately maximum-likelihood trees for large alignments. PLoS One **5**:e9490.

204. **Whelan S**, **Goldman N**. 2001. A general empirical model of protein evolution derived from multiple protein families using a maximum-likelihood approach. Mol. Biol. Evol. **18**:691–699.

205. **Robert X**, **Gouet P**. 2014. Deciphering key features in protein structures with the new ENDscript server. Nucleic Acids Res. **42** :W320–W324.

206. **Gams W**, **Bisset J**. 1998. Morphology and identification of *Trichoderma*. p. 3–34. *In* Kubicek, CP, Harman, GE (eds.), *Trichoderma* and *Gliocladium*

Volume 1: Basic biology, taxonomy and genetics. Taylor & Francis, Bristol, PA.

207. **Staley, J. T**, **Konopka A**. 1985. Measurement of in situ activities of nonphotosynthetic microorganisms in aquatic and terrestrial habitats. Annu. Rev. Microbiol. **39**:321–346.

208. **Blackwell M**. 2011. The Fungi: 1, 2, 3 … 5.1 million species? Am. J. Bot. **98** :426–438.

209. **Hawksworth DL**. 2012. Global species numbers of fungi: are tropical studies and molecular approaches contributing to a more robust estimate? Biodivers. Conserv. **21**:2425–2433.

210. **Brooks MH**, **Smith RL**, **Macalady DL**. 1992. Inhibition of existing denitrification enzyme activity by chloramphenicol. Appl. Environ. Microbiol. **58**:1746–1753.

211. **Ma WK**, **Bedard-Haughn A**, **Siciliano SD**, **Farrell RE**. 2008. Relationship between nitrifier and denitrifier community composition and abundance in predicting nitrous oxide emissions from ephemeral wetland soils. Soil Biol. Biochem. **40**:1114–1123.

212. **Moore D**, **Robson GD**, **Trinci APJ**. 2011. 21st century guidebook to fungi, 1st ed. Cambridge.

213. **Luo C**, **Rodriguez-R LM**, **Konstantinidis KT**. 2013. A user's guide to quantitative and comparative analysis of metagenomic datasets, p. 525–547. *In* Microbial Metagenomics, Metatranscriptomics, and Metaproteomics. Academic Press, San Diego, CA..

214. **Takaya N**, **Shoun H**. 2000. Nitric oxide reduction, the last step in denitrification by *Fusarium oxysporum*, is obligatorily mediated by cytochrome P450nor. Mol. Gen. Genet. MGG **263**:342–348.

215. **Lundberg DS**, **Yourstone S**, **Mieczkowski P**, **Jones CD**, **Dangl JL**. 2013. Practical innovations for high-throughput amplicon sequencing. Nat Meth **10**:999–1002.

216. **Tedersoo L**, **Bahram M**, **Põlme S**, **Kõljalg U**, **Yorou NS**, **Wijesundera R**, **Ruiz LV**, **Vasco-Palacios AM**, **Thu PQ**, **Suija A**, **Smith ME**, **Sharp C**, **Saluveer E**, **Saitta A**, **Rosas M**, **Riit T**, **Ratkowsky D**, **Pritsch K**, **Põldmaa K**, **Piepenbring M**, **Phosri C**, **Peterson M**, **Parts K**, **Pärtel K**, **Otsing E**, **Nouhra E**, **Njouonkou AL**, **Nilsson RH**, **Morgado LN**, **Mayor J**, **May TW**, **Majuakim L**, **Lodge DJ**, **Lee SS**, **Larsson K-H**, **Kohout P**, **Hosaka K**, **Hiiesalu I**, **Henkel TW**, **Harend H**, **Guo L**, **Greslebin A**, **Grelet G**, **Geml J**, **Gates G**, **Dunstan W**, **Dunk C**, **Drenkhan R**, **Dearnaley J**, **De Kesel A**, **Dang T**, **Chen X**, **Buegger F**, **Brearley FQ**, **Bonito G**, **Anslan S**, **Abell S**, **Abarenkov K**. 2014. Global diversity and geography of soil fungi. Science. **346** (6213): 1256688. .

217. **Caporaso JG**, **Kuczynski J**, **Stombaugh J**, **Bittinger K**, **Bushman FD**, **Costello EK**, **Fierer N**, **Pena AG**, **Goodrich JK**, **Gordon JI**, **Huttley GA**, **Kelley ST**, **Knights D**, **Koenig JE**, **Ley RE**, **Lozupone CA**, **McDonald D**, **Muegge BD**, **Pirrung M**, **Reeder J**, **Sevinsky JR**, **Turnbaugh PJ**, **Walters WA**, **Widmann J**, **Yatsunenko T**, **Zaneveld J**, **Knight R**. 2010. QIIME allows analysis of high-throughput community sequencing data. Nat Meth **7**:335–336.

218. **Wang Q**, **Quensen JF**, **Fish JA**, **Kwon Lee T**, **Sun Y**, **Tiedje JM**, **Cole JR**. 2013. Ecological patterns of *nifH* genes in four terrestrial climatic zones explored with targeted metagenomics using FrameBot, a new informatics tool. MBio **4** (5): e00592-13.

219. **Rideout JR**, **He Y**, **Navas-Molina JA**, **Walters WA**, **Ursell LK**, **Gibbons SM**, **Chase J**, **McDonald D**, **Gonzalez A**, **Robbins-Pianka A**, **Clemente JC**, **Gilbert JA**, **Huse SM**, **Zhou H-W**, **Knight R**, **Caporaso JG**. 2014. Subsampled open-reference clustering creates consistent, comprehensive OTU definitions and scales to billions of sequences. PeerJ **2**:e545.

220. **Edgar RC**. 2013. UPARSE: highly accurate OTU sequences from microbial amplicon reads. Nat Meth **10**:996–998.

221. **Gweon HS**, **Oliver A**, **Taylor J**, **Booth T**, **Gibbs M**, **Read DS**, **Griffiths RI**, **Schonrogge K**. 2015. PIPITS: an automated pipeline for analyses of fungal internal transcribed spacer sequences from the Illumina sequencing platform. Methods Ecol. Evol. **6**:973–980.

222. **McMurdie PJ**, **Holmes S**. 2013. phyloseq: An R package for reproducible interactive analysis and graphics of microbiome census data. PLoS One

8:e61217.

223. **Zhang J**, **Kobert K**, **Flouri T**, **Stamatakis A**. 2014. PEAR: a fast and accurate Illumina Paired-End reAd mergeR. Bioinformatics **30**:614–620.

224. **Gordon A, Hannon GJ**. 2010. FASTX Toolkit FASTQ/A short-reads pre-processing tools.

225. **Bengtsson-Palme J**, **Ryberg M**, **Hartmann M**, **Branco S**, **Wang Z**, **Godhe A**, **De Wit P**, **Sánchez-García M**, **Ebersberger I**, **de Sousa F**, **Amend A**, **Jumpponen A**, **Unterseher M**, **Kristiansson E**, **Abarenkov K**, **Bertrand YJK**, **Sanli K**, **Eriksson KM**, **Vik U**, **Veldre V**, **Nilsson RH**. 2013. Improved software detection and extraction of ITS1 and ITS2 from ribosomal ITS sequences of fungi and other eukaryotes for analysis of environmental sequencing data. Methods Ecol. Evol. **4**:914–919.

226. **Rognes T**, **Flouri T**, **Nichols B**, **Quince C**, **Mahé F**. 2016. VSEARCH: a versatile open source tool for metagenomics. PeerJ **4**:e2584.

227. **Abarenkov K**, **Henrik Nilsson R**, **Larsson K-H**, **Alexander IJ**, **Eberhardt U**, **Erland S**, **Høiland K**, **Kjøller R**, **Larsson E**, **Pennanen T**, **Sen R**, **Taylor AFS**, **Tedersoo L**, **Ursing BM**, **Vrålstad T**, **Liimatainen K**, **Peintner U**, **Kõljalg U**. 2010. The UNITE database for molecular identification of fungi – recent updates and future perspectives. New Phytol. **186**:281–285.

228. **Wang Q**, **Garrity GM**, **Tiedje JM**, **Cole JR**. 2007. Naïve bayesian classifier for rapid assignment of rRNA sequences into the new bacterial taxonomy. Appl. Environ. Microbiol. **73**:5261–5267.

229. **Dixon P**, **Palmer MW**. 2003. VEGAN, a package of R functions for community ecology. J. Veg. Sci. **14**:927–930.

230. **Team RDC**. 2012. R: A language and environment for statistical computing. R Foundation for Statistical Computing, Vienna, Austria.

231. **Lee CK**, **Herbold CW**, **Polson SW**, **Wommack KE**, **Williamson SJ**, **McDonald IR**, **Cary SC**. 2012. Groundtruthing next-gen sequencing for microbial ecology–biases and errors in sommunity structure estimates from

PCR amplicon pyrosequencing. PLoS One **7**:e44224.

232. **Penton CR**, **Johnson TA**, **Quensen JF**, **Iwai S**, **Cole JR**, **Tiedje JM**. 2013. Functional genes to assess nitrogen cycling and aromatic hydrocarbon degradation: primers and processing matter. Front. Microbiol. **4**:279.

233. **Wang J-G**, **Xia F**, **Zeleke J**, **Zou B**, **Rhee S-K**, **Quan Z-X**. 2017. An improved protocol with a highly degenerate primer targeting copper-containing membrane-bound monooxygenase genes for community analysis of methane- and ammonia-oxidizing bacteria. FEMS Microbiol. Ecol. **93**:fiw244–fiw244.

234. **Kebschull JM**, **Zador AM**. 2015. Sources of PCR-induced distortions in high-throughput sequencing data sets. Nucleic Acids Res. **43**:e143–e143.

235. **Matsen FA**, **Kodner RB**, **Armbrust EV**. 2010. Pplacer: linear time maximum-likelihood and Bayesian phylogenetic placement of sequences onto a fixed reference tree. BMC Bioinformatics **11**:538.

236. **Rousk J**, **Baath E**, **Brookes PC**, **Lauber CL**, **Lozupone C**, **Caporaso JG**, **Knight R**, **Fierer N**. 2010. Soil bacterial and fungal communities across a pH gradient in an arable soil. ISME J **4**:1340–1351.

237. **Hawkes CV**, **Kivlin SN**, **Rocca JD**, **Huguet V**, **Thomsen MA**, **Suttle KB**. 2011. Fungal community responses to precipitation. Glob. Chang. Biol. **17**:1637–1645.

238. **Tringe SG**, **Mering C von**, **Kobayashi A**, **Salamov AA**, **Chen K**, **Chang HW**, **Podar M**, **Short JM**, **Mathur EJ**, **Detter JC**, **Bork P**, **Hugenholtz P**, **Rubin EM**. 2005. Comparative metagenomics of microbial communities. Science. **308**:554–557.

239. **Vieites JM**, **Guazzaroni M-E**, **Beloqui A**, **Golyshin PN**, **Ferrer M**. 2009. Metagenomics approaches in systems microbiology. FEMS Microbiol. Rev. **33**:236–255.

240. **Brulc JM**, **Antonopoulos DA**, **Berg Miller ME**, **Wilson MK**, **Yannarell AC**, **Dinsdale EA**, **Edwards RE**, **Frank ED**, **Emerson JB**, **Wacklin P**,

Coutinho PM, **Henrissat B**, **Nelson KE**, **White BA**, **Miller MEB**, **Wilson MK**, **Yannarell AC**, **Dinsdale EA**, **Edwards RE**, **Frank ED**, **Emerson JB**, **Wacklin P**, **Coutinho PM**, **Henrissat B**, **Nelson KE**, **White BA**. 2009. Gene-centric metagenomics of the fiber-adherent bovine rumen microbiome reveals forage specific glycoside hydrolases. Proc. Natl. Acad. Sci. **106**:1948–53.

241. **Iwai S**, **Chai B**, **Jesus E da C**, **Penton CR**, **Lee TK**, **Cole JR**, **Tiedje JM**. 2011. Gene-targeted metagenomics (GT Metagenomics) to explore the extensive diversity of genes of interest in microbial communities, p. 235–243. *In* Handbook of Molecular Microbial Ecology I. John Wiley & Sons, Inc. Hoboken, NJ.

242. **Galloway JN**, **Townsend AR**, **Erisman JW**, **Bekunda M**, **Cai Z**, **Freney JR**, **Martinelli L a**, **Seitzinger SP**, **Sutton M a**. 2008. Transformation of the nitrogen cycle: Recent trends, questions, and potential solutions. Science (80-.). **320**:889–892.

243. **Shimizu H**, **Park S-Y**, **Shiro Y**, **Adachi S**. 2002. X-ray structure of nitric oxide reductase (cytochrome P450nor) at atomic resolution. Acta Crystallogr. Sect. D **58**:81–89.

244. **Li Y**, **Liu Q**, **Liang X**, **Xiao Q**, **Fang Y**, **Wu Y**. 2016. A new fluorescence biosensor for nitric oxide detection based on cytochrome P450 55B1. Sensors Actuators B Chem. **230**:405–410.

245. **Jones CM**, **Hallin S**. 2010. Ecological and evolutionary factors underlying global and local assembly of denitrifier communities. ISME J **4**:633–641.

246. **Fierer N**, **Lauber CL**, **Ramirez KS**, **Zaneveld J**, **Bradford MA**, **Knight R**. 2012. Comparative metagenomic, phylogenetic and physiological analyses of soil microbial communities across nitrogen gradients. ISME J **6**:1007–1017.

247. **Blackwell M**, **Hibbett DS**, **Taylor JW**, **Spatafora JW**. 2006. Research coordination networks: a phylogeny for kingdom Fungi (Deep Hypha). Mycologia **98**:829–837.

248. **Moktali V**, **Park J**, **Fedorova-Abrams N**, **Park B**, **Choi J**, **Lee Y-H**, **Kang S**. 2012. Systematic and searchable classification of cytochrome P450

proteins encoded by fungal and oomycete genomes. BMC Genomics **13**:525.

249. **Kizawa H**, **Tomura D**, **Oda M**, **Fukamizu A**, **Hoshino T**, **Gotoh O**, **Yasui T**, **Shoun H**. 1991. Nucleotide sequence of the unique nitrate/nitrite-inducible cytochrome P-450 cDNA from *Fusarium oxysporum*. J. Biol. Chem. **266**:10632–10637.

250. **Chen W**, **Lee M-K**, **Jefcoate C**, **Kim S-C**, **Chen F**, **Yu J-H**. 2014. Fungal cytochrome P450 monooxygenases: their distribution, structure, functions, family expansion, and evolutionary origin. Genome Biol. Evol. **6**:1620–1634.

251. **Shapleigh JP**. 2013. Denitrifying prokaryotes, p. 405–425. *In* Rosenberg, E, DeLong, EF, Lory, S, Stackebrandt, E, Thompson, F (eds.), The prokaryotes: Prokaryotic physiology and biochemistry. Springer Berlin Heidelberg, Berlin, Heidelberg.

252. **Shapleigh JP**. 2013. Denitrifying prokaryotes, p. 405–425. *In* Rosenberg, E, DeLong, EF, Lory, S, Stackebrandt, E, Thompson, F (eds.), The prokaryotes: Prokaryotic physiology and biochemistry. Springer Berlin Heidelberg, Berlin, Heidelberg.

253. **Moody SC**, **Loveridge EJ**. 2014. CYP105—diverse structures, functions and roles in an intriguing family of enzymes in *Streptomyces*. J. Appl. Microbiol. **117**:1549–1563.

254. **Barry SM**, **Kers JA**, **Johnson EG**, **Song L**, **Aston PR**, **Patel B**, **Krasnoff SB**, **Crane BR**, **Gibson DM**, **Loria R**, **Challis GL**. 2012. Cytochrome P450–catalyzed L-tryptophan nitration in thaxtomin phytotoxin biosynthesis. Nat Chem Biol **8**:814–816.

255. **Dodani SC**, **Cahn JKB**, **Heinisch T**, **Brinkmann-Chen S**, **McIntosh JA**, **Arnold FH**. 2014. Structural, functional, and spectroscopic characterization of the substrate scope of the novel nitrating cytochrome P450 TxtE. Chembiochem **15**:2259–2267.

256. **Schmitt I**, **Lumbsch HT**. 2009. Ancient horizontal gene transfer from bacteria enhances biosynthetic capabilities of fungi. PLoS One **4**:e4437.

257. **Simão FA**, **Waterhouse RM**, **Ioannidis P**, **Kriventseva E V**, **Zdobnov EM**. 2015. BUSCO: assessing genome assembly and annotation completeness with single-copy orthologs. Bioinforma. **31**:3210–3212.

258. **She R**, **Chu JS-C**, **Uyar B**, **Wang J**, **Wang K**, **Chen N**. 2011. genBlastG: using BLAST searches to build homologous gene models. Bioinforma. **27**:2141–2143.

259. **Li W**, **Cowley A**, **Uludag M**, **Gur T**, **McWilliam H**, **Squizzato S**, **Park YM**, **Buso N**, **Lopez R**. 2015. The EMBL-EBI bioinformatics web and programmatic tools framework. Nucleic Acids Res. **43**:W580–W584.

260. **Mistry J**, **Bateman A**, **Finn RD**. 2007. Predicting active site residue annotations in the Pfam database. BMC Bioinformatics **8**:298.

261. **Finn RD**, **Mistry J**, **Tate J**, **Coggill P**, **Heger A**, **Pollington JE**, **Gavin OL**, **Gunasekaran P**, **Ceric G**, **Forslund K**, **Holm L**, **Sonnhammer ELL**, **Eddy SR**, **Bateman A**. 2010. The Pfam protein families database. Nucleic Acids Res. **38**::D211–D222.

262. 2015. UniProt: a hub for protein information. Nucleic Acids Res. **43**:D204–D212.

263. **Wisecaver JH**, **Alexander WG**, **King SB**, **Todd Hittinger C**, **Rokas A**. 2016. Dynamic evolution of nitric oxide detoxifying flavohemoglobins, a family of single-protein metabolic modules in *Bacteria* and Eukaryotes. Mol. Biol. Evol. **33** (8):1979-1987.

264. **Pruitt KD**, **Tatusova T**, **Maglott DR**. 2007. NCBI reference sequences (RefSeq): a curated non-redundant sequence database of genomes, transcripts and proteins. Nucleic Acids Res. **35**:D61–D65.

265. **Inglis D**, **Binkley J**, **Skrzypek M**, **Arnaud M**, **Cerqueira G**, **Shah P**, **Wymore F**, **Wortman J**, **Sherlock G**. 2013. Comprehensive annotation of secondary metabolite biosynthetic genes and gene clusters of *Aspergillus nidulans*, *A. fumigatus*, *A. niger* and *A. oryzae*. BMC Microbiol. **13**:91.

266. **Powell S**, **Szklarczyk D**, **Trachana K**, **Roth A**, **Kuhn M**, **Muller J**, **Arnold R**, **Rattei T**, **Letunic I**, **Doerks T**, **Jensen LJ**, **von Mering C**, **Bork P**.

2012. eggNOG v3.0: orthologous groups covering 1133 organisms at 41 different taxonomic ranges. Nucleic Acids Res. **40**:D284–D289.

267. **Mirarab S**, **Warnow T**. 2015. ASTRAL-II: coalescent-based species tree estimation with many hundreds of taxa and thousands of genes. Bioinformatics **31**:i44–i52.

268. **Stamatakis A**. 2006. RAxML-VI-HPC: maximum likelihood-based phylogenetic analyses with thousands of taxa and mixed models. Bioinformatics **22**:2688–2690.

269. **Ronquist F**, **Teslenko M**, **van der Mark P**, **Ayres DL**, **Darling A**, **Höhna S**, **Larget B**, **Liu L**, **Suchard MA**, **Huelsenbeck JP**. 2012. MrBayes 3.2: efficient Bayesian phylogenetic inference and model choice across a large model space. Syst. Biol. **61**:539–542.

270. **Abascal F**, **Zardoya R**, **Posada D**. 2005. ProtTest: selection of best-fit models of protein evolution. Bioinforma. **21** :2104–2105.

271. **Posada D**. 2008. jModelTest: Phylogenetic model averaging. Mol. Biol. Evol. **25**:1253–1256.

272. **Le SQ**, **Gascuel O**. 2008. An improved general amino acid replacement matrix. Mol. Biol. Evol. **25**:1307–1320.

273. **Jones D**, **Taylor W**, **Thornton J**. 1992. The rapid generation of mutation data matrices from protein sequences. Comput Appl Biosci **8** (3):275-282.

274. **Rodriguez R**, **Oliver JL**, **Marin A**, **Medina JR**. 1990. The general stochastic model of nucleotide substitution. J Theor Biol **142** (4):482-501.

275. **Pagel M**, **Meade A**, **Barker D**. 2004. Bayesian estimation of ancestral character states on phylogenies. Syst. Biol. **53**:673–684.

276. **Shimodaira H**, **Hasegawa M**. 2001. CONSEL: for assessing the confidence of phylogenetic tree selection. Bioinformatics **17**:1246–1247.

277. **Stolzer M**, **Lai H**, **Xu M**, **Sathaye D**, **Vernot B**, **Durand D**. 2012. Inferring duplications, losses, transfers and incomplete lineage sorting with nonbinary species trees. Bioinforma. **28** :i409–i415.

278. **Chen K**, **Durand D**, **Farach-Colton M**. 2000. NOTUNG: A program for dating gene duplications and optimizing gene family trees. J. Comput. Biol. **7**:429–447.

279. **Omura T**, **Sato R**. 1964. The carbon monoxide-binding pigment of liver microsomes. J. Biol. Chem. **239**:2370–2378.

280. **Nelson DR**. 2009. The cytochrome P450 homepage. Hum. Genomics **4**:59–65.

281. **Ziemert N**, **Podell S**, **Penn K**, **Badger JH**, **Allen E**, **Jensen PR**. 2012. The natural product domain seeker NaPDoS: A phylogeny based bioinformatic tool to classify secondary metabolite gene diversity. PLoS One **7**:e34064.

282. **Spatafora JW**, **Chang Y**, **Benny GL**, **Lazarus K**, **Smith ME**, **Berbee ML**, **Bonito G**, **Corradi N**, **Grigoriev I**, **Gryganskyi A**, **James TY**, **O'Donnell K**, **Roberson RW**, **Taylor TN**, **Uehling J**, **Vilgalys R**, **White MM**, **Stajich JE**. 2016. A phylum-level phylogenetic classification of zygomycete fungi based on genome-scale data. Mycol. **108** :1028–1046.

283. **Chen S**, **Wang J**, **Lin X**, **Zhao B**, **Wei X**, **Li G**, **Kaliaperumal K**, **Liao S**, **Yang B**, **Zhou X**, **Liu J**, **Xu S**, **Liu Y**. 2016. Chrysamides A–C, three dimeric nitrophenyl trans-epoxyamides produced by the deep-sea-derived fungus *Penicillium chrysogenum* SCSIO41001. Org. Lett. **18**:3650–3653.

284. **Kovacic P**, **Somanathan R**. 2014. Nitroaromatic compounds: Environmental toxicity, carcinogenicity, mutagenicity, therapy and mechanism. J. Appl. Toxicol. **34**:810–824.

285. **Janssen PH**, **Yates PS**, **Grinton BE**, **Taylor PM**, **Sait M**. 2002. Improved culturability of soil bacteria and isolation in pure culture of novel members of the divisions *Acidobacteria*, *Actinobacteria*, *Proteobacteria*, and *Verrucomicrobia*. Appl. Environ. Microbiol. **68** :2391–2396.

286. **Chen H**, **Walsh CT**. 2001. Coumarin formation in novobiocin biosynthesis: β-hydroxylation of the aminoacyl enzyme tyrosyl-S-NovH by a cytochrome P450 NovI. Chem. Biol. **8**:301–312.

287. **Pylypenko O**, **Schlichting I**. 2004. Structural aspects of ligand binding to and electron transfer in bacterial and fungal P450s. Annu. Rev. Biochem. **73**:991–1018.

288. **Kudo T**, **Takaya N**, **Park S-Y**, **Shiro Y**, **Shoun H**. 2001. A positively charged cluster formed in the heme-distal pocket of cytochrome P450nor is essential for interaction with NADH. J. Biol. Chem. **276** :5020–5026.

289. **Zhang L**, **Kudo T**, **Takaya N**, **Shoun H**. 2002. Distribution, structure and function of fungal nitric oxide reductase P450nor—recent advances. Int. Congr. Ser. **1233**:197–202.

290. **Jones CM**, **Welsh A**, **Throbäck IN**, **Dörsch P**, **Bakken LR**, **Hallin S**. 2011. Phenotypic and genotypic heterogeneity among closely related soil-borne N_2- and N_2O-producing *Bacillus* isolates harboring the *nosZ* gene. FEMS Microbiol. Ecol. **76**:541–52.

291. **Walker GC**, **Nicholas DJD**. 1961. An iron requirement for a dissimilatory nitrate reductase in *Neurospora crassa*. Nature **189**:141–142.

292. **Nicholas DJD**, **Wilson PJ**. 1964. A dissimilatory nitrate reductase from *Neurospora crassa*. Biochim. Biophys. Acta. **86**:466–476.

293. **Helen D**, **Kim H**, **Tytgat B**, **Anne W**. 2016. Highly diverse *nirK* genes comprise two major clades that harbour ammonium-producing denitrifiers. BMC Genomics **17**:1–13.

294. **Plouviez M**, **Wheeler D**, **Shilton A**, **Packer MA**, **McLenachan PA**, **Sanz-Luque E**, **Ocana-Calahorro F**, **Fernandez E**, **Guieysse B**. 2017. The biosynthesis of nitrous oxide in the green alga *Chlamydomonas reinhardtii*. Plant J.

295. **Hou C**, **Tian W**, **Kleist T**, **He K**, **Garcia V**, **Bai F**, **Hao Y**, **Luan S**, **Li L**. 2014. DUF221 proteins are a family of osmosensitive calcium-permeable cation channels conserved across Eukaryotes. Cell Res **24**:632–635.

296. **Rai A**, **Suprasanna P**, **D'Souza SF**, **Kumar V**. 2012. Membrane topology and predicted RNA-binding function of the "Early Responsive to Dehydration (ERD4)" plant protein. PLoS One **7**:e32658.

297. **Mallick N**, **Rai LC**, **Mohn FH**, **Soeder CJ**. 1999. Studies on nitric oxide (NO) formation by the green alga *Scenedesmus obliquus* and the diazotrophic cyanobacterium *Anabaena doliolum*. Chemosphere **39**:1601–1610.

298. **Fields S**. 2004. Global nitrogen: cycling out of control. Environ. Health Perspect. **112**:A556–63.

299. **Rohe L**, **Anderson T**, **Braker G**, **Flessa H**, **Giesemann A**, **Lewicka-Szczebak D**, **Wrage-Monnig N**, **Well R**. 2014. Dual isotope and isotopomer signatures of nitrous oxide from fungal denitrification - a pure culture study. Rapid Commun. Mass Spectrom. **28**:1893–1903.

300. **Sutka RL**, **Adams GC**, **Ostrom NE**, **Ostrom PH**. 2008. Isotopologue fractionation during N_2O production by fungal denitrification. Rapid Commun. Mass Spectrom. **22**:3989–3996.

301. **Kibbe WA**. 2007. OligoCalc: an online oligonucleotide properties calculator. Nucleic Acids Res. **35** :W43–W46.

302. **Buttigieg PL**, **Ramette A**. 2014. A guide to statistical analysis in microbial ecology: a community-focused, living review of multivariate data analyses. FEMS Microbiol. Ecol. **90**:543–550.

APPENDIX



Figure 1.1: Comparison of fungal and bacterial denitrification pathways. The red X indicates that the *nosZ* gene is absent in Fungi. Note that Fungi only possess *nirK*, encoding the nitrite reductase, and that *Bacteria* possess alternative nitric oxide reductases, NorB and NorZ.

Table 2.1: NCBI identifiers and species designations for *p450nor* sequences used in PCR primer design.

Gi Number	Accession Number	Protein Name	Organism
14456620	BAB60855.1	cytochrome P450nor	*Trichosporon cutaneum*
85095006	XP_959999.1	cytochrome P450 55A2	*Neurospora crassa* OR74A
115399458	XP_001215318.1	cytochrome P450 55A3	*Aspergillus terreus* NIH2624
116203985	XP_001227803.1	hypothetical protein CHGG_09876	*Chaetomium globosum* CBS 148.51
154283207	XP_001542399.1	cytochrome P450 55A3	*Histoplasma capsulatum* NAm1
169776776	XP_001822854.1	cytochrome P450 55A3	*Aspergillus oryzae* RIB40
171678885	XP_001904391.1	hypothetical protein	*Podospora anserina* S mat+
193735592	ACF20287.1	cytochrome P450	*Metarhizium anisopliae*
225561727	EEH10007.1	cytochrome P450 benzoate 4-monooxygenase	*Histoplasma capsulatum* G186AR
238502137	XP_002382302.1	cytochrome P450, putative	*Aspergillus flavus* NRRL3357
240275331	EER38845.1	cytochrome P450	*Histoplasma capsulatum* H143
258565261	XP_002583375.1	cytochrome P450 55A2	*Uncinocarpus reesii* 1704
261189587	XP_002621204.1	cytochrome P450 55A3	*Blastomyces gilchristii* SLH14081
295670523	XP_002795809.1	cytochrome P450 55A1	*Paracoccidioides lutzii* Pb01
302502800	XP_003013361.1	hypothetical protein ARB_00546	*Arthroderma benhamiae* CBS 112371
302667715	XP_003025438.1	hypothetical protein TRV_00378	*Trichophyton verrucosum* HKI 0517

Table 2.1: (continued)

Gi Number	Accession Number	Protein Name	Organism
302880623	XP_003039249.1	hypothetical protein NECHADRAFT_89386	*Nectria haematococca* mpVI 77-13-4
302887052	XP_003042415.1	predicted protein	*Nectria haematococca* mpVI 77-13-4
302887494	XP_003042635.1	predicted protein	*Nectria haematococca* mpVI 77-13-4
315039865	XP_003169310.1	hypothetical protein MGYG_08858	*Microsporum gypseum* CBS 118893
317030133	XP_001391967.2	cytochrome P450 55A3	*Aspergillus niger* CBS 513.88
322696467	EFY88259.1	cytochrome P450	*Metarhizium acridum* CQMa 102
322702031	EFY93779.1	Cytochrome P450 55A2	*Metarhizium acridum* CQMa 102
322704284	EFY95881.1	Cytochrome P450 CYP55A20	*Metarhizium robertsii* ARSEF 23
325091167	EGC44477.1	cytochrome P450	*Histoplasma capsulatum* H88
326475328	EGD99337.1	cytochrome P450 55A3	*Trichophyton tonsurans* CBS 112818
327292715	XP_003231055.1	cytochrome P450	*Trichophyton rubrum* CBS 118892
336259849	XP_003344723.1	hypothetical protein SMAC_06378	*Sordaria macrospora* k-hell
336467208	EGO55372.1	cytochrome P450 55A2	*Neurospora tetrasperma* FGSC 2508
340966809	EGS22316.1	hypothetical protein CTHT_0018400	*Chaetomium thermophilum* var. *thermophilum* DSM 1495

Table 2.1: (continued)

Gi Number	Accession Number	Protein Name	Organism
342872713	EGU75027.1	hypothetical protein FOXB_14464	*Fusarium oxysporum* Fo5176
342882391	EGU83079.1	hypothetical protein FOXB_06423	*Fusarium oxysporum* Fo5176
358383911	EHK21571.1	hypothetical protein TRIVIDRAFT_186579	*Trichoderma virens* Gv29-8
367048355	XP_003654557.1	hypothetical protein THITE_2117644	*Thielavia terrestris* NRRL 8126
893699238	EGE85793.2	cytochrome P450 55A3	*Blastomyces dermatitidis* ATCC 18188
719932114	EEH22787.2	hypothetical protein PABG_04998	*Paracoccidioides brasiliensis* Pb03
699750017	EEH49581.2	hypothetical protein PADG_05660	*Paracoccidioides brasiliensis* Pb18
734840173	EFY96295.2	Cytochrome P450 CYP55A19	*Metarhizium robertsii* ARSEF 23

Table 2.2: Characteristics of the *p450nor* gene-targeted primers.

Primer[1]	**Primer Sequence (5'→ 3')**	**Melting Temperature Range (°C)**[2]	**GC (%)**[2]	**Fold Degeneracy**[3]
*p450nor*394F	SCIACITTYGTIGAYATGGA	45.6 – 55.9	35-60	8 (256)
*p450nor*809R	ATCATGTTIACBAIIGTIGCIT	45.5 – 56.7	27-55	3 (3072)
*p450nor*1008R	GMSGCRATKATNCCYTC	42.2 – 54.3	41-71	128

[1]Numeric positions of primers are based on *Aspergillus terreus* strain NIH2624 *p450nor* gene sequence.
[2]Ranges were calculated using OligoCalc (301).
[3]Numbers in parentheses indicate fold-degeneracy if the IUPAC symbol "N" had been used instead of an inosine nucleoside.
S = G or C, Y = C or T, B = C, G, or T, M = A or C, R = A or G, K = G or T, N = A, G, C, or T, I = inosine

Table 2.3: Fungal isolate N_2O production and PCR amplification of *p450nor* and *nirK* genes.

Isolate ID	Isolate source[1]	Taxonomic affiliation[2]	N_2O production[3]	Targeted PCR		
				p450nor [4]	***nirK* primer set 1**[5]	***nirK* primer set 2**[6]
30	H	*Helotiales*	+	+	+	-
179	U	*Trichoderma*	+	+	+	-
213	U	*Gibberella*	+	+	+	-
138	H	*Fusarium*	+	+	+	+
210	U	*Hypocreales*	+	+	-	-
184	U	*Hypocreales*	+	+	-	-
185	U	*Hypocreales*	+	+	+	+
67	U	*Fusarium*	+	+	+	-
31	U	*Verticillium*	+	+	+	-
63	H	*Hypocreales*	+	+	+	-
8	H	*Gibberella*	+	+	+	-
74	H	*Gibberella*	+	+	+	-
209	U	*Gibberella*	+	+	+	-
112	H	*Trichoderma*	-	+	-	-
93	H	*Fusarium*	+	+	+	+
107	H	*Bionectria*	+	+	-	-
111	U	*Trichoderma*	+	+	+	-
134	H	*Hypocreales*	-	+	-	-
142	H	*Hypocreales*	-	+	+	-
192	H	*Hypocreales*	-	+	+	-
194	H	*Eurotiales*	+	+	+	-
195	U	*Fusarium*	-	+	-	-
205	H	*Humicola*	-	+	-	+
H2	H	*Hypocreales*	+	+	-	-
136	H	*Trichoderma*	-	+	+	-
72	U	*Guehomyces*	+	+	-	-
48	U	*Humicola*	-	+	-	-
75	U	*Mortierellales*	-	-	-	-
174	U	*Gibberella*	+	+	+	-
89	H	*Podospora*	-	+	-	-
149	H	*Mortierellales*	+	+	+	-
50	U	*Chaetomium*	-	-	+	+
212	H	*Hypocreales*	-	-	-	-
211	H	*Lecythophora*	-	-	-	-
141	H	*Fusarium*	-	-	+	-
AT*	USDA	*Aspergillus*	+	+	-	-
AF*	USDA	*Aspergillus*	+	+	+	-

[1]H and U refer to Havana and Urbana soils, respectively, and USDA refers to the Agricultural Research Service culture collection.
[2]Lowest taxonomic rank based on 18S rRNA gene classification (see Materials and Methods for more information). In some cases, the internal transcribed spacer sequence was used for classification when 18S rRNA gene classification was unsuccessful.
[3]N_2O production was determined in defined mineral salts medium using nitrite as electron acceptor (see Materials and Methods).

[4]*p450nor* was classified as detected (+ symbol) when a visible band was confirmed between 536 and 890 bp by electrophoresis on a 1% (w/v) agarose gel (see Materials and Methods).
[5]*nirK* amplification with primer set nirKfF/nirKfR (130). *nirK* positive detection (+ symbol) was indicated by a visible band at 480 bp by electrophoresis on a 1% (w/v) agarose gel (see Materials and Methods).
[6]*nirK* amplification with primer set fnirK2F/fnirK1R (131). *nirK* was classified as detected (+ symbol) when a visible band was confirmed at 468 bp by electrophoresis on a 1% (w/v) agarose gel (see Materials and Methods).
* AT, *Aspergillus terreus* strain NRRL 255 and AF, Aspergillus flavus strain NRRL 3357.

Table 2.4: The SILVA 18S rRNA gene classification of 37 fungal isolates.

	Lineage				
ID	**Phylum**	**Class**	**Order**	**Family**	**Genus**
138	Ascomycota	Sordariomycetes	Hypocreales	Nectriaceae	*Fusarium*
213	Ascomycota	Sordariomycetes	Hypocreales	Nectriaceae	*Gibberella*
30	Ascomycota	Leotiomycetes	Helotiales	N/A	N/A
179	Ascomycota	Sordariomycetes	Hypocreales	Hypocreaceae	*Trichoderma*
112	Ascomycota	Sordariomycetes	Hypocreales	Hypocreaceae	*Trichoderma*
210	Ascomycota	Sordariomycetes	Hypocreales	N/A	N/A
184	Ascomycota	Sordariomycetes	Hypocreales	N/A	N/A
185	Ascomycota	Sordariomycetes	Hypocreales	N/A	N/A
31	Ascomycota	Sordariomycetes	Glomerellales	Plectosphaerellaceae	*Verticillium*
8	Ascomycota	Sordariomycetes	Hypocreales	Nectriaceae	*Gibberella*
63	Ascomycota	Sordariomycetes	Hypocreales	N/A	N/A
74	Ascomycota	Sordariomycetes	Hypocreales	Nectriaceae	*Gibberella*
209	Ascomycota	Sordariomycetes	Hypocreales	Nectriaceae	*Gibberella*
67	Ascomycota	Sordariomycetes	Hypocreales	Nectriaceae	*Fusarium*
93	Ascomycota	Sordariomycetes	Hypocreales	Nectriaceae	*Fusarium*
111	Ascomycota	Sordariomycetes	Hypocreales	Hypocreaceae	*Trichoderma*
134	Ascomycota	Sordariomycetes	Hypocreales	N/A	N/A
142	Ascomycota	Sordariomycetes	Sordariales	Chaetomiaceae	*Chaetomium*
174	Ascomycota	Sordariomycetes	Hypocreales	Nectriaceae	*Gibberella*
192	Ascomycota	Sordariomycetes	Sordariales	Chaetomiaceae	*Chaetomium*
194	Ascomycota	Eurotiomycetes	Eurotiales	N/A	N/A
195	Ascomycota	Sordariomycetes	Hypocreales	Nectriaceae	*Fusarium*
205	Ascomycota	Sordariomycetes	Sordariales	Chaetomiaceae	*Humicola*
H2	Ascomycota	Sordariomycetes	Hypocreales	N/A	N/A
50	Ascomycota	Sordariomycetes	Sordariales	Chaetomiaceae	*Chaetomium*
89	Ascomycota	Sordariomycetes	Sordariales	Lasiosphaeriaceae	*Podospora*
211	Ascomycota	Sordariomycetes	Sordariales	Coniochaetaceae	*Lecythophora*
48	Ascomycota	Sordariomycetes	Sordariales	Chaetomiaceae	*Humicola*
72	Basidiomycota	Tremellomycetes	Cystofilobasidiales	Cystofilobasidiaceae	N/A
75	Mucoromycotina	N/A	N/A	N/A	N/A
149	Mucoromycotina	N/A	N/A	N/A	N/A
107	Ascomycota	Sordariomycetes	Hypocreales	Bionectriaceae	*Bionectria*
136	N/A	N/A	N/A	N/A	N/A
141	N/A	N/A	N/A	N/A	N/A
212	Ascomycota	Sordariomycetes	Hypocreales	N/A	N/A
AF*	Ascomycota	Eurotiomycetes	Eurotiales	Trichocomaceae	*Aspergillus*
AT*	Ascomycota	Eurotiomycetes	Eurotiales	Trichocomaceae	*Aspergillus*

*AF = Aspergillus flavus NRRL 3357, AT = Aspergillus terreus NRRL 255, N/A = not assigned

Table 2.5: *p450nor* amplicon lengths and number of introns found in amplified regions using primer set *p450nor394F*/*p450nor809R*.

Organism	Genome Accession Number	Amplicon Length	Number of Introns in Amplicon[1]
Uncinocarpus reesii 1704	NW_003052497	661	3
Trichoderma virens Gv29-8	NW_003315617	685	3
Trichophyton verrucosum HKI 0517	GG698521	798	4
Trichophyton tonsurans CBS 112818	GG700661	787	4
Trichophyton rubrum CBS 118192	ABDF02000069	785	4
Sordaria macrospora k-hell	CABT02000035	613	2
Sclerotinia sclerotiorum 1980 UF-70	NW_001820835	657	3
Podospora anserina S mat+	NW_001914839	658	3
Paracoccidioides brasiliensis Pb18	NW_011371363	765	4
Paracoccidioides lutzii Pb01	NW_003217283	772	4
Neurospora tetrasperma FGSC 2508	GL891306	615	2
Neurospora crassa OR74A	NC_026507	617	2
Nectria haematococca mpVI 77-13-4	NW_003315852	648	3
Nectria haematococca mpVI 77-13-4	NW_003315850	649	3
Nectria haematococca mpVI 77-13-4	NW_003315753	688	3
Metarhizium robertsii ARSEF 23	NW_011942182	662	4
Metarhizium robertsii ARSEF 23	NW_011942182	666	2
Metarhizium acridum CQMa 102	NW_006916718	666	2
Marssonina brunnea f. sp. 'multigermtubi' MB_m1	NW_006763048	563	1
Macrophomina phaseolina MS6	AHHD01000221	612	2
Glarea lozoyensis ATCC 20868*	NW_007360999	587	1(2)
Geomyces destructans 20631-21	GL573369	693	4
Gaeumannomyces graminis var. tritici R3-111a-1	NW_008804545	621	2
Fusarium oxysporum MT-811	D14517	649	3
Fusarium oxysporum Fo5176	AFQF01003581	651	3
Fusarium oxysporum f. sp. cubense race 4	KB726480	649	3
Fusarium oxysporum f. sp. cubense race 1	KB730401	649	3
Fusarium lichenicola	D78511	648	3
Fusarium graminearum	HG970332	652	3
Fusarium fujikuroi IMI 58289	HF679033	647	3
Coniosporium apollinis CBS 100218	NW_006913289	684	3
Colletotrichum gloeosporioides Nara gc5	NW_006762233	628	2
Bipolaris sorokiniana ND90Pr	NW_006911899	603	3
Chaetomium thermophilum var. *thermophilum* DSM 1495	NW_006383031	669	2
Chaetomium globosum CBS 148.51	NT_165982	662	3
Aspergillus terreus NIH2624	NT_165931	715	3
Aspergillus oryzae RIB40	NW_001884671	673	3
Aspergillus oryzae 3.042	AKHY01000120	673	3
Aspergillus oryzae	AB055659	673	3
Aspergillus flavus NRRL3357	NW_002477247	673	3
Microsporum gypseum CBS 118893	NW_003345192	800	4
Arthroderma benhamiae CBS 112371	NW_003315100	800	4
Blastomyces gilchristii SLH14081	NW_003101659	776	4
Histoplasma capsulatum NAm1	NW_001813981	890	4
Histoplasma capsulatum H143	GG692430	854	4
Histoplasma capsulatum H88	DS990638	865	4
Histoplasma capsulatum G186AR*	GG663364	861	3(4)

[1] The number in parentheses indicates genetic potential for an additional coding region (and additional intron) present within the gene but additional expressed sequence tags are unavailable to support the alternative gene model.

Figure 2.1: Alignment of P450nor sequences from select organisms displaying primer binding sites (pink), and key residues involved in cofactor (NAD(P)H) binding. The N-terminal region of the alignment has been removed for clarity. Stars below the alignment (blue, red, black) indicate positive, negative and charged amino acids and key residues involved in NAD(P)H binding, respectively. Sites outlined in black with all bold amino acid characters indicate 100% amino acid identity. Columns highlighted yellow and outlined in black indicate ≥ 80% amino acid similarity. Stars with a white "S" and "H" indicate involvement in a salt bridge and proton channel, respectively. PP stands for a residue believed to be involved in binding pyrophosphate on the NAD(P)H molecule. The B' helix (helix 3α above) is a hypervariable region of P450 proteins and represents an area of NAD(P)H recognition by P450nor. P450nor secondary structure is provided by the PDB accession 1JFB and was added using the ESPript 3.0 web server. F_oxysorum = *Fusarium oxysporum*, F_lichenicola = *Fusarium lichenicola*, C_globosum = *Chaetomium globosum*, T_virens = *Trichoderma virens*, S_macrospora = *Sordaria macrospora*, G_graminis = *Gaeumannomyces graminis*, A_terreus = *Aspergillus terreus* NRRL 255, A_flavus = *Aspergillus flavus* NRRL 3357, U_reesii = *Uncinocarpus reesii*, C_apollinis = *Coniosporium apollinis*, M_gypseum = *Microsporum gypseum*, M_brunnea = *Marssonina brunnea*, M_phaseolina = *Macrophomina phaseolina*, T_cutaneum = *Trichosporon cutaneum*, C_reinhardtii = *Chlamydomonas rheinhardtii*, C_variabilis = *Chlorella variabilis*.

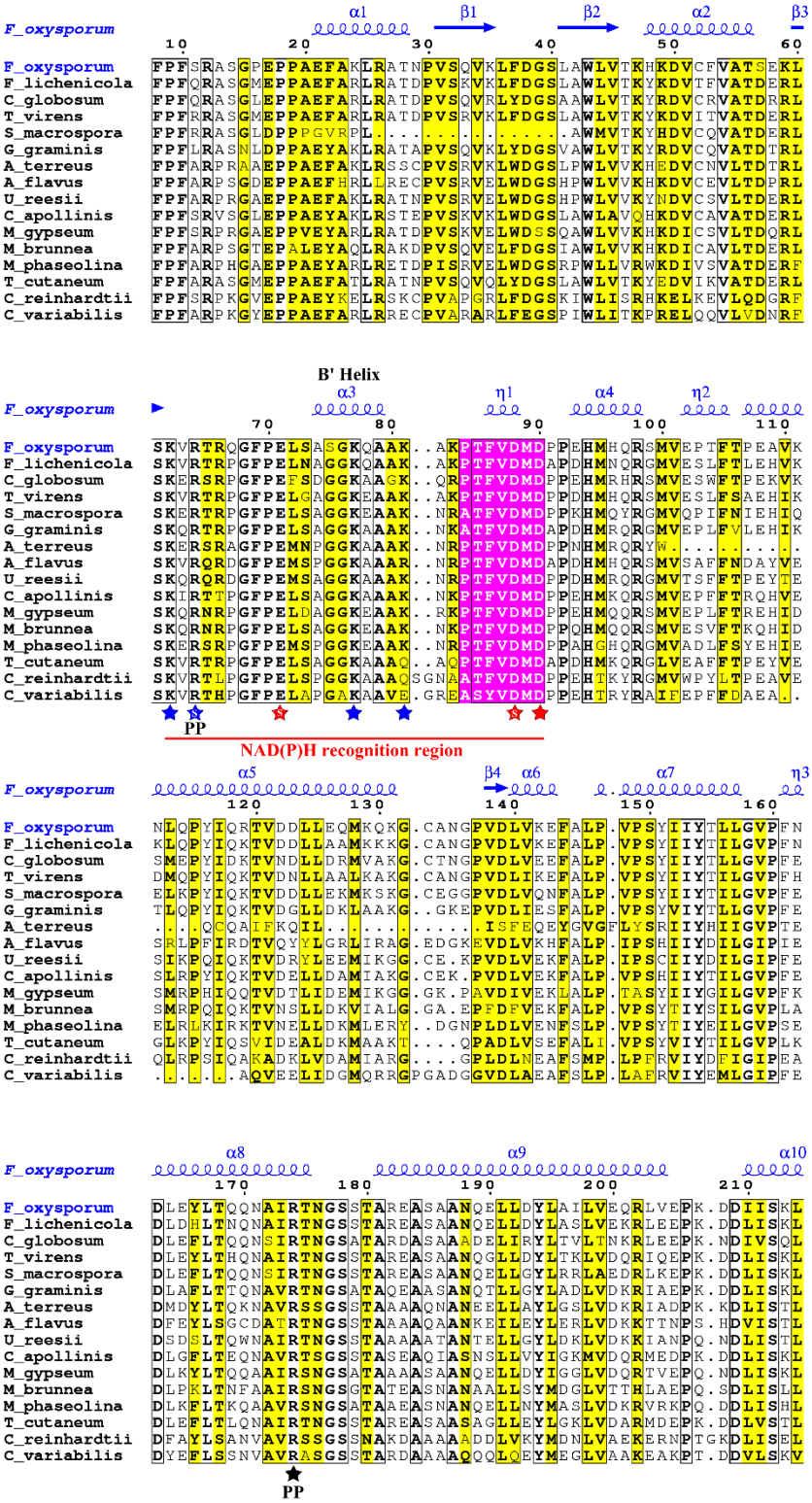
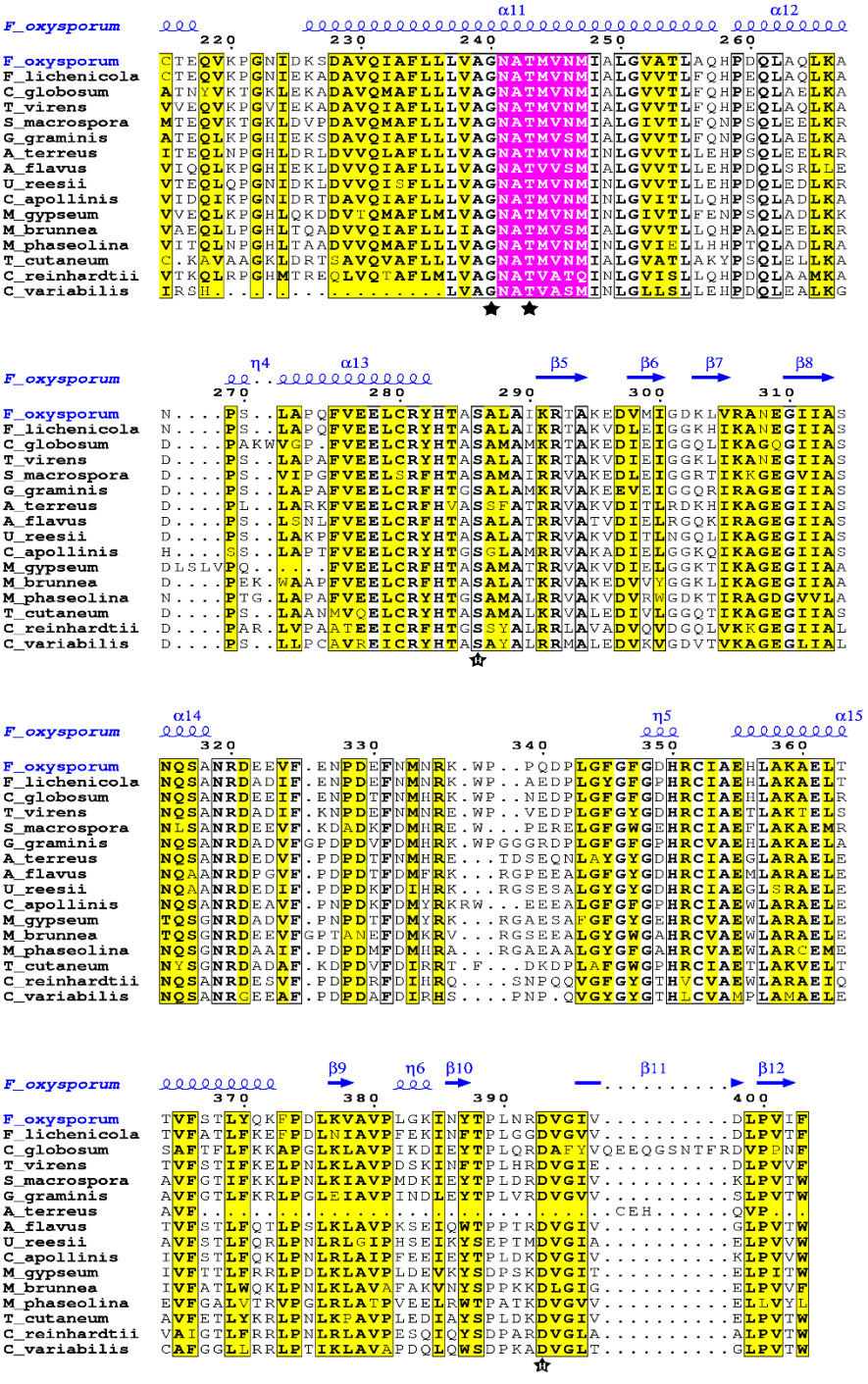

F_oxysporum
α1
β1
β2
α2
β3
F_oxysporum
F_lichenicola
C_globosum
T_virens
S_macrospora
G_graminis
A_terreus
A_flavus
U_reesii
C_apollinis
M_gypseum
M_brunnea
M_phaseolina
T_cutaneum
C_reinhardtii
C_variabilis
B' Helix
α3
η1
α4
η2
PP
NAD(P)H recognition region
α5
β4
α6
α7
η3
α8
α9
α10
PP

Figure 2.1: (continued)



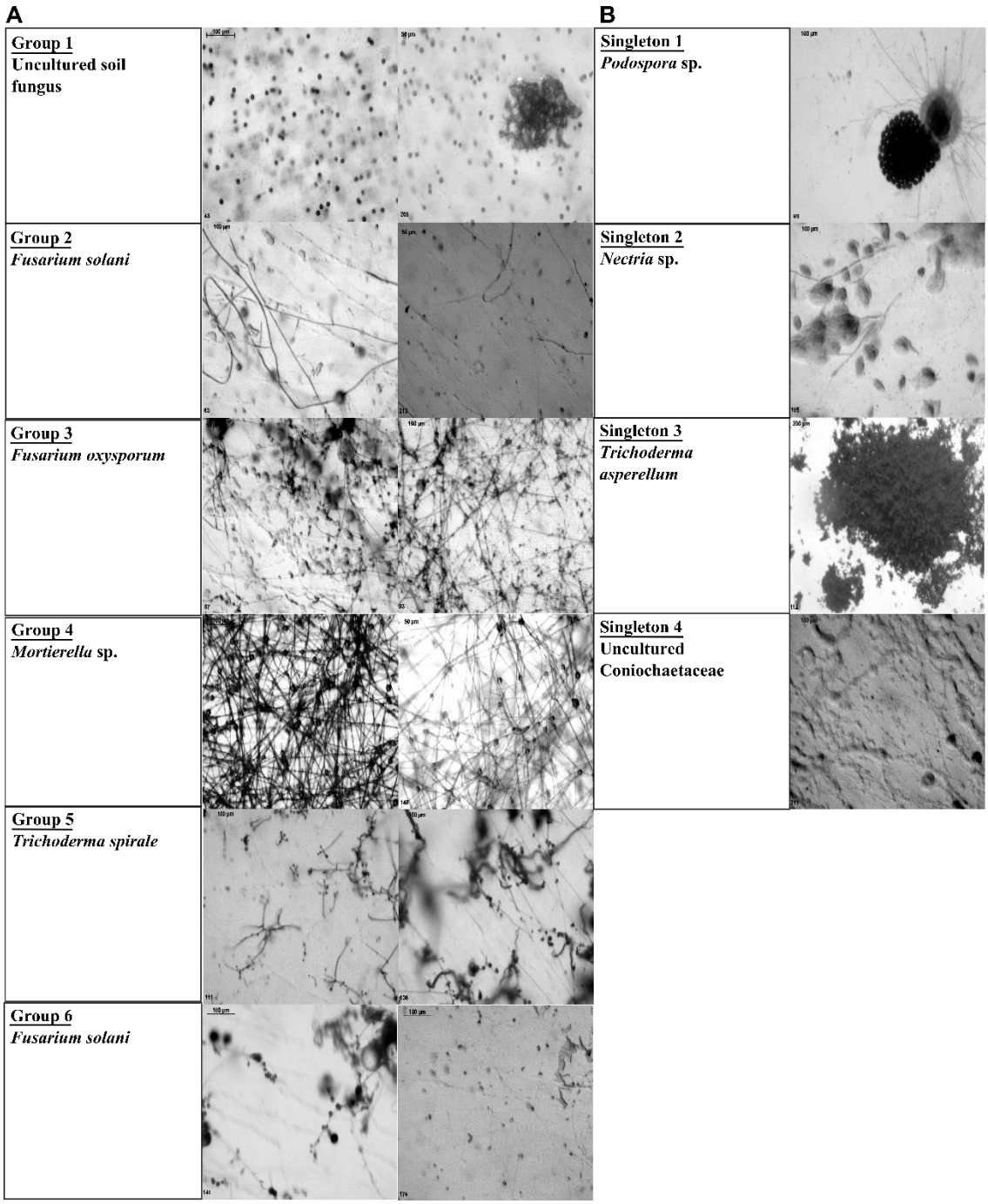


Figure 2.2: Stereoscopic images of isolate fungal groups (A) and singleton isolates (B).

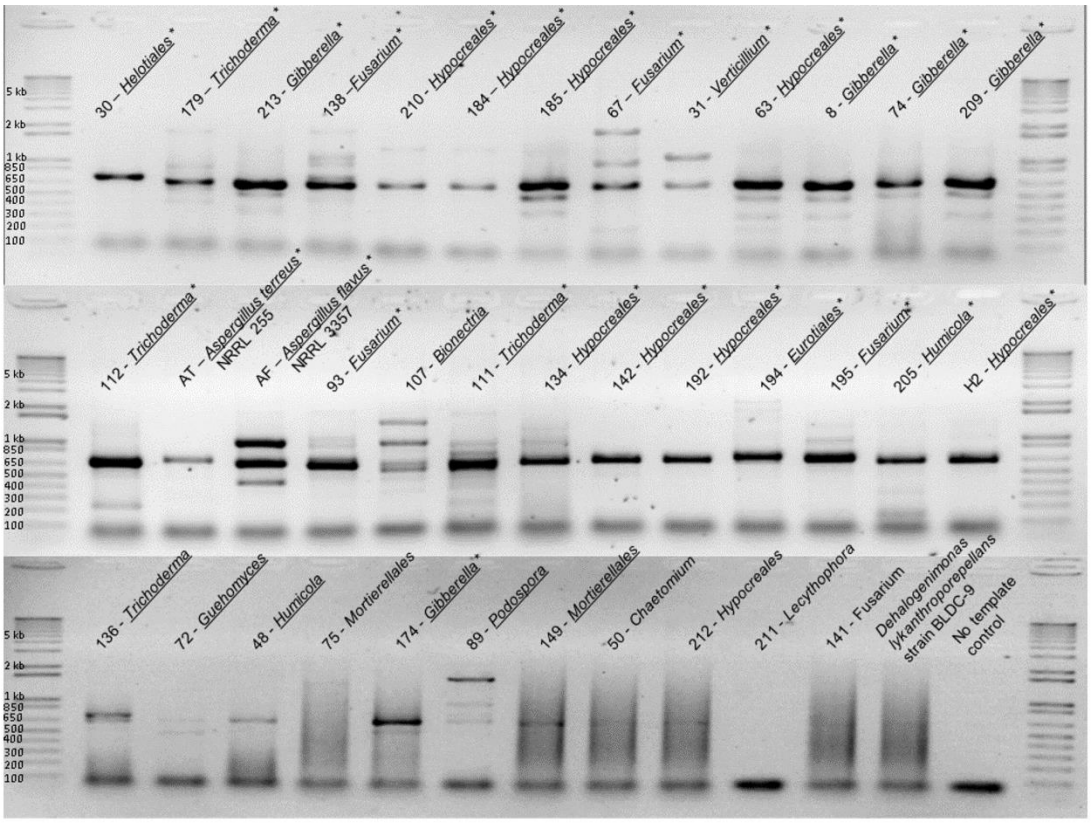


Figure 2.3: PCR amplification of *p450nor* in fungal isolates.

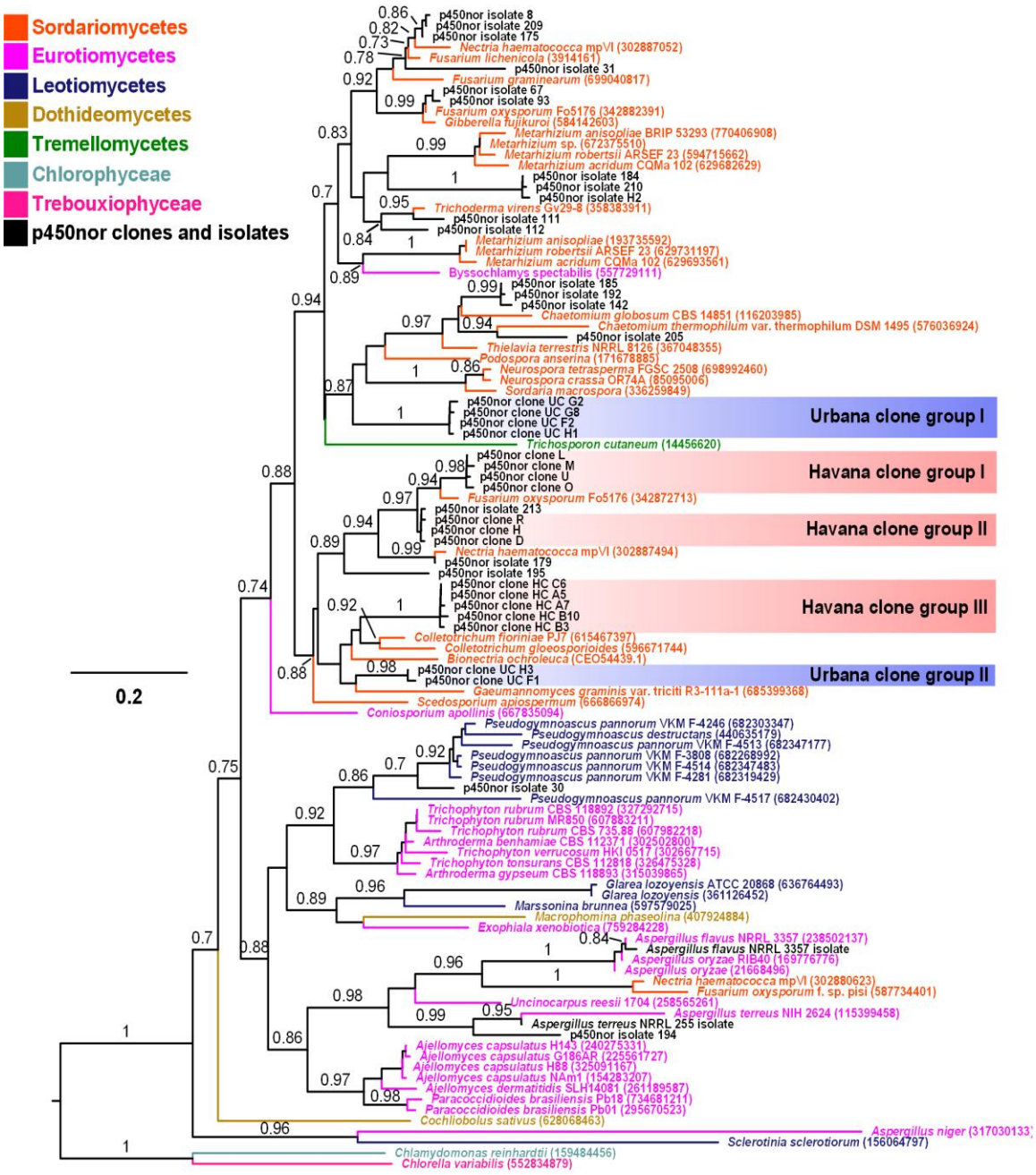


Figure 2.4: Phylogeny of full length p450nor and *p450nor* amplicon sequences generated using PCR primers *p450nor394F/p450nor809R*.

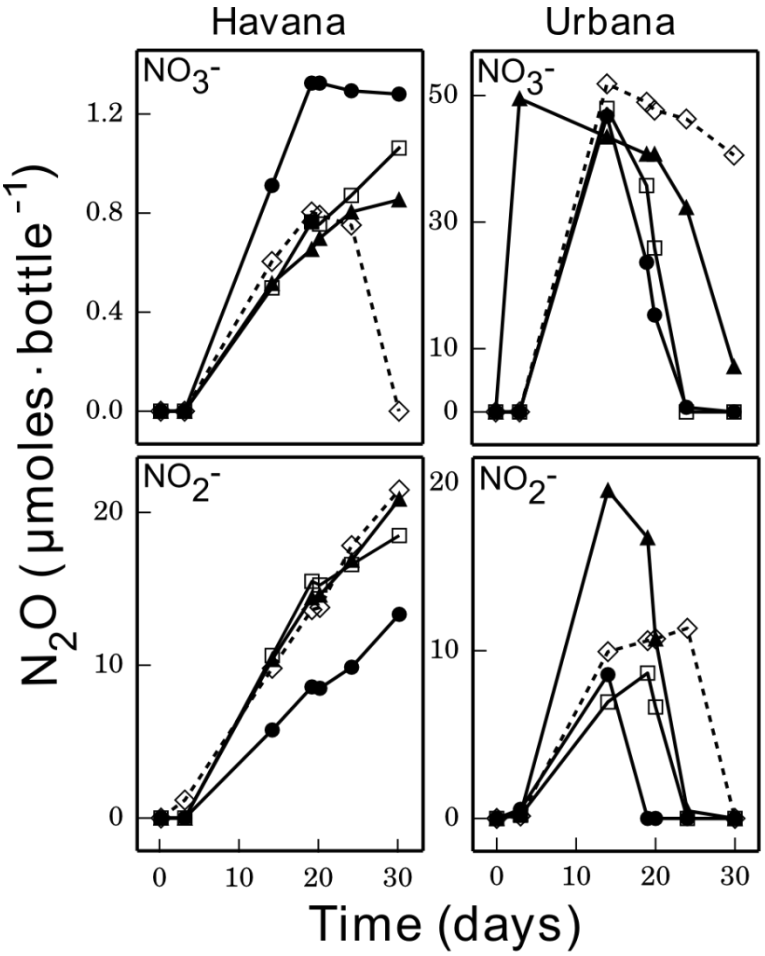


Figure 2.5: N_2O production in soil microcosms amended with streptomycin and chloramphenicol to inhibit bacterial activity. The symbols indicate a carbon source of either acetate (●), pyruvate (▲), formate (□), and milled corn and soybean plant residues (◊, dashed line).

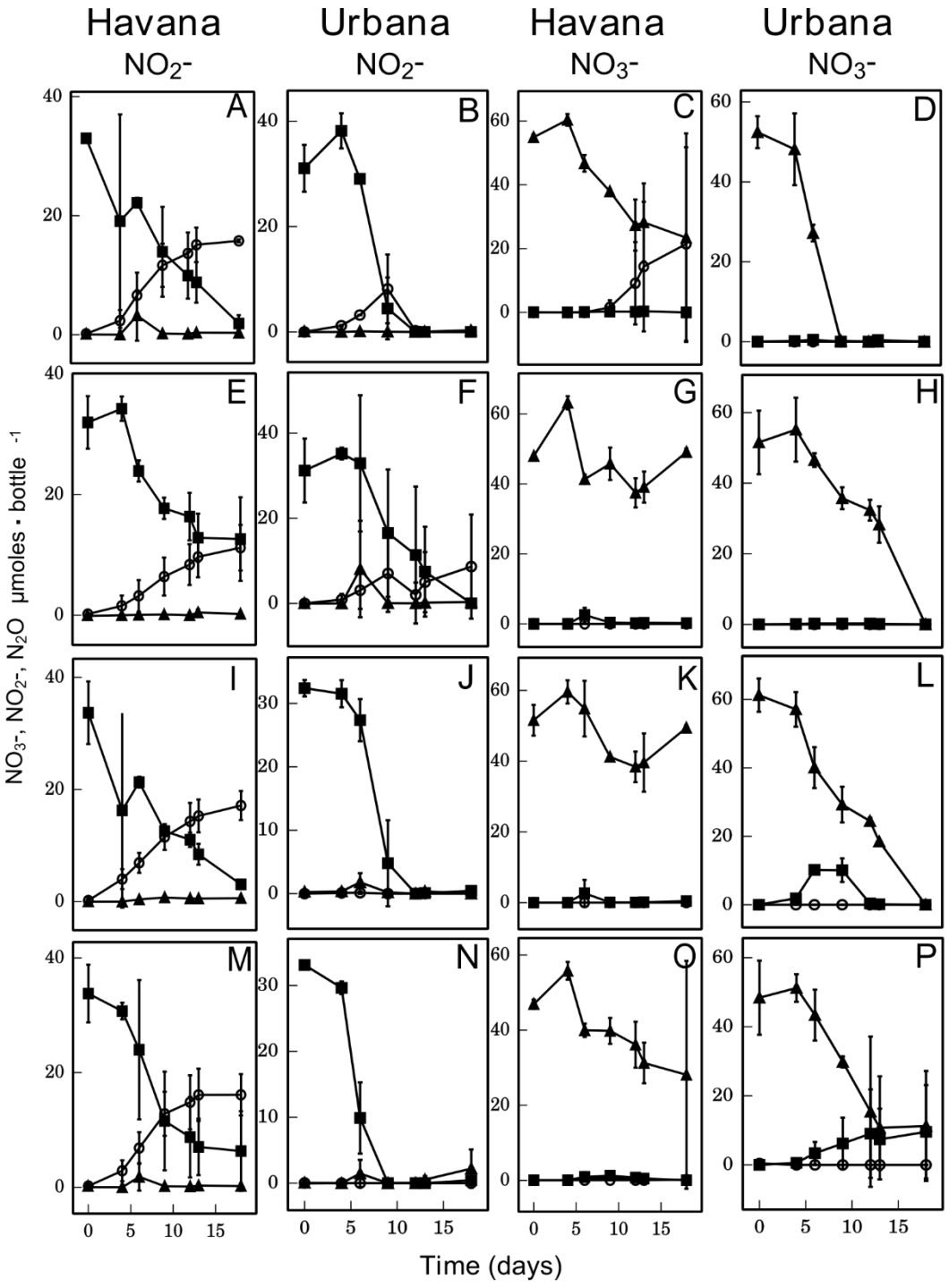


Figure 2.6: NO_3^- (▲), NO_2^-(■), and N_2O (○) quantities measured in Havana and Urbana soil transfer cultures.

Figure 2.7: Intron structure of the region amplified by primer set *p450nor394F*/*p450nor809R* in 47 *p450nor* sequences.

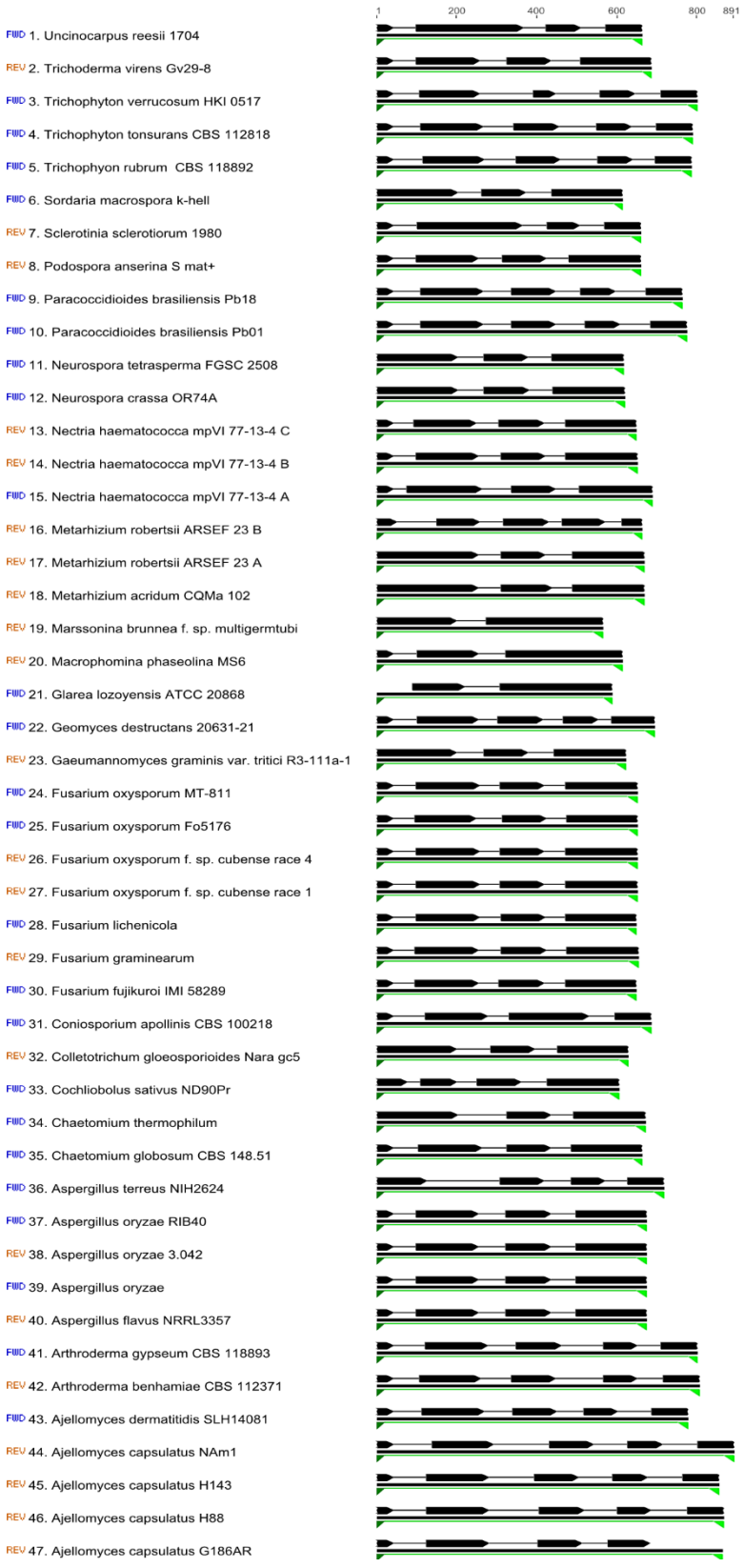

1
200
400
600
800
891
FWD 1. Uncinocarpus reesii 1704
REV 2. Trichoderma virens Gv29-8
FWD 3. Trichophyton verrucosum HKI 0517
FWD 4. Trichophyton tonsurans CBS 112818
FWD 5. Trichophyon rubrum CBS 118892
FWD 6. Sordaria macrospora k-hell
REV 7. Sclerotinia sclerotiorum 1980
REV 8. Podospora anserina S mat+
FWD 9. Paracoccidioides brasiliensis Pb18
FWD 10. Paracoccidioides brasiliensis Pb01
FWD 11. Neurospora tetrasperma FGSC 2508
FWD 12. Neurospora crassa OR74A
REV 13. Nectria haematococca mpVI 77-13-4 C
REV 14. Nectria haematococca mpVI 77-13-4 B
FWD 15. Nectria haematococca mpVI 77-13-4 A
REV 16. Metarhizium robertsii ARSEF 23 B
REV 17. Metarhizium robertsii ARSEF 23 A
REV 18. Metarhizium acridum CQMa 102
REV 19. Marssonina brunnea f. sp. multigermtubi
REV 20. Macrophomina phaseolina MS6
FWD 21. Glarea lozoyensis ATCC 20868
FWD 22. Geomyces destructans 20631-21
REV 23. Gaeumannomyces graminis var. tritici R3-111a-1
FWD 24. Fusarium oxysporum MT-811
FWD 25. Fusarium oxysporum Fo5176
REV 26. Fusarium oxysporum f. sp. cubense race 4
REV 27. Fusarium oxysporum f. sp. cubense race 1
FWD 28. Fusarium lichenicola
REV 29. Fusarium graminearum
FWD 30. Fusarium fujikuroi IMI 58289
FWD 31. Coniosporium apollinis CBS 100218
REV 32. Colletotrichum gloeosporioides Nara gc5
FWD 33. Cochliobolus sativus ND90Pr
FWD 34. Chaetomium thermophilum
FWD 35. Chaetomium globosum CBS 148.51
FWD 36. Aspergillus terreus NIH2624
FWD 37. Aspergillus oryzae RIB40
REV 38. Aspergillus oryzae 3.042
FWD 39. Aspergillus oryzae
REV 40. Aspergillus flavus NRRL3357
FWD 41. Arthroderma gypseum CBS 118893
REV 42. Arthroderma benhamiae CBS 112371
FWD 43. Ajellomyces dermatitidis SLH14081
REV 44. Ajellomyces capsulatus NAm1
REV 45. Ajellomyces capsulatus H143
REV 46. Ajellomyces capsulatus H88
REV 47. Ajellomyces capsulatus G186AR

Table 3.1: Number of *p450nor* sequences generated per DNA sample and other quality control statistics per sample.

Sample ID	No. sequences	No. Sequences passing QC	% Passed QC	% Failed QC	Median sequence length
US2S	375276	222853	59.38	40.62	367
US2J	356555	183884	51.57	48.43	366
HW2S	344991	170986	49.56	50.44	379
HW2J	249300	184002	73.81	26.19	374
UN3J	349710	184307	52.7	47.3	362
HW2N	208481	158684	76.11	23.89	377
HW2A	275646	193260	70.11	29.89	375
US1A	151872	110440	72.72	27.28	371
UN3N	293994	209438	71.24	28.76	364
HM1N	331054	260737	78.76	21.24	377
HM3A	340192	203511	59.82	40.18	375
HE3J	342718	238613	69.62	30.38	374
HM1J	268611	190749	71.01	28.99	378
HE1S	231610	159893	69.04	30.96	375
HE3N	286300	191337	66.83	33.17	377
US2A	254026	172433	67.88	32.12	367
UN1J	686406	487490	71.02	28.98	364
HE3A	265195	189826	71.58	28.42	375
HM3J	230583	167776	72.76	27.24	375
UN1N	276288	204966	74.19	25.81	374
HM3N	310208	214040	69	31	377
HM1A	329288	239502	72.73	27.27	376
UM1A	402009	276365	68.75	31.25	374
UN1S	339853	190900	56.17	43.83	370
HM3S	301130	209778	69.66	30.34	379
UM3N	525576	159095	30.27	69.73	374
HE1A	330560	186578	56.44	43.56	373
HE1N	412558	203666	49.37	50.63	376
HE3S	463551	221388	47.76	52.24	378
HE1J	280207	211346	75.42	24.58	379
HM1S	285196	214772	75.31	24.69	375
UM1N	409264	267196	65.29	34.71	367
UN2N	207384	153469	74	26	364
UM3J	323423	230360	71.23	28.77	363
US1S	275204	188536	68.51	31.49	367
HW3S	259547	195610	75.37	24.63	379
HW3N	317028	140184	44.22	55.78	374
HW1A	275162	204809	74.43	25.57	375
HW3J	161406	117462	72.77	27.23	372
US1N	283562	207574	73.2	26.8	367

Table 3.1: (continued)

Sample ID	No. sequences	No. Sequences passing QC	% Passed QC	% Failed QC	Median sequence length
UN2A	253884	168261	66.27	33.73	365
HW1J	338814	200519	59.18	40.82	376
HW1N	300709	223735	74.4	25.6	378
HW3A	318371	196595	61.75	38.25	377
US3A	173747	110893	63.82	36.18	358
HE2J	214519	150814	70.3	29.7	373
UM2J	355664	240991	67.76	32.24	371
UM1J	313865	208201	66.33	33.67	368
UN3A	403442	234581	58.14	41.86	362
HE2N	255423	162118	63.47	36.53	375
UM2N	343988	227130	66.03	33.97	365
US1J	193129	139518	72.24	27.76	372
HM2J	269836	195227	72.35	27.65	375
HE2A	241666	155642	64.4	35.6	376
UN2J	422669	288888	68.35	31.65	365
UM3S	425594	312184	73.35	26.65	365
UN2S	507596	289313	57	43	373
UM2A	329276	235042	71.38	28.62	364
HE2S	249595	170553	68.33	31.67	374
UM2S	267955	185095	69.08	30.92	366
UM3A	222130	156675	70.53	29.47	367
UM1S	431613	305690	70.83	29.17	371
Total	19444409	12675480	65.19	34.81	374

Table 3.2: Relative abundance of *p450nor* sequences aligned to reference OTUs in DNA extracted from Havana or Urbana soils.

	Relative abundance (%)	
Organism	**Havana**	**Urbana**
Isolate 74	13.43	12.09
Isolate 67	12.99	22.81
Isolate 213	9.30	0.88
Isolate 179	8.21	5.41
Clone HC C1	8.06	0.98
Clone HC A7	5.79	1.80
Colletotrichum gloeosporioides Nara gc5	3.44	3.85
Fusarium oxysporum f. sp. *cubense* race 4	3.39	6.38
Ajellomyces capsulatus NAm1	3.34	1.78
Isolate L	3.08	0.31
Trichoderma virens Gv29-8	2.82	2.11
Paracoccidioides sp. Pb01	2.67	0.51
Pseudogymnoascus destructans 20631-21	2.43	1.97
Clone D	2.10	0.87
Aspergillus terreus NRRL 255	2.06	2.05
Isolate 112	1.59	7.37
Fusarium oxysporum Fo5176	1.55	0.50
Metarhizium anisopliae	1.46	0.16
Clone R	1.36	0.51
Paracoccidioides brasiliensis Pb18	1.26	0.50
Trichophyton tonsurans CBS 112818	1.15	2.14
Fusarium lichenicola	1.14	1.59
Isolate 209	1.10	1.23
Clone UC H3	1.02	1.28
Ajellomyces dermatitidis SLH14081	0.70	1.84
Marssonina brunnea MB m1	0.66	0.63
Clone M	0.42	0.07
Isolate 184	0.41	0.37
Aspergillus flavus NRRL 3357	0.36	0.62
Isolate 185	0.34	3.96
Fusarium fujikuroi IMI 58289	0.34	0.55
Ajellomyces capsulatus G186AR	0.28	0.07
Trichophyton rubrum CBS 118892	0.23	1.84
Aspergillus oryzae RIB40	0.19	0.58
Microsporum gypseum CBS 118893	0.16	0.44
Isolate 31	0.15	0.07
Arthroderma benhamiae CBS 112371	0.12	1.17
Aspergillus oryzae 3.042	0.11	0.03
Clone HC B10	0.10	0.01

Table 3.2: (continued)

	Relative abundance (%)	
Organism	**Havana**	**Urbana**
Thielavia terrestris NRRL 8126	0.09	0.49
Chaetomium globosum CBS 148.51	0.08	0.17
Uncinocarpus reesii 1704	0.07	0.06
Clone O	0.06	1.10
Clone HC B3	0.04	0.01
Clone U	0.04	0.01
Clone HC A5	0.04	0.29
Nectria haematococca mpVI 77-13-4 A	0.03	0.21
Ajellomyces capsulatus H143	0.02	0.00
Trichophyton verrucosum HKI 0517	0.02	0.21
Bipolaris sorokiniana ND90Pr	0.02	0.00
Clone UC F2	0.02	2.97
Aspergillus terreus NIH2624	0.02	0.03
Nectria haematococca mpVI 77-13-4 B	0.02	0.08
Podospora anserina S mat+	0.01	0.53
Nectria haematococca mpVI 77-13-4	0.01	0.01
Metarhizium acridum CQMa 102 B	0.01	0.03
Fusarium oxysporum	0.01	0.13
Metarhizium anisopliae ARSEF 23 B	0.01	0.00
Clone H	0.01	0.00
Macrophomina phaseolina MS6	0.01	0.06
Metarhizium acridum CQMa 102 A	0.01	0.04
Metarhizium anisopliae ARSEF 23	0.01	0.00
Fusarium oxysporum f. sp. *cubense* race 1	0.01	0.01
Clone UC F1	0.00	0.01
Glarea lozoyensis 74030	0.00	0.19
Chaetomium thermophilum DSM 1495	0.00	0.00
Neurospora crassa OR74A	0.00	0.64
Sordaria macrospora k-hell	0.00	1.18
Trichosporon asahii CBS 2479	0.00	0.00
Ajellomyces capsulatus H88	0.00	0.00
Clone UC G2	0.00	0.12
Neurospora tetrasperma FGSC 2508	0.00	0.00
Isolate 210	0.00	0.00
Trichosporon cutaneum	0.00	0.00
Aspergillus oryzae	0.00	0.04
Glarea lozoyensis ATCC 20868	0.00	0.00
Clone UC G8	0.00	0.02
Clone UC H1	0.00	0.01
Aspergillus flavus NRRL 3357 B	0.00	0.00
Thielavia terrestris NRRL 8126	0.09	0.49
Chaetomium globosum CBS 148.51	0.08	0.17

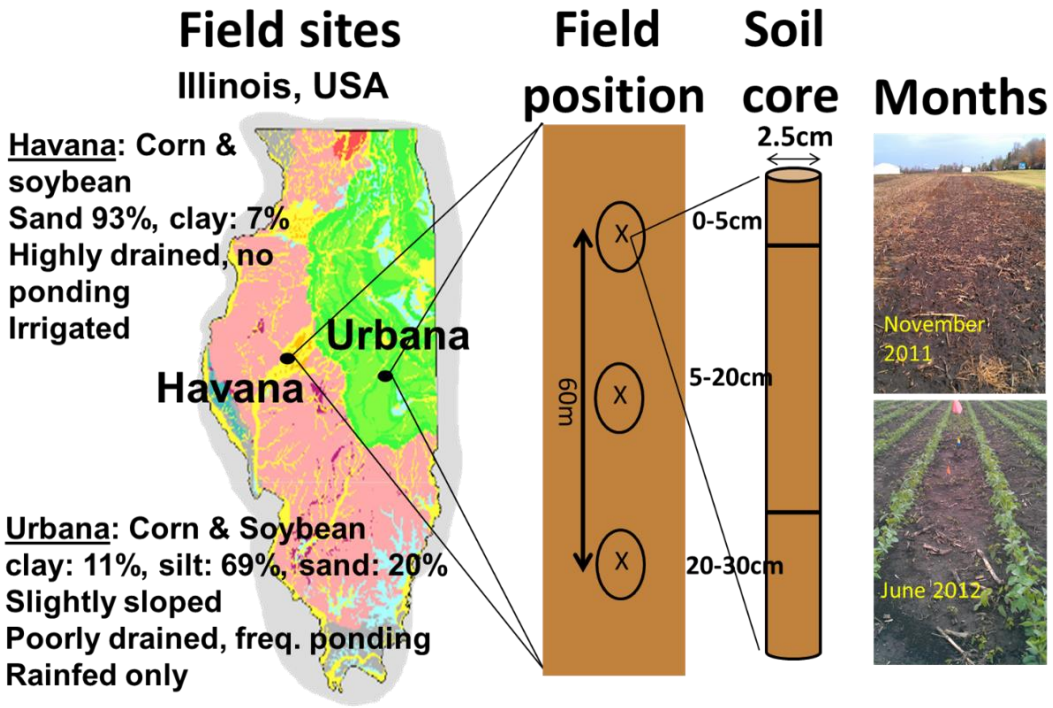


Figure 3.1: Schematic of the locations of soil sampling sites within Havana and Urbana, IL. The large brown rectangle represents the agricultural field at each site. The transect and the associated centroid sampling locations are marked by a line with arrows and circles with an X, respectively. This figure is courtesy of Drs. Allana Welsh, Joanne Chee-Sanford, and Robert Sanford (University of Illinois at Urbana-Champaign).

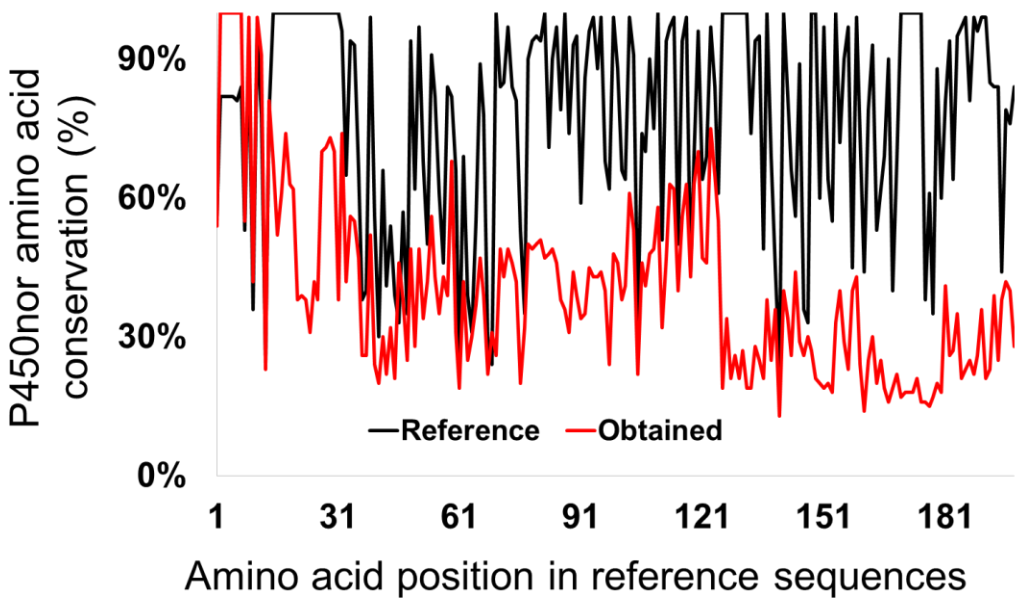


Figure 3.2: Plot of amino acid conservation of translated and aligned P450nor amplicon sequences (red) compared to amino acid conservation in the reference (black).

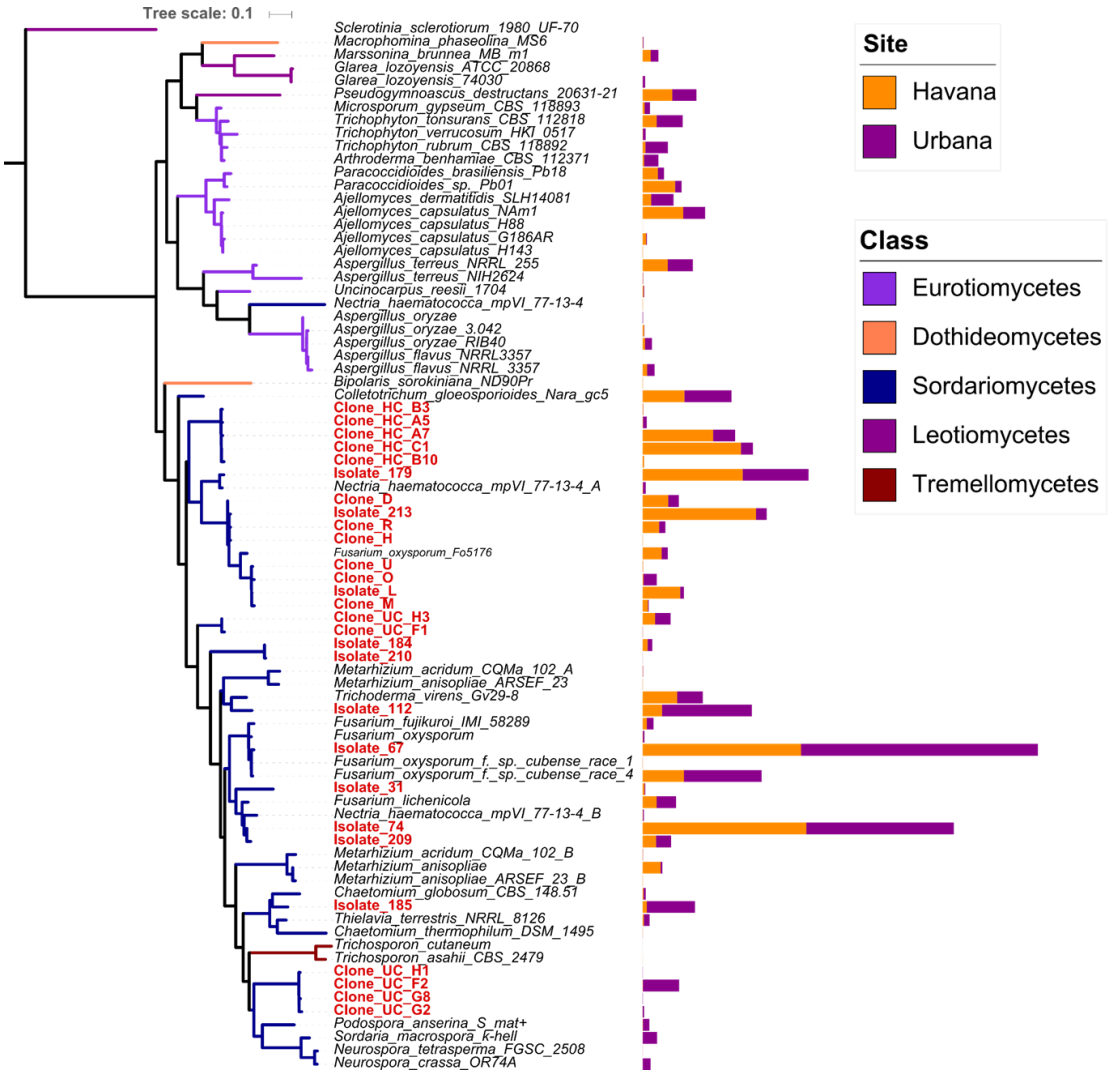


Figure 3.3: Phylogenetic tree of amino acid sequence alignment of P450nor OTUs identified in DNA extracted from Havana (gold) and Urbana (purple) soils. Relative abundances of each OTU in the soil DNA are indicated by bars on the right. OTUs colored red are either P450nor soil clones from Havana and Urbana or fungal isolates previously isolated from each site. Tree scale represents amino acid substitutions per site.

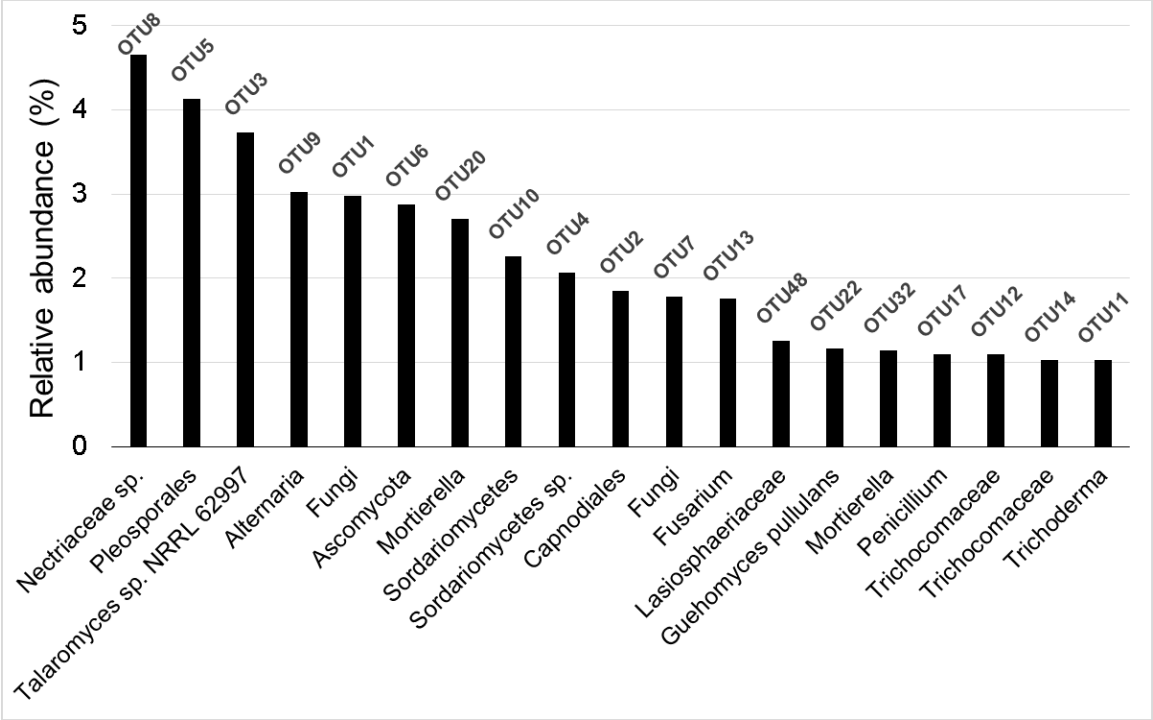


Figure 3.4: Relative abundance of ITS2 OTUs identified in DNA extracted from soil samples collected at Havana and Urbana, IL sites. The lowest taxonomic affiliation for a given OTU is presented on the x axis and the OTU label (for reference purposes) is located above each bar.

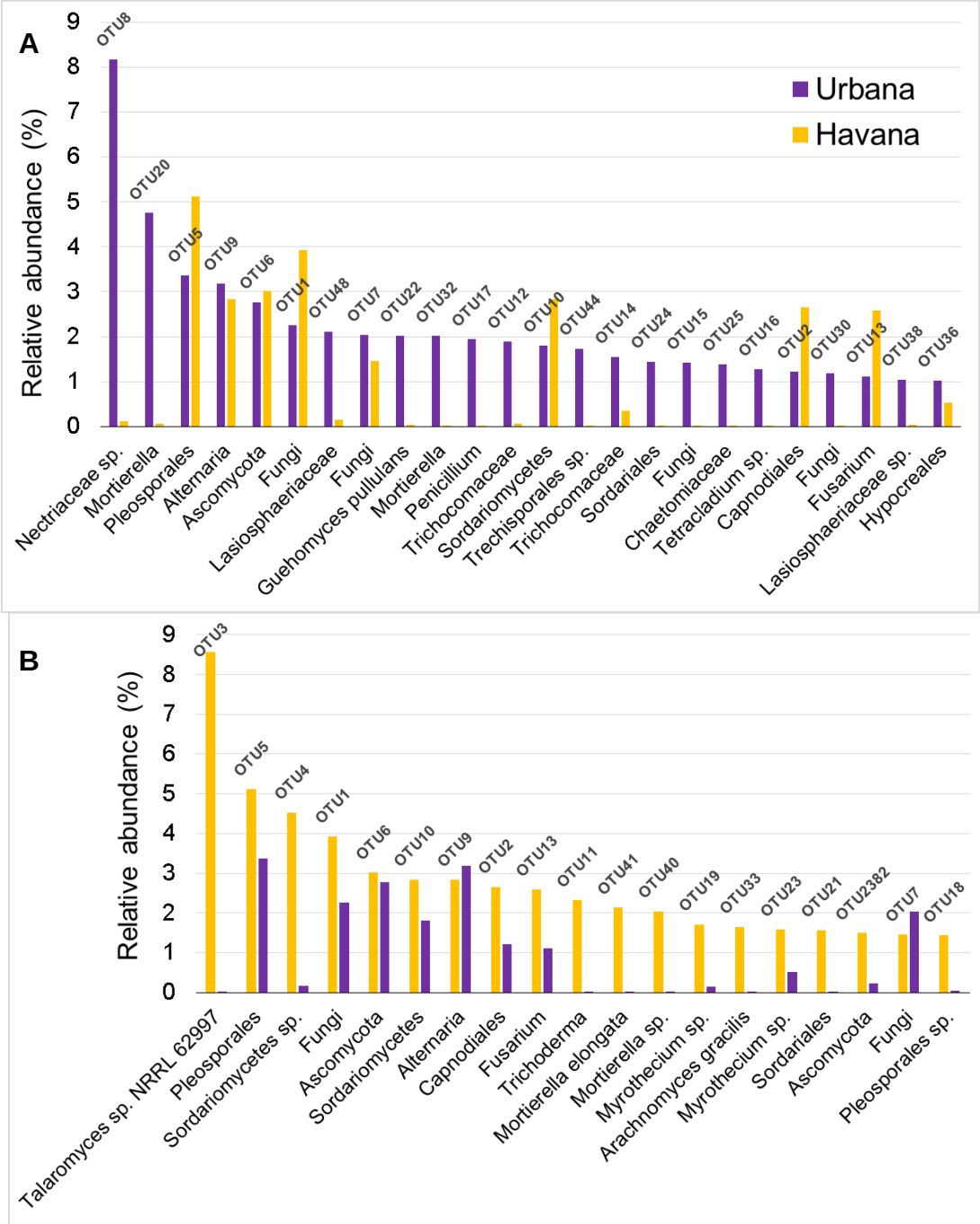


Figure 3.5: ITS2 OTUs with ≥ 1 % relative abundance in (A) Urbana and (B) Havana soils. Relative abundances of OTUs between sites are displayed for comparison purposes. The OTU label is displayed above each bar as a reference and the lowest taxonomic rank assigned to an OUT is provided on the x-axis.

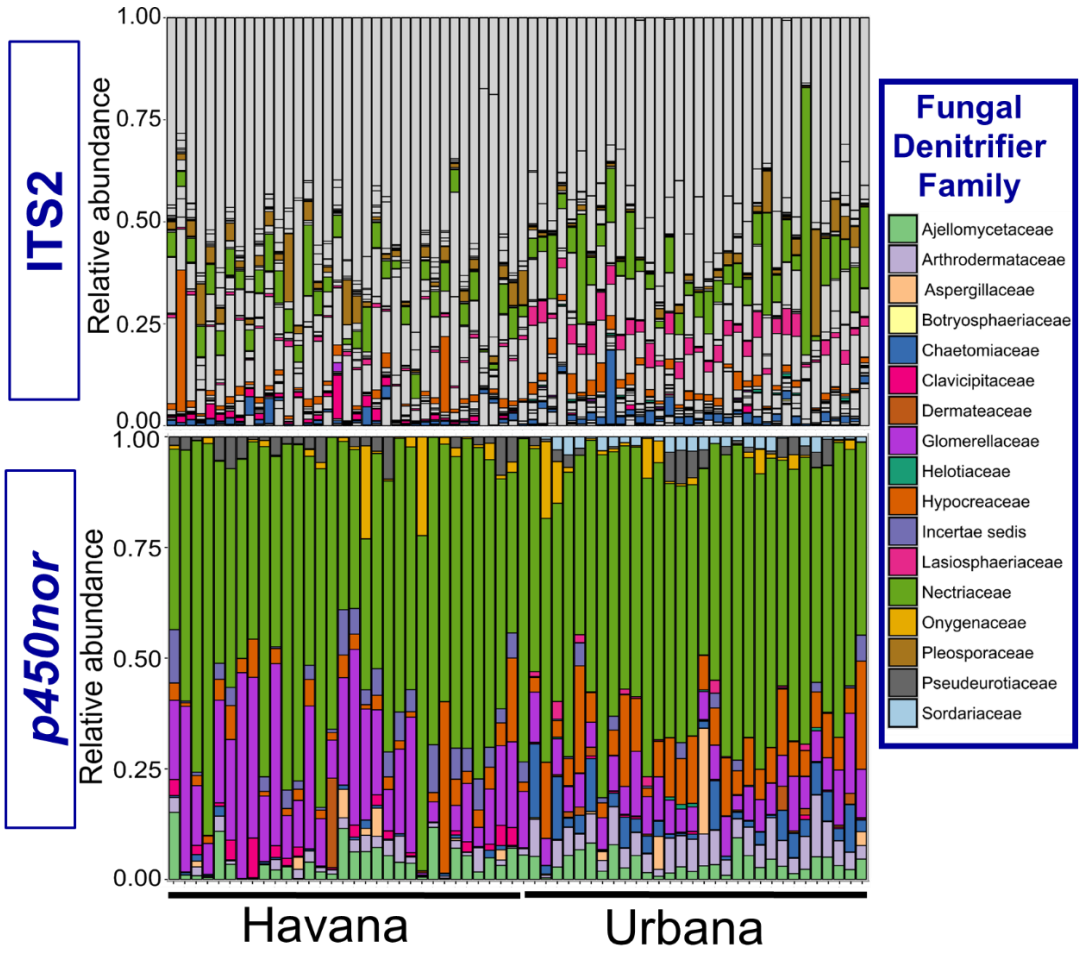


Figure 3.6: Relative abundance of fungal OTUs at the family rank within the ITS2 (above) and *p450nor* (below) amplicons. Potential for denitrification within the entire fungal community is suggested by shared taxonomic classifications between data sets. The grey bar color (top image) indicate fungal families not matching those fungal families detected in the *p450nor* data set.

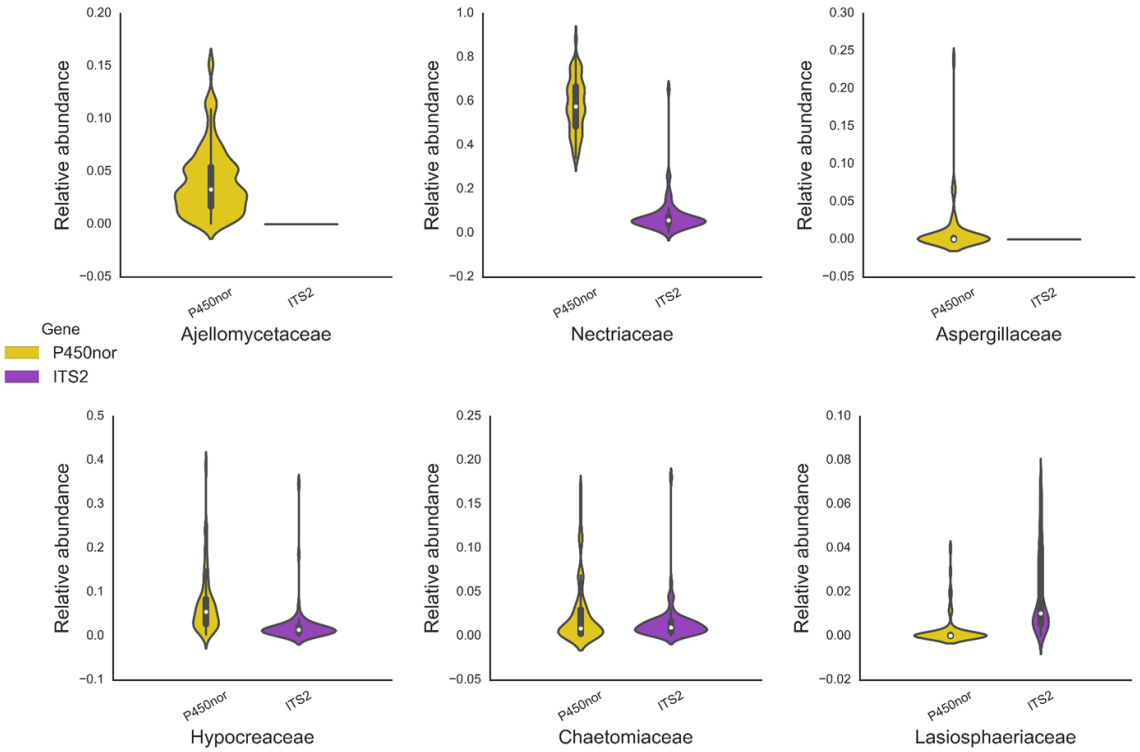


Figure 3.7: Distribution of OTU relative abundances for *p450nor* (gold) and ITS2 (purple) based on family rank classifications. OTU relative abundance distributions of OTUs within Ajellomycetaceae, Nectriaceae, Aspergillaceae (top row) display little overlap, whereas OTUs within Hypocreaceae, Chaetomiaceae, and Lasiosphaeriaceae display more similar distributions.

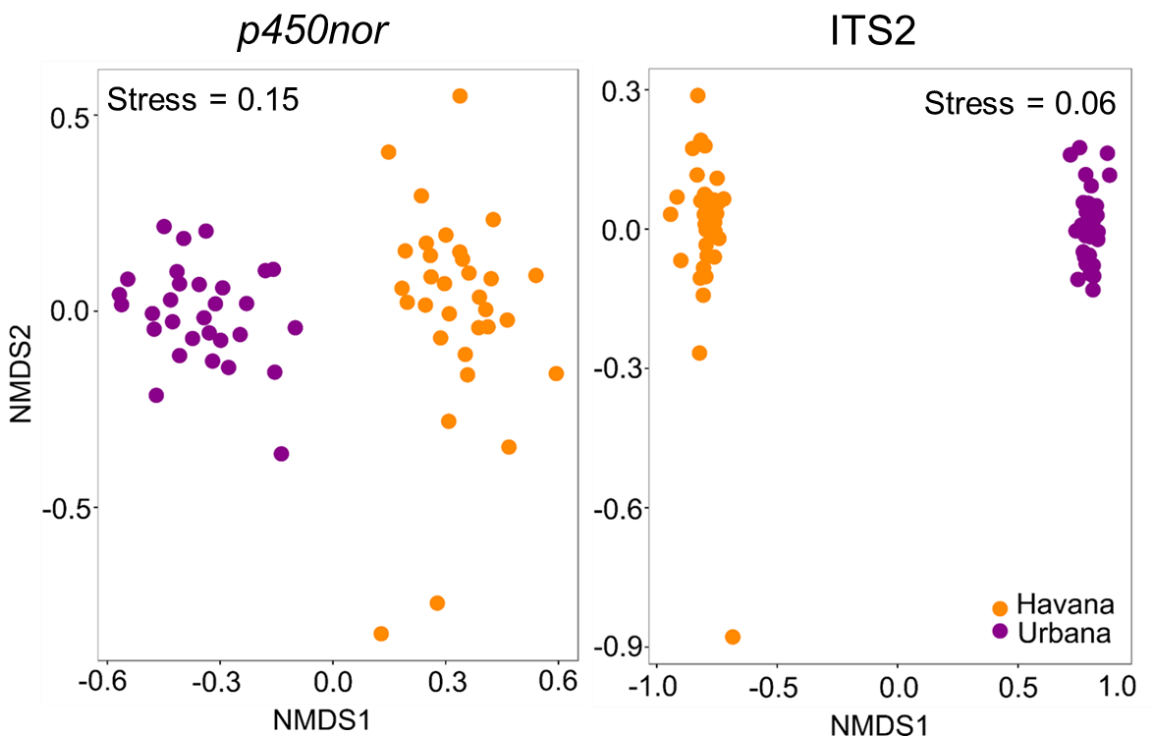


Figure 3.8: Non-metric multidimensional scaling ordination of Bray-Curtis dissimilarity matrix of *p450nor* and ITS2 OTU relative abundances for Havana and Urbana soils. Stress values are reported to indicate goodness-of-fit of the ordination. Stress values ≤ 0.2 indicate suitable fit, and values ≤ 0.05 indicate a good fit (302).

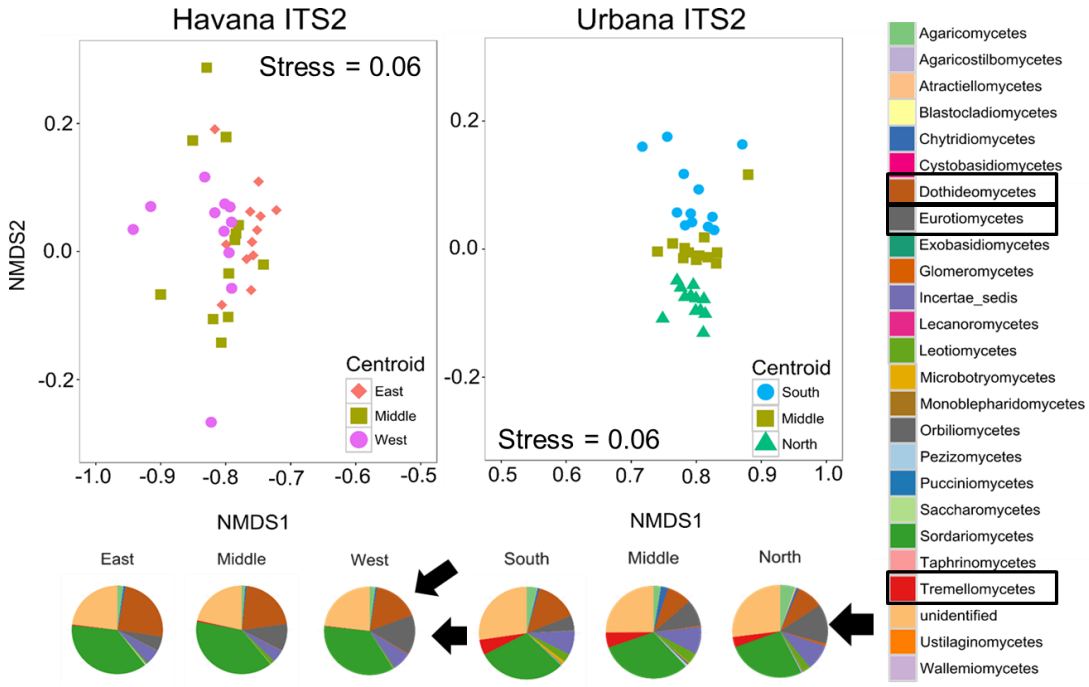


Figure 3.9: NMDS ordination of Bray-Curtis pairwise distances computed for fungal ITS2 OTU relative abundances observed in Havana and Urbana soil DNA samples (top). Points within the NMDS plots are colored by centroid location within the site. Pie charts (below) detail class level taxonomic ranks of ITS2 OTUs within each centroid. Black arrows highlight specific shifts in class relative abundance between centroids that are likely driving separation between the points. Class level designation (right) for the pie charts, with black boxes highlighting classes in the pie charts that change in relative abundance between centroids.

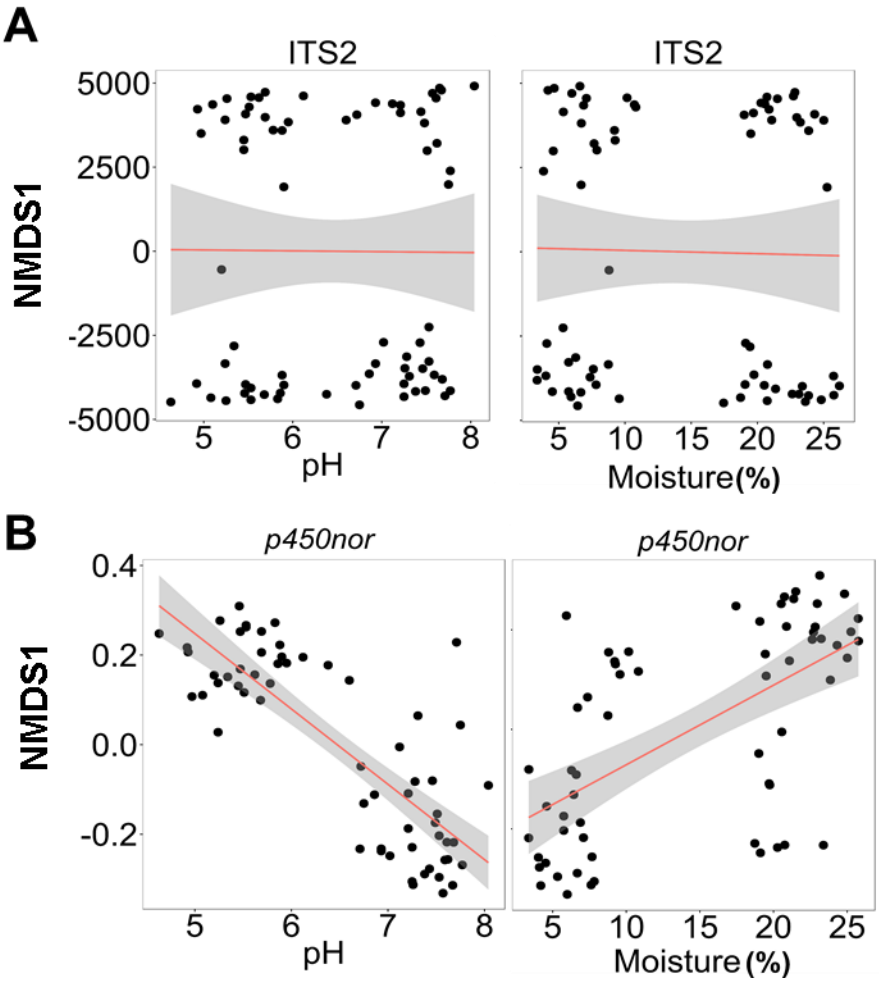


Figure 3.10: Regression of NMDS ordination values (first axis) against measured pH and moisture of Havana and Urbana soil samples for the (A) ITS2 NMDS ordination and (B) *p450nor* NMDS ordination.

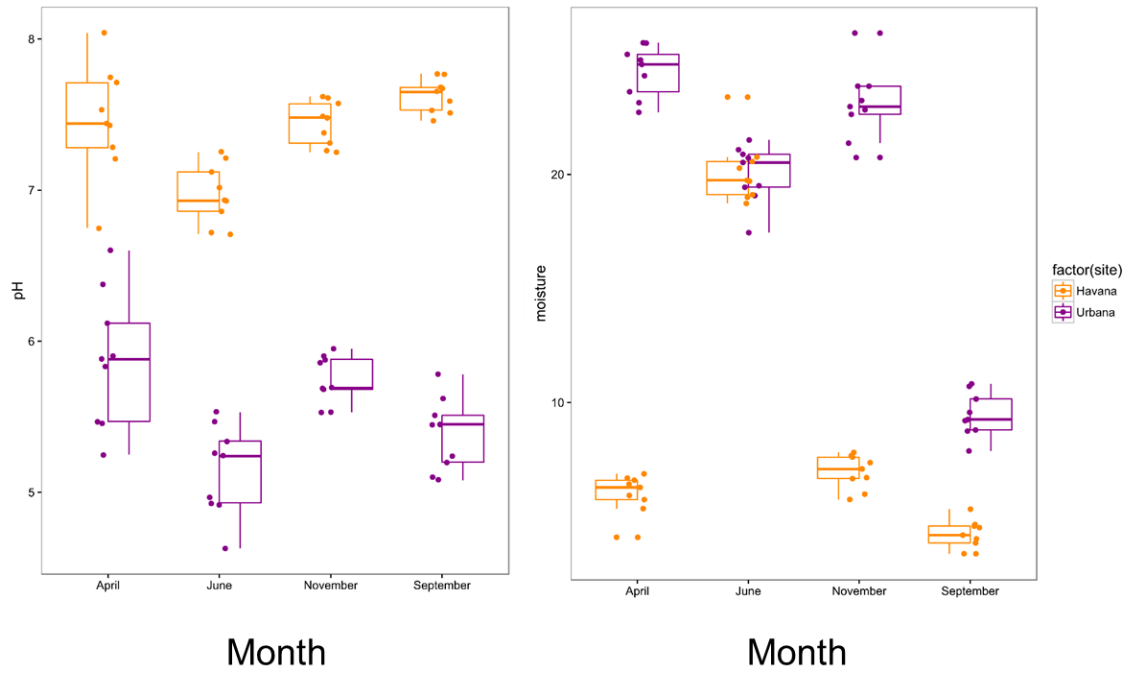


Figure 3.11: pH and moisture measurements by month within Havana (gold) and Urbana (purple) soil samples.

Table 4.1: TxtE enzyme assay reaction components and final concentrations.

Ingredient	Stock concentration	Stock solution	Volume (µL)	Final concentration
Purified TxtE	53 µM	25 mM Tris buffer, pH 8	18	1.9 µM
L-tryptophan	250 mM	0.5 M NaOH	10	5 mM
Ferredoxin NADP+ reductase	4 U/mL	1 M Trizma solution	10	0.08 U/mL
Ferredoxin	1-3 mg/mL	25 mM Tris buffer, pH 8	10	0.02-0.06 mg/mL
DiethylamineNONOate diethylammonium salt	10 mM	10 mM NaOH, diluted to 10 mM DEANO in 25 mM Tris buffer prior to addition	25	0.5 mM * 1.5 mol NO per mol DEANO = 0.75 mM NO produced
β nicotinamide adenine dinucleotide 2' phosphate, reduced	18.5 mM	25 mM Tris buffer	27	0.99 mM
Tris buffer	25 mM, pH 8	--	343	17.2 mM

Table 4.2: Results from AU tests (see Materials and Methods) for the monophyly of fungal classes within *napA*, *nirK,* and *p450nor* gene trees. Where indicated, the monophyly of two lineages was also assessed. Bold font data indicate that the AU test rejected the monophyly of the taxa. Test significance was evaluated at $p \leq 0.05$.

							AU test of Monophyly			
Gene	**Lineage**	**No. Genes**	**No. Taxa**	**No. Genera**	**Monophyletic**		**Amino acid**		**Nucleotide**	
					Amino acid	*Nucleotide*	*Diff - lnL*	*P value*	*Diff - lnL*	*P value*
napA	Agaricomycetes	2	1	1	Yes	Yes	-	-	-	-
	Dothideomycetes	7	7	6	**No**	**No**	**40**	**0.015**	**40**	**0.001**
	Eurotiomycetes	36	34	14	**No**	**No**	**753**	**2.00E-06**	**550**	**4.00E-04**
	Lecanoromycetes (Lec)	1	1	1	Yes	Yes	-	-	-	-
	Leotiomycetes (L)	2	2	2	Yes	Yes	-	-	-	-
	Microbotryomycetes	4	4	1	Yes	Yes	-	-	-	-
	Pucciniomycetes	2	2	2	**No**	**No**	**1303**	**9.00E-05**	**1088**	**2.00E-08**
	Sordariomycetes (S)	23	23	18	**No**	**No**	**806**	**7.00E-61**	**770**	**9.00E-56**
	Tremellomycetes	1	1	1	Yes	Yes	-	-	-	-
	L+S share MRCA				**No**	**No**	**908**	**2.00E-71**	**973**	**6.00E-74**
	Lec+E share MRCA				**No**	**No**	**75**	**3.00E-05**	**257**	**9.00E-06**
nirK	Dothideomycetes	1	1	1	Yes	Yes	-	-	-	-
	Eurotiomycetes	52	52	17	No	No	19	0.142	**33**	**0.003**
	Leotiomycetes	10	9	1	Yes	Yes	-	-	-	-
	Sordariomycetes	20	20	8	Yes	Yes	-	-	-	-
	D+E share MRCA				**No**	**No**	**15**	**0.042**	**30.1**	**0.004**
	L+S share MRCA				No	No	18	0.142	35.3	0.001
p450nor	Dothideomycetes (D)	28	28	26	**No**	**No**	**1153**	**4.00E-05**	**1294**	**8.00E-51**
	Eurotiomycetes (E)	36	35	17	**No**	**No**	**891**	**1.00E-32**	**917**	**2.00E-37**
	Leotiomycetes (L)	37	36	16	**No**	**No**	**465**	**2.00E-39**	**694**	**4.00E-40**
	Sordariomycetes (S)	72	63	32	**No**	**No**	**1159**	**5.00E-10**	**1206**	**5.00E-15**
	Tremellomycetes	3	3	2	**No**	**No**	**125**	**3.00E-04**	**125**	**3.00E-08**
	Atractiellomycetes	1	1	1	Yes	Yes	-	-	-	-
	Pezizomycetes	1	1	1	Yes	Yes	-	-	-	-
	L+S share MRCA				**No**	**No**	**1386**	**3.00E-43**	**1420**	**5.00E-72**
	D+E share MRCA				**No**	**No**	**1481**	**0.001**	**1481**	**2.00E-63**
	Ascomycota (A)				**No**	**No**	**139**	**5.00E-05**	**140**	**6.00E-06**
	Basidiomycota (B)				**No**	**No**	**139**	**4.00E-56**	**139**	**1.00E-39**
	A+B share MRCA				**No**	**No**	**139**	**3.00E-11**	**140**	**3.00E-04**

Table 4.3: Results from species-tree gene-tree reconciliation using NOTUNG software for *napA*, *nirK*, and *p450nor* genes in fungi. Values are averages of solutions with standard deviations reported in parentheses.

Gene	Phylogeny	Duplications	Codivergences	Transfers	Losses	Duplication cost	Transfer cost	Loss cost	Solutions
p450nor	amino acid	-	-	-	-	2	3	1	0
		-	-	-	-	2	5	1	0
		-	-	-	-	2	7	1	0
		-	-	-	-	2	9	1	0
		49.0 (0.0)	0.0 (0.0)	15.0 (0.0)	253.0 (0.0)	2	11	1	1000
		61.0 (0.0)	0.0 (0.0)	6.0 (0.0)	333.0 (0.0)	2	13	1	180
		62.1 (1.0)	0.0 (0.0)	5.4 (0.5)	339.3 (5.4)	2	15	1	420
p450nor	nucleotide	-	-	-	-	2	3	1	0
		-	-	-	-	2	5	1	0
		-	-	-	-	2	7	1	0
		45.0 (0.0)	0.0 (0.0)	16.0 (0.0)	215.0 (0.0)	2	9	1	1000
		53.6 (0.8)	0.0 (0.0)	8.2 (0.4)	277.6 (2.8)	2	11	1	1000
		56.0 (0.0)	0.0 (0.0)	6.0 (0.0)	299.0 (0.0)	2	13	1	100
		60.0 (0.0)	0.0 (0.0)	4.0 (0.0)	319.0 (0.0)	2	15	1	60
napA	amino acid	1.4 (0.5)	0.0 (0.0)	30.8 (0.8)	14.9 (1.7)	2	3	1	1000
		9.2 (1.4)	0.0 (0.0)	19.8 (1.4)	43.7 (4.3)	2	5	1	1000
		15.0 (0.0)	0.0 (0.0)	14.0 (0.0)	64.0 (0.0)	2	7	1	36
		22.0 (1.3)	0.0 (0.0)	7.8 (1.0)	100.8 (6.4)	2	9	1	20
		28.0 (0.0)	0.0 (0.0)	3.0 (0.0)	135.0 (0.0)	2	11	1	1
		28.0 (0.0)	0.0 (0.0)	3.0 (0.0)	135.0 (0.0)	2	13	1	1
		31.0 (1.0)	0.0 (0.0)	0.5 (0.5)	165.5 (5.5)	2	15	1	2
napA	nucleotide	-	-	-	-	2	3	1	0
		-	-	-	-	2	5	1	0
		-	-	-	-	2	7	1	0
		-	-	-	-	2	9	1	0
		-	-	-	-	2	11	1	0
		28.0 (1.0)	0.0 (0.0)	2.5 (0.5)	142.5 (4.5)	2	13	1	2
		30.0 (0.0)	0.0 (0.0)	1.0 (0.0)	159.0 (0.0)	2	15	1	1

Table 4.3: (continued).

Gene	Phylogeny	Duplications	Codivergences	Transfers	Losses	Duplication cost	Transfer cost	Loss cost	Sample size
nirK	amino acid	0.0 (0.0)	0.0 (0.0)	31.0 (0.0)	19.0 (0.0)	2	3	1	1000
		16.6 (1.1)	0.0 (0.0)	10.4 (1.1)	71.8 (3.3)	2	5	1	1000
		24.3 (0.5)	0.0 (0.0)	2.7 (0.5)	101.7 (2.4)	2	7	1	3
		25.5 (0.5)	0.0 (0.0)	1.5 (0.5)	108.5 (3.5)	2	9	1	2
		26.0 (0.0)	0.0 (0.0)	1.0 (0.0)	112.0 (0.0)	2	11	1	1
		28.0 (0.0)	0.0 (0.0)	0.0 (0.0)	120.0 (0.0)	2	13	1	1
		28.0 (0.0)	0.0 (0.0)	0.0 (0.0)	120.0 (0.0)	2	15	1	1
nirK	nucleotide	-	-	-	-	2	3	1	0
		-	-	-	-	2	5	1	0
		21.0 (0.0)	0.0 (0.0)	2.0 (0.0)	90.0 (0.0)	2	7	1	2
		24.0 (0.0)	0.0 (0.0)	0.0 (0.0)	100.0 (0.0)	2	9	1	1
		24.0 (0.0)	0.0 (0.0)	0.0 (0.0)	100.0 (0.0)	2	11	1	1
		24.0 (0.0)	0.0 (0.0)	0.0 (0.0)	100.0 (0.0)	2	13	1	1
		24.0 (0.0)	0.0 (0.0)	0.0 (0.0)	100.0 (0.0)	2	15	1	1

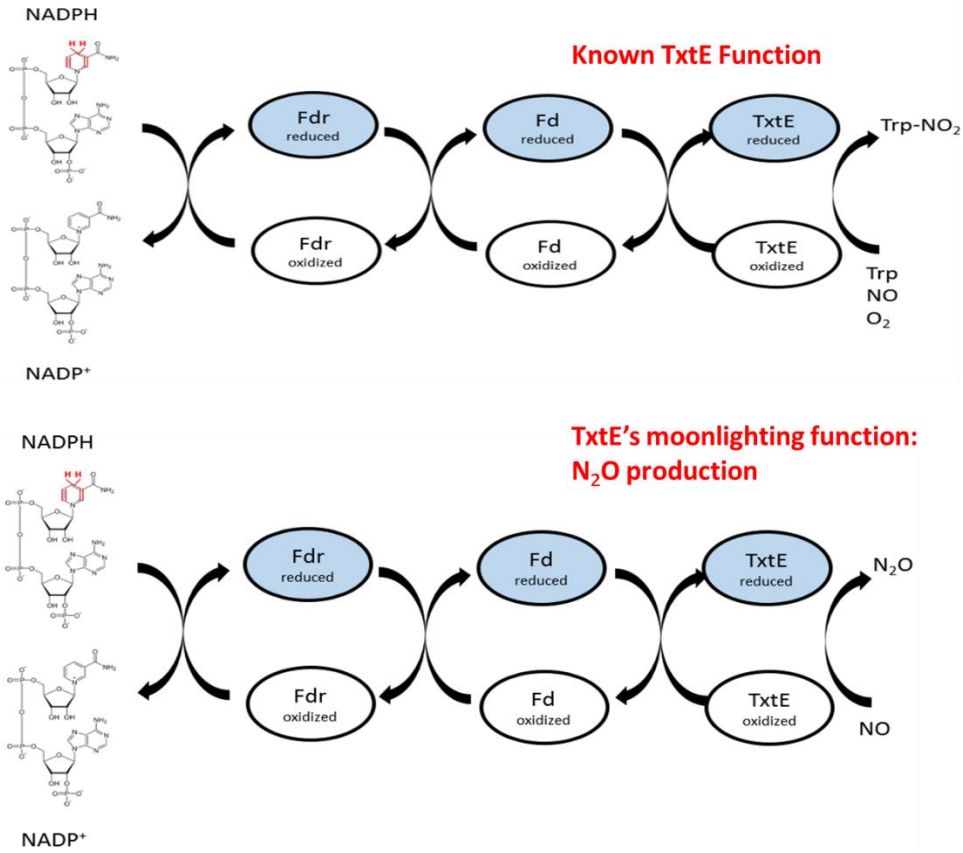


Figure 4.1: Schematic of the proposed TxtE nitration reaction of L-tryptophan that has been demonstrated to occur *in vitro* (254) (top) and the hypothesized side reaction of TxtE in N_2O formation (bottom). In some cases, presumably without the substrates for nitration (L-tryptophan, O_2) present, TxtE may react with two NO molecules to produce N_2O as demonstrated for P450nor.

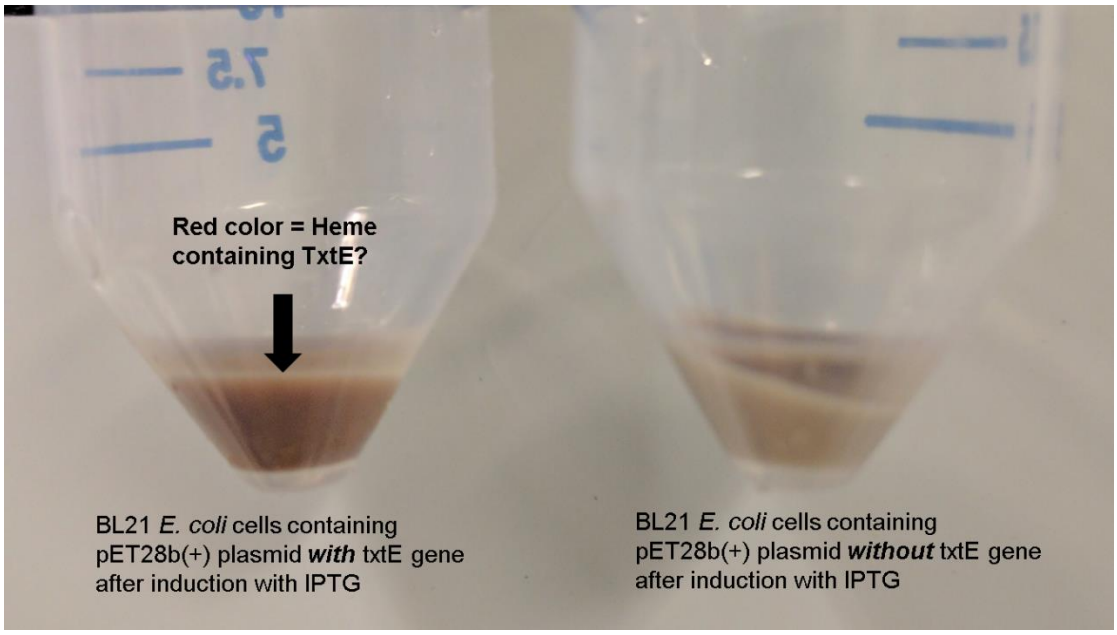


Figure 4.2: BL21 *Escherichia coli* cell pellets following induction of cells with IPTG. Both sets of cells contain a pET28b(+) vector with or without the *txtE* gene, encoding a nitrating cytochrome P450. The darker red color of induced *E. coli* containing plasmid with the *txtE* gene suggests a large production of heme-containing protein.

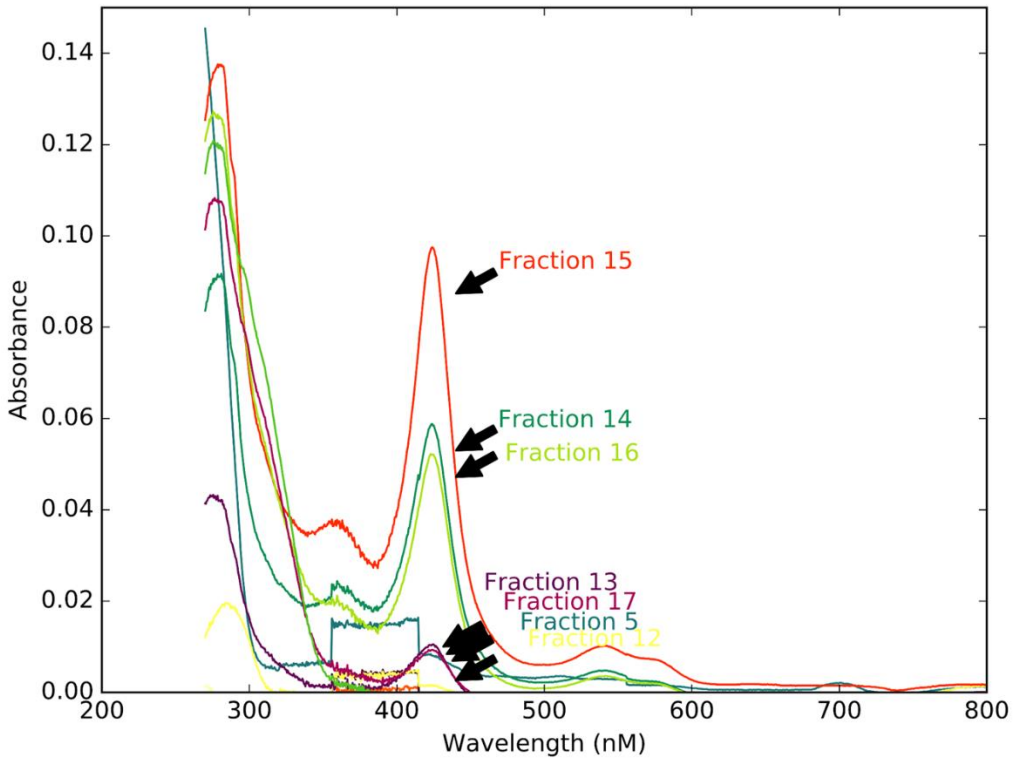


Figure 4.3: Plot of absorbance of eluted protein fractions from metal ion affinity chromatography. An increasing absorbance at 417 nm indicates a heme-containing protein, possibly the target protein TxtE, was eluted from the column in the collected fractions. Peaks at 280 nm represent absorbance of aromatic amino acid moieties of proteins present within these fractions.

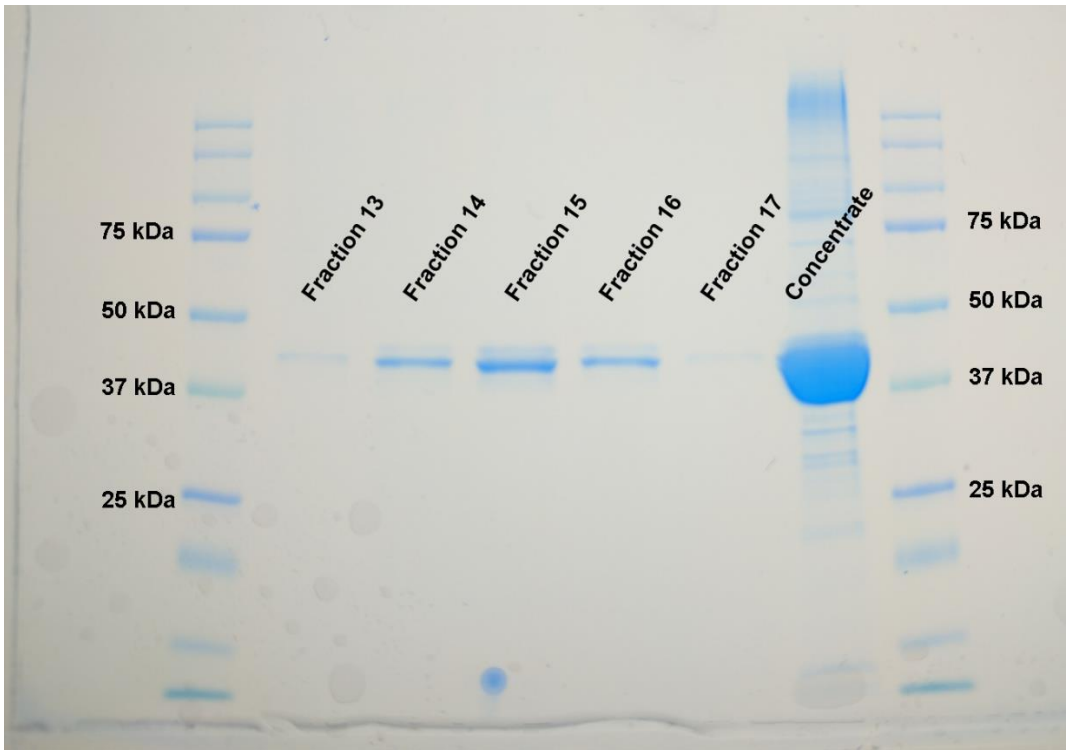
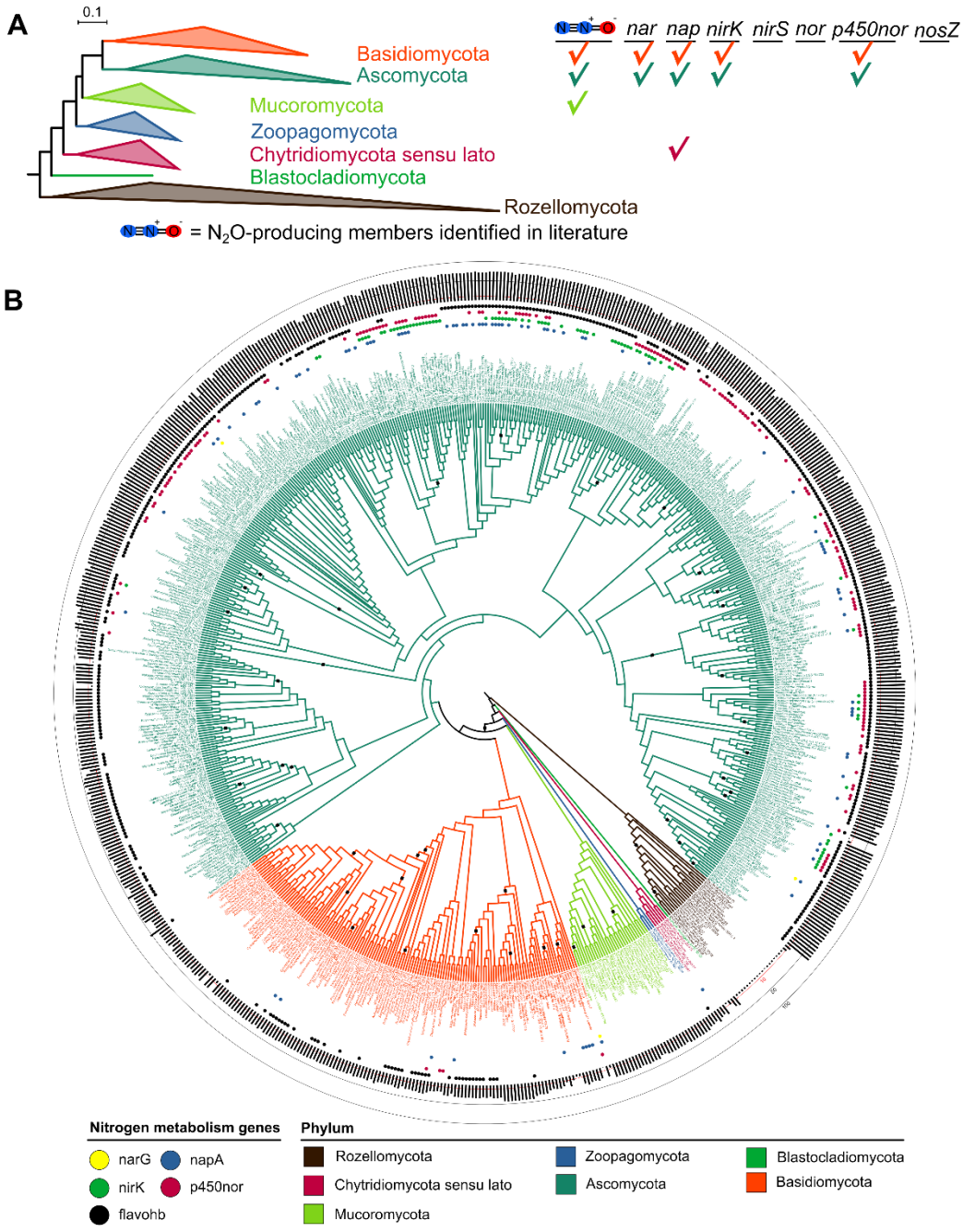


Figure 4.4: SDS-PAGE gel of purified TxtE protein (20 µL) produced in IPTG-induced BL21 *Escherichia coli* cells containing the *txtE* gene in a pET28b(+) vector. Lanes contain his-tagged protein-containing fractions eluted from a nickel ion embedded affinity chromatography column. Lane labeled “Concentrate” shows the pooled fractions (13-17) after concentration using a 30 kDa cutoff MWCO filter. Outer most lanes are precision protein plus kaleidoscope protein standards. kDa, kilodalton.

Figure 4.5: Maximum likelihood phylogeny of the kingdom Fungi inferred from a concatenated alignment of 238 single copy marker gene amino acid sequences (see Materials and Methods). The presence/absence of key denitrification genes within fungal phyla queried in the present study (A) and within individual members (B). Black squares marking branches indicate nodes with bootstrap percentages below 90%. The scale bar in (A) represents amino acid substitutions per site. The outer black bars in (B) represent the percentage (out of 1438) of conserved single copy genes in kingdom Fungi that were detected in the fungal genomes queried in the present study. Additional colored markers surrounding the tree indicate presence or absence of each gene within a fungal genome. Flavohb, flavohemiglobin genes involved in NO detoxification to NO_3^-.


A
0.1
Basidiomycota
Ascomycota
Mucoromycota
Zoopagomycota
Chytridiomycota sensu lato
Blastocladiomycota
Rozellomycota
nar
nap
nirK
nirS
nor
p450nor
nosZ
= N2O-producing members identified in literature
B
Nitrogen metabolism genes
narG
napA
nirK
p450nor
flavohb
Phylum
Rozellomycota
Chytridiomycota sensu lato
Mucoromycota
Zoopagomycota
Ascomycota
Blastocladiomycota
Basidiomycota

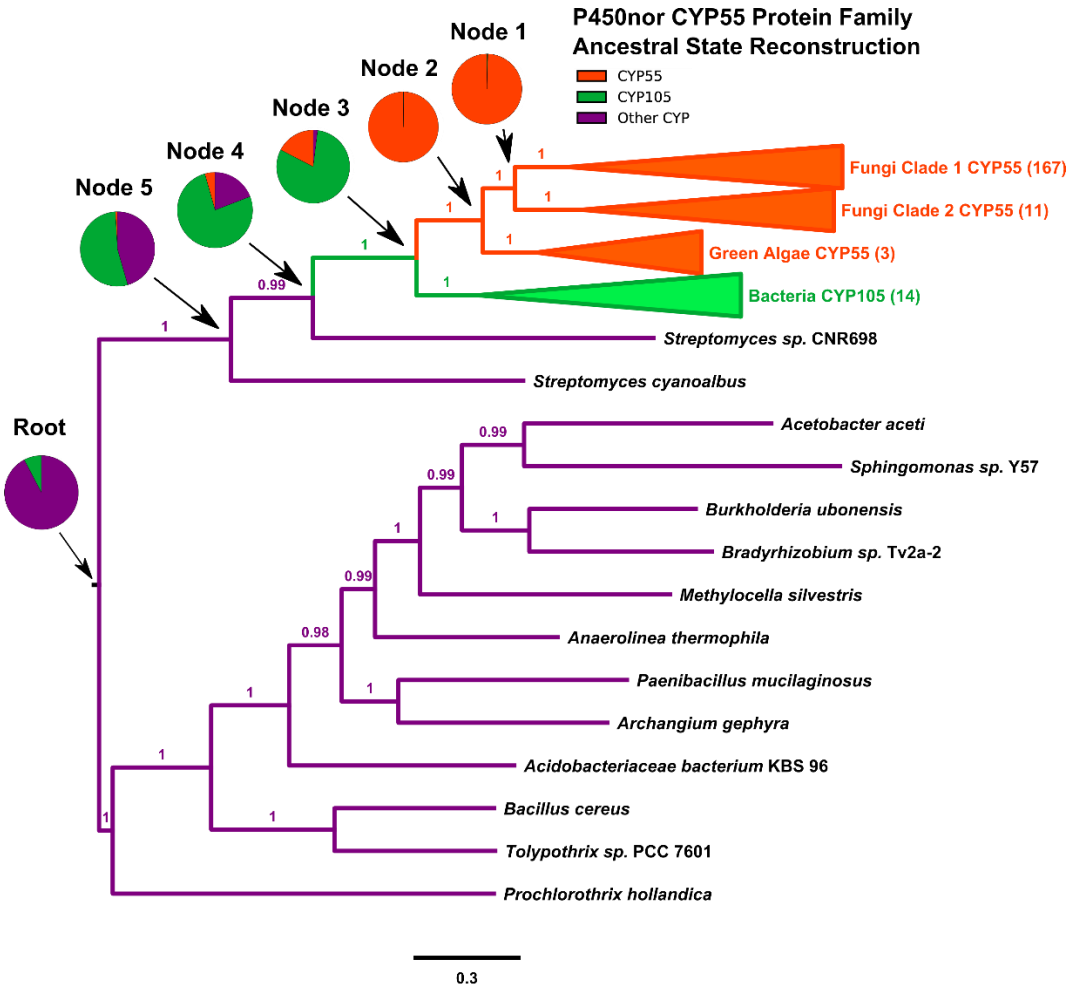


Figure 4.6: Midpoint-rooted Bayesian phylogeny of select families of cytochrome P450 amino acid sequences from fungi, algae, and bacteria. Ancestral state reconstruction was performed using CYP55 (orange), CYP105 (green), and other CYPs (purple) to uncover the shared ancestry of algal and fungal N_2O-producing cytochrome P450s with their most recent common bacterial ancestor. The scale bar indicates substitutions per site and values above branches are posterior probabilities of the Bayesian MCMC analysis. Numbers in parentheses next to collapsed clades indicate the number of sequences in the clade. Values in pie charts are average probabilities of each character across a representative Bayesian MCMC analysis.

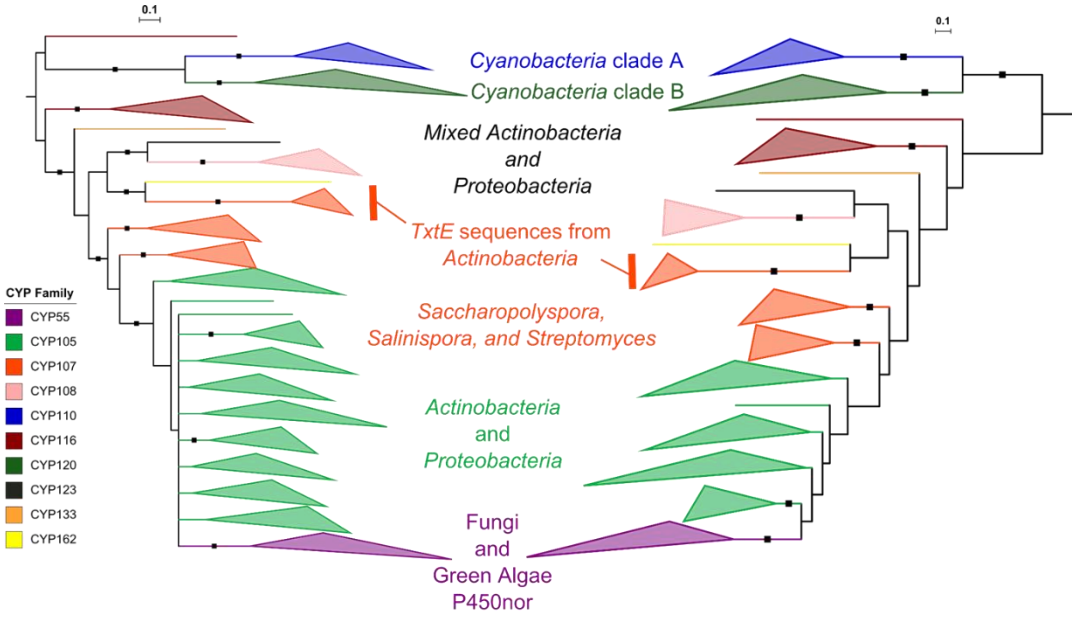


Figure 4.7: Midpoint rooted Bayesian (left) and Maximum-Likelihood phylogenies (right) of 301 cytochrome P450 sequences demonstrating the affiliation of P450nor with other sequences belonging to members of the bacterial phyla *Actinobacteria* and *Proteobacteria*. Black squares on branches (left tree) indicate ≥0.95 posterior probability or ≥90 % bootstrap replication (right tree). The colored legend indicates the cytochrome P450 family specified by shared amino acid identity of ≥40 % (280).



Figure 4.8: Bayesian tree reconstruction of actinobacterial and proteobacterial 16S rRNA gene (left) and cytochrome P450 family 105 amino acid sequences (right). Both phylogenies represent 50% majory-rule consensus trees. The tree on the left is rooted with proteobacterial sequences as outgroup to the Actinobacteria. The tree on the right is midpoint rooted. Nodes with posterior probabilites ≥ 0.95 are indicated by black circles on an adjacent branch.

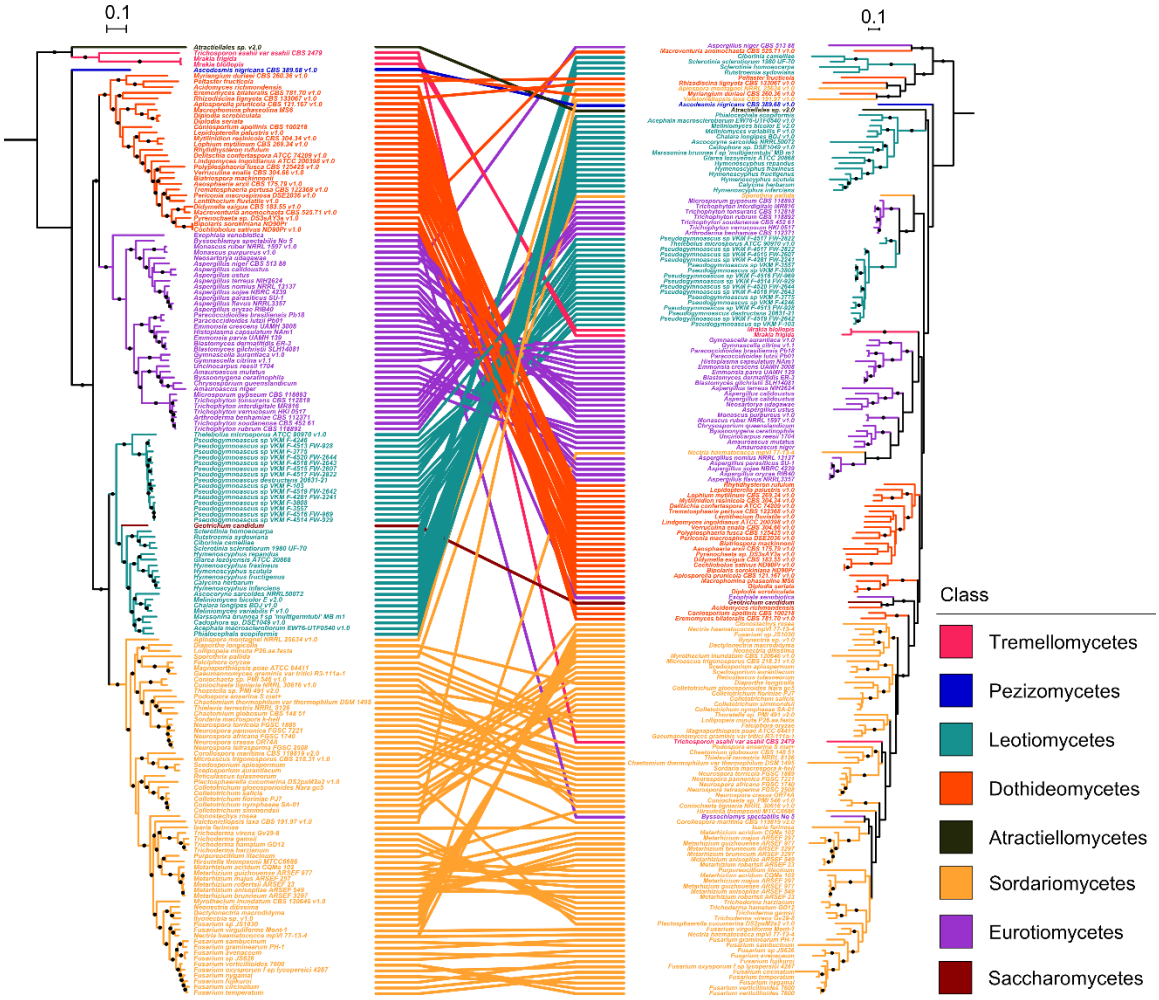


Figure 4.9: Maximum-likelihood phylogenies connecting fungal species with their respective nitric oxide reductase (*p450nor*) gene sequence(s). On the left, an amino acid phylogeny of 238 concatenated single copy orthologues from fungal species in which one or more *p450nor* gene(s) were detected. The *p450nor* nucleotide phylogeny (right) demonstrates many instances of incongruence with the fungal species phylogeny. Black dots in each phylogeny represent bootstrap percentages greater than or equal to 90%. Scale bars represent substitutions per site.

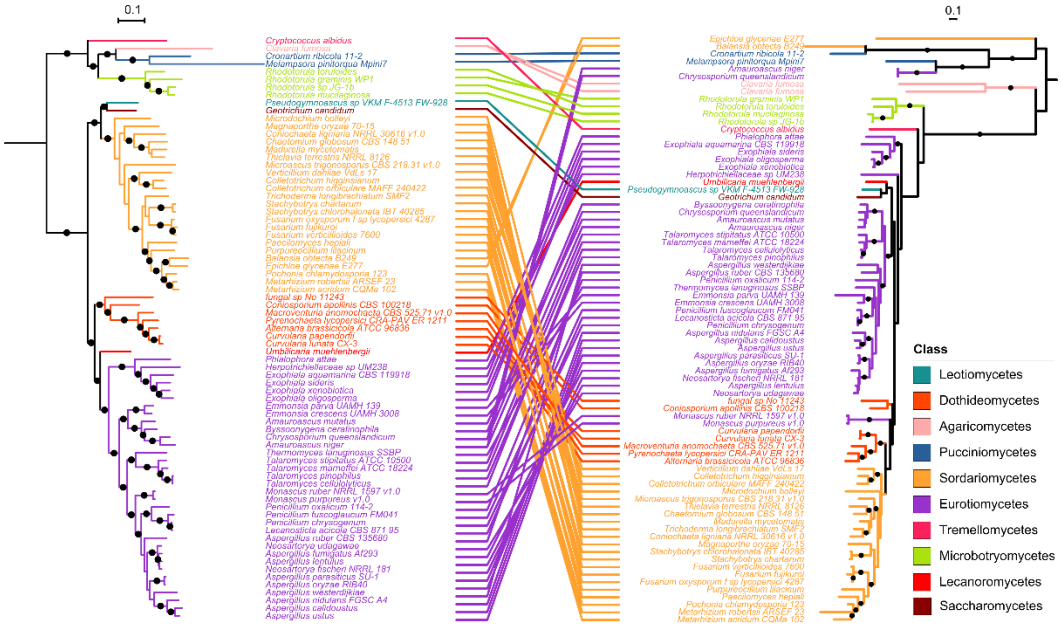


Figure 4.10: Cophylogenetic plot of *napA*-containing fungal species (left) and the *napA* nucleotide tree (right). Both are ML trees where blacks dots represent bootstrap percentages ≥90 %. Scale bars indicate substitutions per site for the concatenated amino acid species phylogeny and nucleotide phylogeny, respectively.

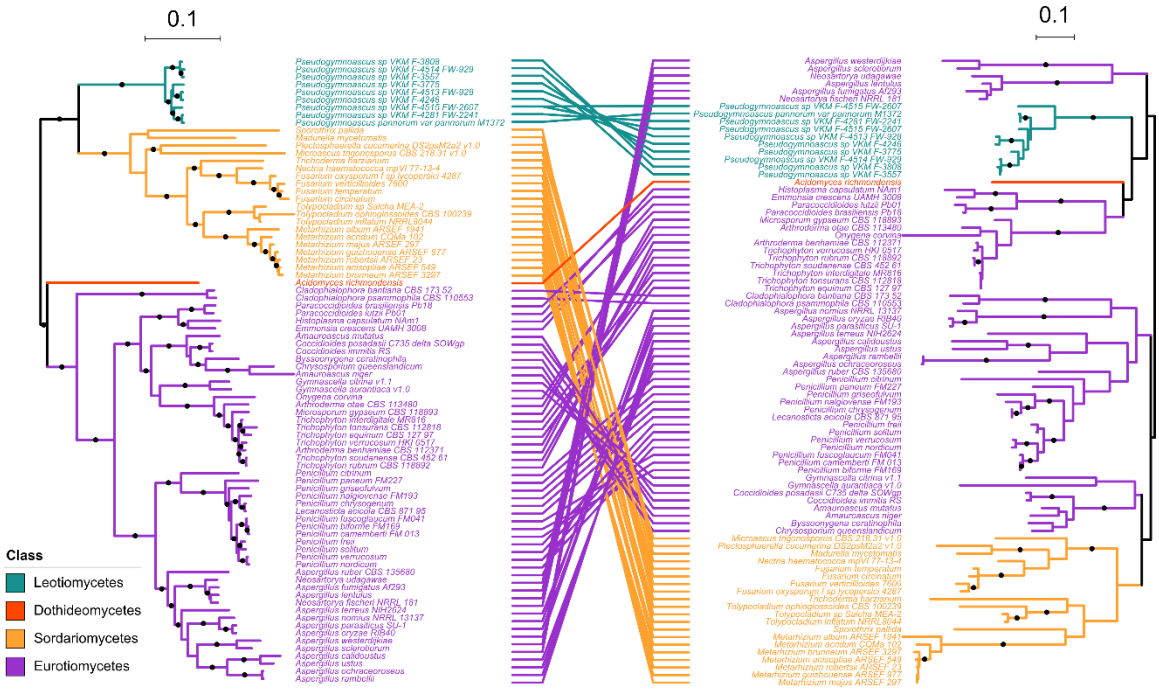
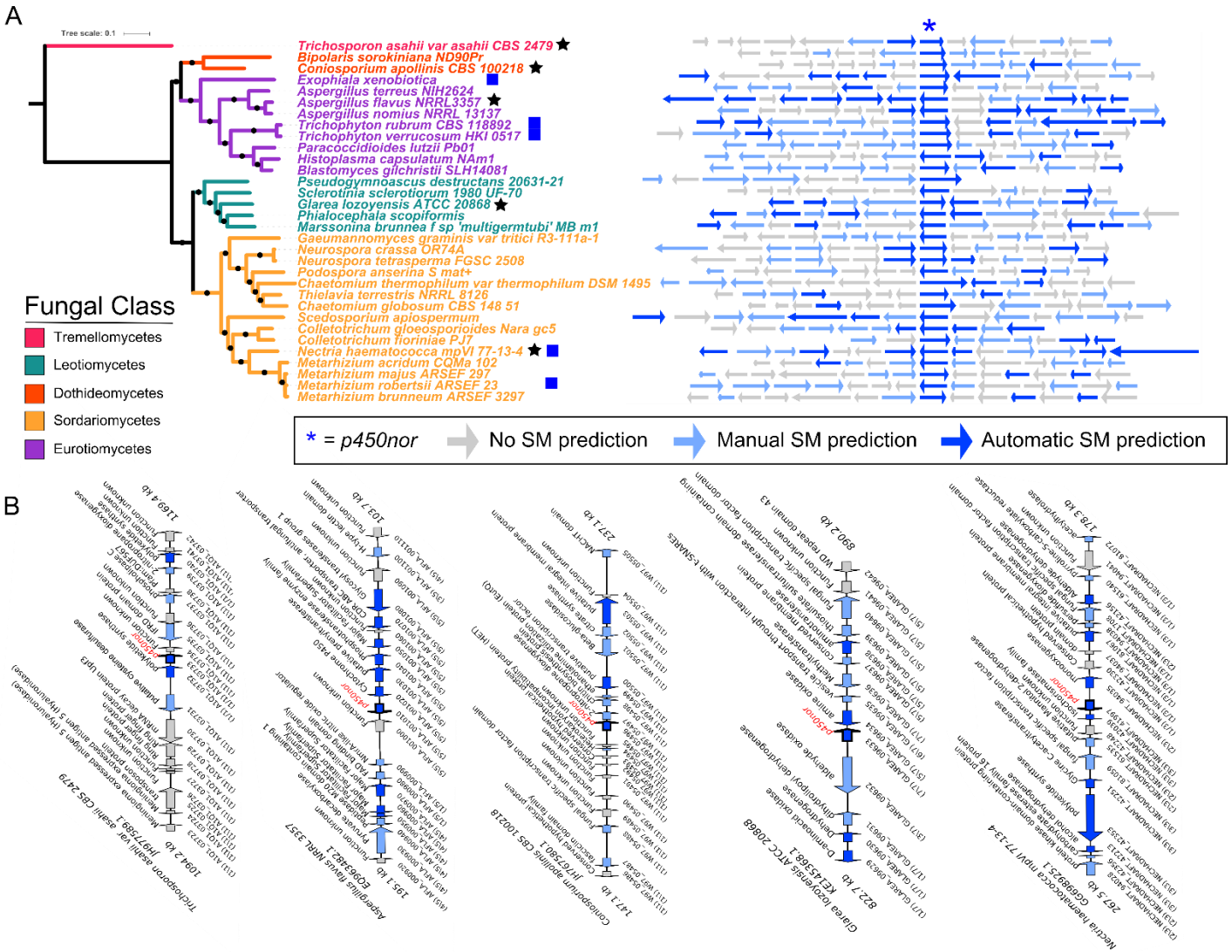


Figure 4.11: Cophylogenetic plot of *nirK*-containing fungal species (left) and the *nirK* nucleotide tree (right). Both are ML trees where blacks dots represent bootstrap percentages ≥90 %. Scale bars indicate substitutions per site for the concatenated amino acid species phylogeny and nucleotide phylogeny, respectively.

Figure 4.12: ML phylogeny of a concatenated set of 238 amino acid sequences (A) and zoomed in view of genes surrounding *p450nor* in five of the 32 fungi (B). Black stars at the tips of the phylogeny in (A) indicate the zoomed in gene regions are depicted in (B). Fungi predicted to have *p450nor* contained within an SM cluster are indicated with a blue square at the end of the phylogeny. Arrows at the tips of the phylogeny represent the genomic arrangement of *p450nor* (blue asterisk) and surrounding genes. Distance between arrows are scaled representations of actual genomic distances within the genomes. Grey, light blue, and dark blue arrows represent no SM annotation, manual SM annotation, and automatic SM annotation (see Materials and Methods for details). The scale bar indicates amino acid substitutions per site and black circles indicate bootstrap percentages ≥90 %.


A
Tree scale: 0.1
Trichosporon asahii var asahii CBS 2479
Bipolaris sorokiniana ND90Pr
Coniosporium apollinis CBS 100218
Exophiala xenobiotica
Aspergillus terreus NIH2624
Aspergillus flavus NRRL3357
Aspergillus nomius NRRL 13137
Trichophyton rubrum CBS 118892
Trichophyton verrucosum HKI 0517
Paracoccidioides lutzii Pb01
Histoplasma capsulatum NAm1
Blastomyces gilchristii SLH14081
Pseudogymnoascus destructans 20631-21
Sclerotinia sclerotiorum 1980 UF-70
Glarea lozoyensis ATCC 20868
Phialocephala scopiformis
Marssonina brunnea f sp 'multigermtubi' MB m1
Gaeumannomyces graminis var tritici R3-111a-1
Neurospora crassa OR74A
Neurospora tetrasperma FGSC 2508
Podospora anserina S mat+
Chaetomium thermophilum var thermophilum DSM 1495
Thielavia terrestris NRRL 8126
Chaetomium globosum CBS 148 51
Scedosporium apiospermum
Colletotrichum gloeosporioides Nara gc5
Colletotrichum fioriniae PJ7
Nectria haematococca mpVI 77-13-4
Metarhizium acridum CQMa 102
Metarhizium majus ARSEF 297
Metarhizium robertsii ARSEF 23
Metarhizium brunneum ARSEF 3297
Fungal Class
Tremellomycetes
Leotiomycetes
Dothideomycetes
Sordariomycetes
Eurotiomycetes
* = p450nor
No SM prediction
Manual SM prediction
Automatic SM prediction
B

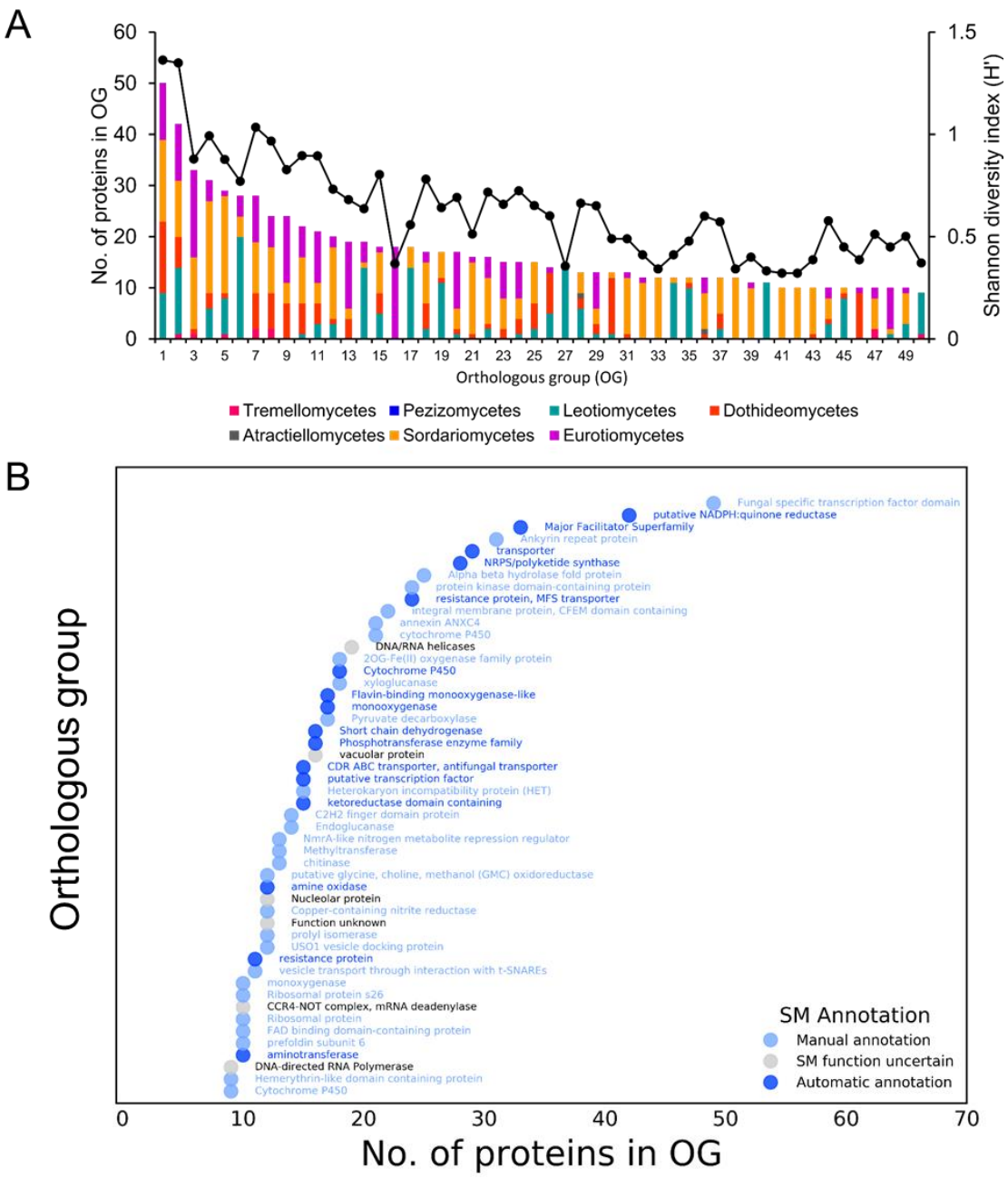


Figure 4.13: Taxonomic representation of the top 50 orthologous groups (A) and their functional annotations (B). Bars in (A) are colored by fungal class. Data points in (B) are colored according to whether they were automatically (dark blue), manually (light blue), or were not predicted (grey) to be involved in SM.

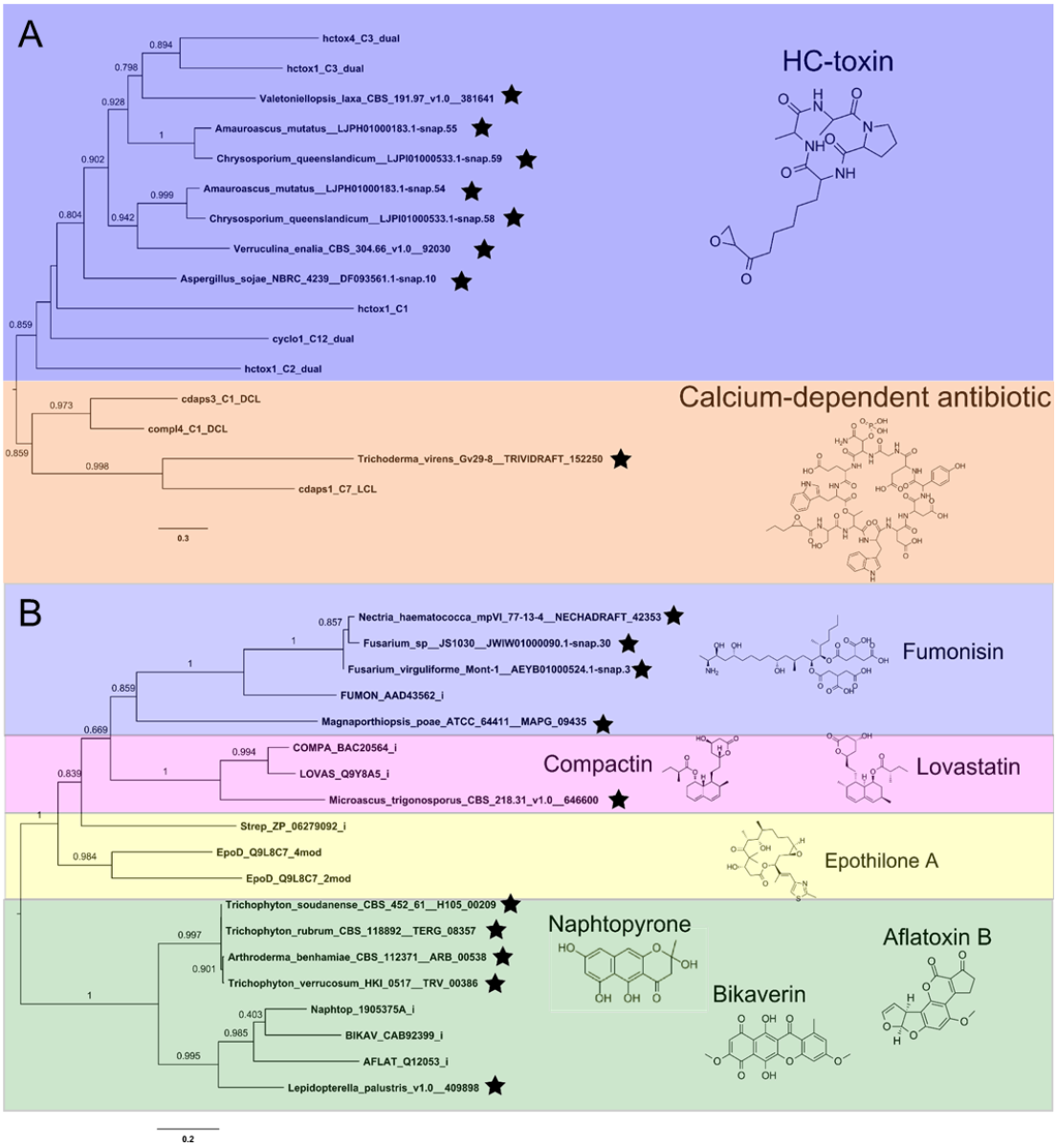


Figure 4.14: ML phylogenetic trees of amino acid sequences corresponding to non-ribosomal peptide synthase (A) and polyketide synthase domains (B). Domains identified in fungal genomes nearby *p450nor* are indicated by a black star. Reference domains from the NAPDOS database and their corresponding chemical products are indicated by colored sections. Scale bars indicate amino acid substitutions per site. Values along branches indicate bootstrap support for the adjacent node.

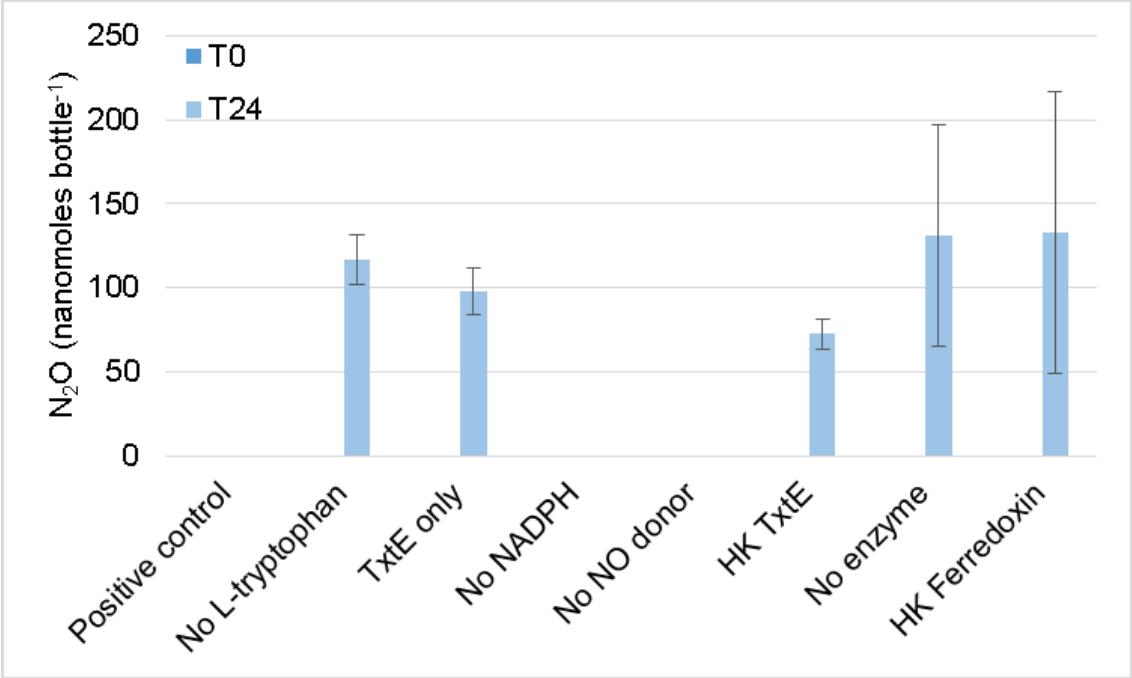


Figure 4.15: N_2O formation at time 0 and 24 h after incubation of TxtE under anoxic conditions.

VITA

Steven Adam Higgins was born in Lowell, MA in 1986. He grew up in Lowell until the 1st grade, where he then moved to live with his father in the small town of Littleton, MA. He attended high school at the Littleton public school system and played football and enjoyed life growing up as a teen in a small Boston suburb. He attended college at the University of Massachusetts, Amherst and received his bachelor of science in biology. During his time at UMass Amherst, Steven became interested in the field of herpetology due to the excellent teachings of a Dr. Alan Richmond and his teaching assistant, Dr. Mike Jones. Steven participated in an internship at the University of South Dakota assisting with a population study on false map and smooth softshell turtles with Dr. Aaron Gregor along the Missouri river. After graduating from UMass Amherst in 2008, Steven moved to South Dakota to participate as a field technician in the ongoing population study from the previous summer, and in 2009, began to pursue his own Master's thesis studying the physiology of freezing tolerance in the boreal chorus frog, *Pseudacris maculata* under the guidance of Dr. David Swanson. He was especially indebted to his committee members, Dr. Karen Koster and Miles Koppang for their advice and research assistance during his M.S. thesis. In 2011, Steven graduated with a Master of Science in biology from the University of South Dakota in 2011, and moved to Knoxville, TN to pursue a doctor of philosophy degree in microbiology under the guidance of Dr. Frank Löffler, a governor's chair and professor at the University of Tennessee (UTK) in the Department of Microbiology. During his time at UTK, Steven applied to multiple fellowships and awards, and received both an two-year NSF funded IGERT fellowship (SCALE-IT) to develop expertise in computer science and one year Department of Energy SCGSR fellowship to work at the Oak Ridge National laboratory with Dr. Christopher W. Schadt. Steven is very grateful for the education he has received at University of Tennessee and the research opportunities he took part in. Steven finished his doctoral thesis in 2017, and

accepted a two-year, NSF-funded postdoctoral position to work with Dr. Dan Buckley at Cornell University in Ithaca, NY. He hopes to continue to pursue a career in academia and mentor his own students one day, or branch out and pursue an entrepreneurial career developing and selling fungal products or services enabled by fungal physiology.